

Aus der Medizinischen Klinik des Universitätsklinikums Heidelberg

Geschäftsführender Direktor: Prof. Dr. med. Hugo A. Katus

Abteilung Klinische Pharmakologie und Pharmakoepidemiologie

Ärztlicher Direktor: Prof. Dr. med. Walter E. Haefeli

**Midazolam Microdosing and Population Pharmacokinetic Modelling to Assess
CYP3A Drug-Drug Interactions in Early Clinical Development**

Inauguraldissertation
zur Erlangung des Doctor scientiarum humanarum
an der
Medizinischen Fakultät Heidelberg
der
Ruprecht-Karls-Universität

vorgelegt von
Sabrina Wiebe

aus
Nipigon, Kanada

2020

Dekan: Herr Prof. Dr. med. Hans-Georg Kräusslich

Doktorvater: Herr apl. Prof. Dr. med. Gerd Mikus

TABLE OF CONTENTS

| | |
|---|-----------|
| Abbreviations..... | 1 |
| 1. INTRODUCTION..... | 5 |
| 1.1 General Introduction | 5 |
| 1.2 Brief Overview of Drug-Drug Interactions | 7 |
| 1.2.1 Guidelines for Assessment | 8 |
| 1.2.2 Cytochrome P450 3A | 11 |
| 1.3 Characteristics of Midazolam..... | 14 |
| 1.3.1 Pharmacokinetic Properties | 15 |
| 1.3.2 Metabolites..... | 15 |
| 1.3.3 Microdosing | 16 |
| 1.3.4 Limited Sampling Approaches..... | 18 |
| 1.4 Overview of Population Pharmacokinetic Models..... | 20 |
| 1.4.1 Definition and Theory..... | 20 |
| 1.4.2 Model Development and Evaluation | 22 |
| 1.4.3 Review of Available Midazolam Population Pharmacokinetic Models..... | 34 |
| 1.5 Aim of Thesis..... | 37 |
| 2. MATERIALS AND METHODS | 37 |
| 2.1 Implementation of Midazolam Microdosing..... | 37 |
| 2.1.1 Subjects | 40 |
| 2.1.2 Study Design | 40 |
| 2.1.3 Study Conduct..... | 41 |
| 2.2 Midazolam and Metabolite Population PK Model Development..... | 44 |
| 2.2.1 Datasets..... | 45 |
| 2.2.2 Software..... | 46 |
| 2.2.3 Base Midazolam Model Development..... | 46 |
| 2.2.4 Base 1'-OH Midazolam Model Development | 47 |
| 2.2.5 Statistical Models..... | 48 |
| 2.2.6 Composite Model..... | 48 |
| 2.2.7 Model Testing for Drug-Drug Interactions..... | 49 |
| 2.2.8 Limited Sampling Testing..... | 50 |
| 3. RESULTS..... | 50 |
| 3.1 Midazolam Microdosing Implementation | 50 |
| 3.1.1 Study 1..... | 51 |
| 3.1.2 Study 2..... | 54 |
| 3.1.3 Study 3..... | 58 |

TABLE OF CONTENTS

| | | |
|-------|---|-----|
| 3.1.4 | Exploratory Analysis of Partial AUC | 63 |
| 3.2 | Model Development Results | 64 |
| 3.2.1 | Midazolam Model | 64 |
| 3.2.2 | 1'-OH Midazolam Model | 70 |
| 3.2.3 | Composite Model | 76 |
| 3.2.4 | Model Assessment of Drug-Drug Interaction | 80 |
| 3.2.5 | Limited Sampling | 83 |
| 4. | DISCUSSION | 87 |
| 4.1 | Midazolam Microdosing Implementation | 87 |
| 4.1.1 | Limitations | 91 |
| 4.1.2 | Midazolam microdosing conclusion | 92 |
| 4.2 | Model Development | 93 |
| 4.2.1 | Structural models | 93 |
| 4.2.2 | Statistical and covariate models | 95 |
| 4.2.3 | Final models with constitutive CYP3A activity | 96 |
| 4.2.4 | Drug-drug interaction assessment | 97 |
| 4.2.5 | Limited sampling assessment | 99 |
| 4.2.6 | Limitations | 99 |
| 4.2.7 | Model development conclusion | 100 |
| 4.3 | Overall Conclusions | 100 |
| 5. | SUMMARY | 101 |
| 5.1 | English | 101 |
| 5.2 | Deutsch | 103 |
| 6. | REFERENCES | 105 |
| 7. | PUBLICATIONS | 117 |
| | APPENDICES | 118 |
| | PK Parameter Tables for Midazolam Microdosing Implementation | 118 |
| | Figure A1: Composite Model Diagnostic Plots | 121 |
| | Figure A2: Composite Model VPC | 122 |
| | Figure A3: Midazolam Individual Fits for Interaction Model | 124 |
| | Figure A4: 1'-OH Midazolam Individual Fits for Interaction Model | 127 |
| | Figure A5: Midazolam Interaction Model VPC | 130 |
| | Figure A6: Simulations Based on Limited Sampling – Internal Set | 132 |
| | Figure A7: Simulations Based on Limited Sampling – External Set | 133 |
| | Adopted Midazolam Model Control Stream with Interaction and Food Effect | 134 |
| | Adopted 1'-OH Midazolam Control Stream with Food Effect | 138 |

TABLE OF CONTENTS

| | |
|---|------------|
| Adopted Composite Model Control Stream with Interaction..... | 141 |
| CURRICULUM VITAE | 146 |
| ACKNOWLEDGMENTS..... | 147 |
| EIDESSTÄTTLICHE VERSICHERUNG | 148 |

Abbreviations

| | |
|---------------------|--|
| -2LL | -2 times the log of the likelihood |
| 1'-OH MDZ | 1-hydroxymidazolam |
| AE | Adverse Event |
| ANOVA | Analysis of variance |
| AUC | Area under the concentration-time curve |
| AUC ₂₋₄ | Area under the concentration-time curve from time 2 to 4 hours |
| AUC _{0-tz} | Area under the concentration-time curve from time 0 until the last quantifiable time point |
| AUC _{0-∞} | Area under the concentration-time curve from time 0 extrapolated up to infinity |
| BCS | Biopharmaceutics Classification System |
| BLQ | Below the Lower limit of Quantification |
| C _{max} | Maximum measured concentration |
| C _{max,u} | Maximum unbound concentration |
| CI | Confidence Interval |
| CL | Clearance |
| CL/F | Apparent clearance |
| CL _{int} | Intrinsic clearance |
| CL _{met} | Clearance of the metabolite |
| C _p | Unbound concentration of a substrate |
| CPRED | Conditional population predictions |
| CWRES | Conditional weighted residual error |
| CYP | Cytochrome P450 |
| DDI | Drug-drug interaction |
| EBE | Empirical Bayes estimate |
| EC ₅₀ | Concentration required for half-maximal effect |
| EFV | Efavirenz |
| EMA | European Medicines Agency |
| E _{max} | Maximum induction effect |
| F | Bioavailability |

ABBREVIATIONS

| | |
|-------------|--|
| FDA | United States Food and Drug Administration |
| fm | Fraction metabolised |
| FOCE-I | First order conditional estimation method with interaction |
| gCV | geometric coefficient of variation |
| gMean | geometric mean |
| IIV | Inter-individual variability |
| IOV | Inter-occasion variability |
| IPRED | Individual predictions |
| iv | Intravenous |
| IWRES | Individual weighted residual error |
| ka | Absorption rate constant |
| k_{deg} | Degradation rate constant of an enzyme |
| keto | Ketoconazole |
| k_{inact} | Maximal inactivation rate constant |
| k_{obs} | Observed inactivation rate of an enzyme |
| K_i | Unbound inhibition rate constant |
| K_I | Inhibitor concentration required for half-maximal inactivation |
| K_m | Michaelis-Menten constant; represents the unbound concentration at which half-maximal rate of metabolism is achieved |
| k_{met} | Rate of (pre-systemic) metabolism |
| MDZ | Midazolam |
| MI-Complex | Metabolite intermediate complex |
| mRNA | Messenger ribonucleic acid |
| nM | Nanomolar |
| nmol | Nanomole |
| NPDE | Normalised Prediction Distribution Error |
| OFV | Objective Function Value |
| PBPK | Physiologically Based Pharmacokinetic model |
| P_{ij} | Individual parameter value at the jth occasion |
| PK | Pharmacokinetic |
| pM | Picomolar |
| PMDA | Pharmaceuticals & Medical Devices Agency |

ABBREVIATIONS

| | |
|-------------------|--|
| pmol | Picomole |
| po | <i>per os</i> ; oral |
| PopPK | Population pharmacokinetic model |
| PsN | Pearl-speaks-NONMEM |
| PXR | Pregnane X receptor |
| Q_x | Inter-compartmental clearance for compartment X |
| QSP | Quantitative Systems Pharmacology model |
| R | Reference treatment |
| R_1 | Reversible inhibition predicted AUC ratio |
| R_2 | Time dependent inhibition predicted AUC ratio |
| R_3 | Induction predicted AUC ratio |
| RIS | Relative Induction Score |
| RSE | Relative Standard Error |
| RTV | Ritonavir |
| RUV | Residual Unexplained Variance |
| SAEM | Stochastic Approximation Expectation-Maximization |
| SJW | St. John's Wort |
| T | Test treatment |
| $t_{1/2}$ | Half-life |
| t_{max} | Time of maximum measured concentration |
| UGT | Uridine 5'-diphospho-glucuronosyltransferase |
| V_c | Volume of central compartment |
| VCZ | Voriconazole |
| V_{max} | Maximum rate of metabolism at high substrate concentrations |
| V_{met} | Volume of metabolite central compartment |
| V_{MPX} | Volume of peripheral metabolic compartment X |
| VPC | Visual Predictive Check |
| V_{pX} | Volume of peripheral compartment X |
| ϑ_{pop} | Typical population value of a parameter |
| ϑ_{cov} | Covariate effect for the population |
| η_i | Random effect for a parameter for the <i>i</i> th individual |
| κ_{ij} | Random effect for a parameter for the <i>i</i> th individual at the <i>j</i> th occasion |

ABBREVIATIONS

| | |
|--------------------|--|
| ε_{ij} | Residual error for the i th individual at the j th time occasion |
| ω^2 | Inter-individual variance |
| π^2 | Inter-occasion variance |

1. INTRODUCTION

1.1 General Introduction

An important challenge encountered when developing drugs derives from drugs with competing metabolic mechanisms interacting with one another. Specifically, a drug compound may act on drug metabolising enzymes in numerous ways: as a substrate, an inhibitor, an inactivator, an inducer, an activator, or a combination thereof (e.g. (Liu et al. 2007; Zhou 2008)), resulting in multiple ways in which drugs may inadvertently interact with each other. With the ever growing rate of polypharmacy, this is becoming particularly problematic, especially in populations such as the elderly or in patients with comorbid conditions (Guthrie et al. 2015; Murphy et al. 2018; Qato et al. 2008).

Cytochrome P450s (CYPs) are a family of heme-containing isoenzymes which have been found to be important in the metabolism of most drugs (Anzenbacher and Anzenbacherova 2001). Within this family, CYP3A is the most plentiful and contributes to metabolism in both the liver and the intestine (Paine et al. 2006; Thelen and Dressman 2009). Consequently, CYP3A is responsible for metabolism of almost half of the small molecule drugs currently marketed (Anzenbacher and Anzenbacherova 2001; Rendic 2002). Despite the preclinical methods that exist for testing drug-drug interaction (DDI) liability, clinical outcomes are not necessarily consistent with *in vitro* findings. In particular, *in vitro*-based models for inhibition in the gut and for time-dependent inhibition, as described in the FDA and EMA drug-drug interaction guidances, have been found to produce 14.8-21.3% positive prediction error, meaning that despite a positive *in vitro* signal for inhibition, no clinically relevant DDI is seen (Vieira et al. 2014). Furthermore, it has been noted that when both time-dependent inhibition and induction are present, the potential for clinically relevant DDIs tends to be overestimated (Einolf et al. 2014). The conservative criteria given by the major health authorities (e.g. FDA and EMA) are meant to provide a safeguard for patients and, thus, it is understandably preferred to have studies with a higher potential for a negative DDI result to be conducted than to miss a DDI that is actually present (EMA-CHMP 2012 Jun; US-FDA 2020a; US-FDA 2020b). Consequently, many DDI trials are conducted without any clinically relevant interactions, resulting in individuals (usually healthy volunteers) who are needlessly exposed to investigational substances, increased drug development timelines, and increased expenditure on clinical trials. An approach that can be used early in drug development to

INTRODUCTION

accurately predict the overall CYP3A interaction liability would allow for better judgment on viability of a compound, would give earlier information regarding which drugs need to be excluded during Phase II/III clinical trials, would inform potential dose adjustments, and can help get much-needed drugs to the market faster.

Due to its extensive metabolism via CYP3A, midazolam is the probe drug recommended by the FDA, EMA, and PMDA to examine the liability of an investigational compound as a perpetrator of CYP3A (EMA-CHMP 2012 Jun; PMDA 2014; US-FDA 2020a; US-FDA 2020b). Guidances state that a victim drug (enzyme substrate) needs to be within the dose proportional range of the drug when DDIs are tested. As midazolam has been found to be dose proportional over at least a 30,000-fold range (Bornemann et al. 1985; Halama et al. 2013), midazolam microdosing is an appealing method for assessing CYP3A DDI liability. Microdosing results in pharmacologically inactive systemic concentrations, meaning that neither therapeutic nor adverse effects should be present and there should be no interference with other administered drugs. Consistently, in research settings where midazolam microdosing has been employed, neither benzodiazepine effects nor adverse events were observed (Eap et al. 2004). Furthermore, DDI results were found to be scalable from midazolam microdoses to therapeutic doses, which is congruent with its large range of linearity (Halama et al. 2013; Hohmann et al. 2016)). Thus, combining midazolam microdosing with early clinical development studies may be a viable alternative to conducting a dedicated CYP3A DDI study.

In order to increase the attractiveness of microdosing methods and to further decrease subject burden, it has been proposed that a limited sampling scheme may be used for midazolam. Limited sampling schemes have previously been shown to be predictive of midazolam metabolic clearance and/or midazolam exposure both following administration of midazolam alone and in the presence of a CYP3A modulator (Katzenmaier et al. 2010; Katzenmaier et al. 2011; Mueller and Drewelow 2013).

Population pharmacokinetic modelling (PopPK) may also be used to enhance the predictability of limited sampling approaches. PopPK models are generally established using rich data and can then be applied to sparse sampling protocols; they identify relevant pharmacokinetic parameters, along with associated sources of variability, which are then entered into the model to predict exposure (Mould and Upton 2012). In the case of DDIs, this would allow for

the prediction of AUC ratios and clearance changes, thereby increasing the ability of limited sampling approaches to detect the presence of DDIs.

Thus, it is proposed that through the implementation of multiple methods, including microdosing, limited sampling, and PopPK, earlier and accurate detection of DDIs may be feasible, without the need for dedicated studies.

1.2 Brief Overview of Drug-Drug Interactions

Drug-drug interactions can be a major concern both during drug development and when co-prescribing medications. Such interactions can result due to a medication influencing what the body does to another medication (i.e. a pharmacokinetic interaction), due to a medication influencing how another drug affects the body (i.e. a pharmacodynamic interaction), or it can be a combination thereof. The focus of the current work is on pharmacokinetic interactions, thus, this overview will not cover pharmacodynamic interactions.

Pharmacokinetic drug-drug interactions can be either metabolic in nature (i.e. interactions with one or more enzymes) or due to interactions with transporters involved in the absorption, distribution or elimination of drugs. The result of such interactions may be an increase in exposure that result in more safety concerns (e.g. a greater number or greater severity of adverse events (AEs)) or the result may be a decrease in exposure that results in a loss of efficacy of a drug (Lin and Lu 1998). Inhibitory interactions may be competitive, non-competitive, or mechanism-based (Burk and Wojnowski 2004). Mechanism-based interactions are irreversible and time-dependent, meaning that either a covalent bond is formed with the enzyme or a reactive intermediate irreversibly alters part of the enzyme; maximal inhibition is slow to be achieved and usually requires multiple days to disappear, as the interaction duration is dependent upon the rate of the affected enzyme's re-synthesis. In contrast, competitive and non-competitive inhibition is generally reversible and usually occurs rapidly, as weaker, non-covalent bonds between the substance and enzyme are formed. In the case of reversible inhibition, the effects are generally seen immediately (Lin and Lu 1998) and disappear shortly after the inhibitor is removed. A third type of inhibition, which is similar to irreversible inhibition, is termed 'quasi-irreversible' inhibition (Riley and Wilson 2015). Quasi-irreversible inhibition occurs due to the formation of an MI-complex – i.e. a complex created between the enzyme and a metabolic intermediate of the inhibitor. As with irreversible inhibition, the inhibitory effects are not immediately apparent and following

removal of the inhibitor, baseline activity levels are slow to return. The interaction persists, as either the complexation with the metabolic intermediate needs to be reversed before the enzyme can be activated again or enzyme re-synthesis is required (Lin and Lu 1998). While *in vitro* methods have been found to reverse the complexation, *in vivo*, such situations appear to be uncommon and, thus, interactions tend to last until the synthesis of new enzymes occurs. Finally, while less common, drug interactions may also result in the induction or activation of enzyme activity, with induction usually occurring through transcriptional activation (Thummel and Wilkinson 1998). Transcriptional activation persists as long as the inducer is present and the return to baseline levels of activity is dependent upon the affected enzyme's rate of degradation. With enzyme activation, the rate of metabolite formation by a specific enzyme is increased due to the presence of another compound, resulting in much faster appearance of an induction-like effect than that seen with traditional induction (Atkins 2005; Mikus et al. 2017).

The superfamily of isoenzymes referred to as the cytochrome P450 (CYP) enzymes are responsible for the majority of Phase I metabolism of drugs (Evans and Relling 1999). Phase I metabolism refers to the metabolic reactions of oxidation, reduction, and/or hydrolysis, which result in a more polar compound. CYPs are a superfamily of oxidising enzymes located mainly on the endoplasmic reticulum membrane and the inner mitochondrial membrane of cells (Thelen and Dressman 2009). They are classified according to families ($\geq 40\%$ of amino acid sequence is similar), such as CYP1, CYP2, and CYP3, and subfamilies ($\geq 55\%$ of amino acid sequence is similar), such as CYP1A and CYP1B (Nebert and Russell 2002). Although at least 18 CYP families have been discovered in humans to date, only three main families appear to be involved in drug metabolism. These families are CYP1, CYP2, and CYP3, with the CYP3A subfamily being responsible for the metabolism of $\sim 50\%$ of small molecule drugs on the market. Due to its importance in drug metabolism, the current work focuses on CYP3A, which will be discussed in more detail following an overview of the drug-drug interaction guidelines from the main health authorities (FDA, EMA, and PMDA).

1.2.1 Guidelines for Assessment

To ensure the safety of patients receiving medications, the main regulatory authorities, such as the FDA, the EMA, and the PMDA, have established guidelines for when drug-drug interaction studies need to be conducted *in vivo* (EMA-CHMP 2012 Jun; PMDA 2014; US-FDA

2020a; US-FDA 2020b). Although the guidelines refer to requirements for both DDIs relating to metabolism and to transport, only the metabolism-related aspects are covered here.

In vitro assessments are required to see if a drug is a substrate, an inhibitor, and/or an inducer of specific metabolising enzymes. For inhibition, the guidelines refer to reversible inhibition and time-dependent inhibition (which can be slow reversible/'quasi-irreversible' or mechanism-based/irreversible, as described in Section 1.2). For substrate and inhibition testing, CYP1A2, 2B6, 2C8, 2C9, 2C19, 2D6, 3A4/5 should be routinely tested, while for induction, only CYP1A2, CYP2B6, and CYP3A4/5 are required for initial testing. If no induction signal is seen for CYP3A4/5, then testing of the CYP2C enzymes is not required, as these are induced via the same pathway (pregnane X receptor) as CYP3A4/5 (Wilkinson 2005). However, if a positive induction signal is seen for CYP3A4/5, then CYP2C8, 2C9, and 2C19 should also be tested for induction. Although it is clear which CYPs to assess for DDI testing, the criteria for determining if a positive signal is seen for a specific enzyme can be relatively complex and, although mostly aligned between guidelines, does have slight differences from one health authority to the next.

Enzyme modulation potential is initially assessed using a basic model, which provides cut-offs to assess interaction signals from *in vitro* data. If the cut-offs are exceeded, a mechanistic or physiologically-based pharmacokinetic (PBPK) model may then be further used to assess inhibition and/or induction potential. As both the basic and the mechanistic models given by the authorities are static models, the change in concentrations over time is not accounted for and, thus, the models tend to overestimate drug interaction potential.

1.2.1.1 Inhibition Testing

Two main basic models exist for inhibition testing: one for reversible inhibition and one for time-dependent inhibition. For CYPs that have considerable presence in the gastrointestinal tract, the models are further broken down to try and determine the potential for interactions both at the hepatic level and at the level of the gut. The equation for determining the predicted area under the concentration-time curve (AUC) ratio based on reversible inhibition is the following:

$$R_1 = 1 + ([I]/K_i)$$

where [I] refers to the maximum unbound concentration ($C_{max,u}$) of the inhibitor (for hepatic interactions) or dose/250 mL (interactions in the gut), and K_i is the unbound inhibition rate constant. The lowest unbound fraction to be used in the equation is 1%, even if lower unbound fractions are determined. When $R_1 \geq 1.02$ for hepatic level interactions or $R_1 \geq 11$ for interactions at the level of the gut, a DDI study using a sensitive substrate for the enzyme should be conducted *in vivo*.

With regards to time-dependent inhibition, the following equation is to be used for predicting the AUC ratio:

$$R_2 = (k_{obs} + k_{deg})/k_{deg}$$

Where k_{obs} refers to the observed inactivation rate constant and k_{deg} refers to the degradation rate constant. To determine k_{obs} , the following formula is used:

$$k_{obs} = (k_{inact} * [I]) / (K_i + [I])$$

where k_{inact} is the maximal inactivation rate constant and K_i refers to the inhibitor concentration resulting in half-maximal inactivation; the meaning of [I] is different between guidelines, such that for the EMA, [I] is equal to the $C_{max,u}$, while for the FDA and PMDA, [I] refers to $50 * C_{max,u}$. When $R_2 \geq 1.25$ (all guidelines), a DDI examining time-dependent inhibition using a sensitive substrate for the enzyme should be conducted *in vivo*.

1.2.1.2 Induction Testing

For induction testing, multiple methods are given in the guidances. Specifically, the guidances refer to the fold-change method, the correlation method, and the basic kinetic model, which uses a given equation to determine a predicted AUC ratio in the presence and absence of the test substance. Note that in the guidance from the EMA, no basic kinetic model is given.

For the fold-change method, the change in mRNA of the given enzyme within human hepatocytes from at least 3 donors is investigated following incubation with the test substance. This change is then compared to what is seen with positive and negative controls. If a ≥ 2 -fold increase in mRNA is observed in at least one donor, the substance is considered to be an enzyme inducer. If the change in mRNA is $\geq 20\%$ of the positive control, then even if less than 2-fold change is seen, the substance cannot be excluded as an inducer.

The FDA presents two possible methods for evaluating induction with a correlational method, while the EMA and PMDA only refer to one of these methods (the relative induction score [RIS] method). An RIS is calculated based on the following formula:

$$\text{RIS} = E_{\text{max}} * [I] / (EC_{50} + [I])$$

where E_{max} is the maximum induction effect, EC_{50} is the concentration required to obtain the half-maximal induction effect, and $[I]$ is the $C_{\text{max,u}}$. The RIS should be calculated both for the test substrate, as well as for several other known inducers of the particular enzyme.

The basic kinetic model consists of the following formula:

$$R_3 = 1 / [1 + (d * E_{\text{max}} * 10 * [I]) / (EC_{50} + (10 * [I]))]$$

where $[I]$ refers to $C_{\text{max,u}}$, d is a scaling factor (usually 1), E_{max} is the maximum induction effect, and EC_{50} is the concentration required to achieve the half-maximal induction effect. If $R_3 \leq 0.8$, then the substance is considered to be an inducer of the particular enzyme.

As noted earlier, the cut-offs implemented by the regulatory agencies result in numerous dedicated DDI trials without any clinically relevant effects observed, particularly in the cases of induction and time-dependent inhibition (Einolf et al. 2014; Vieira et al. 2014). This is particularly true for CYP3A, given its importance in drug metabolism. Due to the prominence of CYP3A, much research has been conducted regarding mechanisms associated with DDI liability, as well as with regards to the best ways to assess CYP3A activity. The following section gives an overview of the current knowledge pertaining to CYP3A.

1.2.2 Cytochrome P450 3A

CYP3A is one of the most abundant drug-metabolising enzymes, making up around 40% of the CYPs found in the liver (following induction, this can be increased to greater than 60% (Anzenbacher and Anzenbacherova 2001)) and almost 80% of CYPs in the gut (Paine et al. 2006; Thelen and Dressman 2009). A broad spectrum of xenobiotics and endogenous substances are able to be metabolised by this subfamily of CYPs, with multiple substrates able to bind simultaneously (Sevrioukova and Poulos 2013). Thus, the potential for DDIs involving the inhibition, inactivation or induction of CYP3A is particularly high. Of the CYP3A genes, CYP3A4 is the most prominent (e.g. 71-99.5% of CYP3A transcripts), although CYP3A5 and CYP3A7 may also be important for metabolism, each accounting for, on average, 2.5% of the

CYP3A transcripts (Koch et al. 2002). Notably, CYP3A7 is generally found in the fetal liver, while reports of its existence in adults appears to be conflicting (e.g. (Dresser et al. 2000; Koch et al. 2002)). While CYP3A5 has been shown *in vitro* to contribute to the metabolism of substances such as midazolam, its relevance *in vivo* remains controversial and may be partly tied to the relative expression of CYP3A5 to CYP3A4 (Thummel and Wilkinson 1998). At most, however, it plays a minor role in metabolism when compared to the CYP3A4 enzyme.

Due to the high proportion of CYP3A, oral drugs which are mainly metabolised by CYP3A often undergo extensive first-pass metabolism (i.e. metabolism that occurs pre-systemically) both at the level of the liver and the gut. This extensive first-pass metabolism is a big contributing factor to low oral bioavailability of drugs that are mainly metabolised by CYP3A. Although the liver has traditionally been thought of as the main contributor to first-pass metabolism (due to its much higher enzyme content), intestinal first-pass metabolism has been shown to have an important role for several CYP3A substrates (Thelen and Dressman 2009). In the intestine, CYP enzymes are mostly present in the tips of the villi, as this increases the likelihood of an absorbed compound coming in contact with the enzyme and being metabolised for elimination purposes. Factors such as increased blood flow which change the amount of time spent intracellularly in the villi can have considerable influence on first-pass metabolism and, thus, bioavailability (Thelen and Dressman 2009).

The expression and activity of CYP3A enzymes displays large inter-individual variability. Specifically, expression of CYP3A has been found to vary by factors of 32 (CYP3A5) to 118 (CYP3A4) (Koch et al. 2002) and inter-individual variability in CYP3A4 expression in the intestine has been found to be as much as 30-fold (Thelen and Dressman 2009). It should be noted that such high inter-individual differences in expression do not necessarily mean similarly high levels of inter-individual variability in activity (Thummel and Wilkinson 1998). *In vivo*, baseline CYP3A activity has generally been found to vary by up to 10-14-fold (Dresser et al. 2000; He et al. 2005; Stoll et al. 2013), which is still considerably lower than the 118-fold difference in expression of CYP3A4 transcripts. Taking interactions into account, however, a 400-fold range of variability in CYP3A activity may be seen (Wilkinson 2005). Although various factors have been postulated to influence the inter-individual variability in CYP3A activity, including age, disease state, and sex (Chen et al. 2006; Dresser et al. 2000), the findings regarding these factor have generally been conflicting or non-conclusive. For example, while

Chen et al. (Chen et al. 2006) have noted higher clearance in women following both iv and oral dosing of midazolam, a substrate used to measure CYP3A activity, other researchers have found no sex-related differences (He et al. 2005; Kashuba et al. 1998; Thummel et al. 1996) or lower clearance in women following oral administration (Krecic-Shepard et al. 2000).

Some of the more potent inhibitors of CYP3A are known to include azole antifungals (e.g. ketoconazole), macrolide antibacterials (e.g. erythromycin), HIV protease inhibitors (e.g. ritonavir) and grapefruit juice. Rifampicin, efavirenz, and St. John's Wort are some of the known potent inducers and/or activators of CYP3A (Dresser et al. 2000; Keubler et al. 2012; Mikus et al. 2017; Thummel and Wilkinson 1998; Wilkinson 2005). Interestingly, some perpetrators (e.g. grapefruit juice) appear to be selective for intestinal CYP3A, likely due to the comparatively low quantity of CYP3A in the enterocytes, along with the fact that orally administered substances have to go through the gastrointestinal tract before being metabolised in the liver (Wilkinson 2005). Generally, however, perpetrators that are administered orally have been found to inhibit both intestinal and hepatic CYP3A. For reversible inhibitors of CYP3A (e.g. voriconazole), inhibition of activity is often immediate and CYP3A activity has been found to return with a $t_{1/2}$ of 24 h following discontinuation of the inhibitor (Katzenmaier et al. 2011). In contrast, substances such as ritonavir, which display mechanism-based/irreversible inhibition, have been noted to take 48 h to achieve maximal CYP3A inhibition, with long-lasting effects, even once the inhibitor is removed (Katzenmaier et al. 2011). In the study by Katzenmaier et al., 3 days after discontinuing ritonavir, CYP3A inhibition was still found to be strong, thus, it is important to ascertain not just if a substance is a perpetrator, but also how long such effects might be likely to last.

Induction of CYP3A is controlled by the pregnane X receptor, which influences multiple enzymes and transporters (Kliwer et al. 2002; Nebert and Russell 2002). As substrates of CYP3A are often also substrates of the P-glycoprotein transporter, it can be unclear to what extent drug interaction effects are due to changes in CYP3A metabolism and to what extent they are due to transport factors (Benet 2009). This problematic further complicates the ability to predict *in vivo* reactions from *in vitro* assessments. The upregulation of transcription factors is a relatively slow process and maximal inductive effects of CYP3A may only be achieved after approximately 2 weeks of dosing; thus, induction is generally thought to be more a problem for chronically administered drug. However, recent evidence suggests that

CYP3A inductive effects may actually be activation effects and, thus, are not dependent on achievement of maximal induction, as even following a single dose, the effects can still be significant 16 or more days later (Mikus et al. 2017). This is also evidence of the long-lasting effects of induction and/or activation, which for CYP3A have been found to last up to 3 weeks or more following removal of the inducer (Mikus et al. 2017; Reitman et al. 2011). These effects can be particularly problematic, as potent inducers of CYP3A have been found to reduce drug exposure up to 40-fold (Kirby et al. 2006), which effectively eradicates any efficacy of a CYP3A substrate drug.

While *in vitro* assessments of CYP3A metabolism or of CYP3A modulator potential provide a good first step in assessing DDI liability, these methods still leave much uncertainty and often do not translate into a similar impact on pharmacokinetics in the clinic. Furthermore, while *in vitro* methods are generally able to reflect the potential for CYP3A inhibition, CYP3A induction is much harder to predict. The fact that substances can simultaneously be a substrate, an inhibitor/inactivator and/or an inducer of CYP3A (Liu et al. 2007; Zhou 2008) leads to additional complexity in the prediction of whether a substance is likely to cause clinically relevant interactions. Given the complexity of substance-enzyme interactions, it is often unclear from pre-clinical data which results to expect in clinical studies *in vivo*.

Finding innovative and resource-saving approaches to accurately predict DDIs early on in drug development is important for academia, pharmaceutical companies, and the public, because it means that needed drugs can get to patients faster, with reduced costs associated with the drug development process. Thus, further efforts need to be made to develop such methodologies. As midazolam is an accepted means of assessing CYP3A activity, methods using midazolam measurement most advantageously appear to be a promising route to go.

1.3 Characteristics of Midazolam

Midazolam is a short-acting, benzodiazepine derivative, used as a sedative-hypnotic (Kanto 1985). It is administered intravenously, intramuscularly, or orally. However, due to its pharmacokinetic properties, it is also the recommended probe drug (proposed by the main food and drug regulatory authorities) for CYP3A-related drug-drug interaction liabilities, both *in vitro* and *in vivo* (EMA-CHMP 2012 Jun; US-FDA 2020a; US-FDA 2020b).

1.3.1 Pharmacokinetic Properties

Midazolam is a BCS Class I substance, meaning that it has both good solubility and good permeability. Despite its BCS Class I classification, midazolam has a relatively low oral bioavailability (~30% (Heizmann et al. 1983)), due to the extensive first-pass metabolism that it undergoes (Thummel et al. 1996). Absorption of midazolam is quite rapid, with peak concentrations reached between 15 and 60 min (Heizmann et al. 1983; Thummel et al. 1996). The volume of distribution for midazolam is quite variable, ranging from 38.6 L – 146.6 L following iv administration, which is generally higher than the total volume of water (42 L) in humans, suggesting that midazolam is highly distributed within the tissues of the body (Heizmann et al. 1983; Smith et al. 1981). Less than 1% of midazolam is excreted unchanged in urine, with the majority of midazolam metabolised via CYP3A (Heizmann et al. 1983; Heizmann and Ziegler 1981; Smith et al. 1981). In studies examining iv and oral administration of midazolam, hepatic and enteric extraction ratios have been found to be of similar magnitude, further indicating the importance of first-pass metabolism in the bioavailability of midazolam (Hohmann et al. 2015; Thummel et al. 1996). It is not known to be a substrate of any transporters (Cummins et al. 2004; Ziesenitz et al. 2012).

The disposition of midazolam is usually described as being at least biexponential. Elimination is also quite rapid, with the elimination half-life ranging from 1.3-3.4 h (Heizmann et al. 1983). Although less than 1% of midazolam is excreted unchanged in urine, the main route of elimination (as metabolite) is renal, as evidenced by the fact that approximately 90% of radioactivity is recovered in urine 24 h following administration of ¹⁴C midazolam (Heizmann and Ziegler 1981). Clearance of midazolam is approximately 300-500 ml/min (18-30 L/h) (Heizmann et al. 1983).

1.3.2 Metabolites

Midazolam is metabolised into three main metabolites: 1'-OH midazolam, 4-OH midazolam, and 1',4-dihydroxymidazolam, all of which are produced via CYP3A4/5 (Kronbach et al. 1989; Thummel et al. 1996). Metabolites are further metabolised via Uridine 5'-diphosphoglucuronosyltransferase (UGT) enzymes, producing glucuronide conjugates of each of the metabolites (Heizmann et al. 1983). 1'-OH midazolam (and its glucuronide conjugate) is the most plentiful of midazolam's metabolites, making up approximately 60 to 80% of the recovered dose in urine over 24 h following either iv or oral dosing (Heizmann et al. 1983;

Heizmann and Ziegler 1981). The 4-OH and 1',4-dihydroxymidazolam metabolites each account for only around 1-3% of the recovered midazolam dose. The metabolites are formed rapidly, with concentrations of 1'-OH midazolam already measurable by at least 5 minutes post-midazolam dose (Thummel et al. 1996). As with the parent compound, maximum concentrations of 1'-OH midazolam are reached around 15 to 60 minutes post-midazolam dose. Elimination tends to parallel that of midazolam, with an elimination half-life around 1.5 to 2 hours (Bornemann et al. 1985). Due to the considerably lower concentrations of 4-OH midazolam and 1',4-dihydroxymidazolam, the rest of this dissertation will focus on midazolam and its primary metabolite, 1'-OH midazolam.

1.3.3 Microdosing

Microdosing of drugs is a technique that has been gaining popularity and is supported by main regulatory authorities in early phases of development (CHMP 2004; FDA 2006). The dose of a small molecule is considered a microdose if it is 1/100th of the expected therapeutic dose or a maximum of 100 µg, whichever amount is smaller. This technique has been applied to promising drug candidates for early assessment of pharmacokinetics, including basic pharmacokinetic profiles and bioavailability, metabolic profiles, and tissue distribution (Sugiyama and Yamashita 2011), as well as in the investigation of pharmacogenomic impact on kinetics and of victim drug-drug interaction liability (Burt et al. 2016; Svendsen et al. 2016). Use of a microdose is considered advantageous, as concentrations within the body do not reach pharmacologically active levels and, thus, no adverse reactions are likely, nor is interference with other administered drugs expected (Mikus 2019; Sugiyama and Yamashita 2011). Additionally, the limited exposure to drugs with microdosing reduces potential harm to subjects or patients which could arise when inhibition of an enzyme or transporter results in greatly increased exposure (Burt et al. 2016).

Despite the limited systemic exposure resulting from microdosing, various analytical tools exist which are sensitive enough to measure such low concentrations, including accelerator mass spectrometry, positron emission tomography, and liquid chromatography-tandem mass spectrometry (LC-MS/MS). Of these methods, LC-MS/MS is also regularly employed in the measurement of therapeutic drug levels, meaning that costs and/or difficulty associated with the bioanalytical technique are not necessarily increased (Burt et al. 2016). With regards to midazolam, assays have been developed using ultra performance LC-MS/MS that are able to

adequately measure concentrations as low as 50 fg/mL for midazolam and 250 fg/mL for 1'-OH midazolam (Burhenne et al. 2012). Therefore, the feasibility of applying microdosing to clinical studies should not be limited by lack of reasonable analytical techniques.

Although some concern has been raised regarding the predictability of microdosing results for therapeutic doses, studies comparing pharmacokinetics have found approximately 80% or more of substances display linear (and, thus, scalable) pharmacokinetics from microdoses to therapeutic doses (Croft et al. 2012; EUMAPP 2012; Hohmann et al. 2016; Lappin et al. 2013). In cases where microdosing is not predictive, there is indication that one can already see preclinically that processes are likely to be saturable and, thus, microdosing would either not be an appropriate tool or could be used together with an appropriate model to scale to therapeutic doses (Bosgra et al. 2016). Midazolam has received considerable attention with regards to its ability to predict outcomes based on a microdose, due to its use for phenotyping CYP3A activity. Doses as low as 100 ng have been administered and results compared to those following microdosing, low milligram doses, and therapeutic doses (Halama et al. 2013). Midazolam was found to display linear pharmacokinetics over the full range of doses; such findings regarding midazolam's dose proportionality have been confirmed by multiple researchers, both for orally administered doses and for iv infusions (Bornemann et al. 1985; Croft et al. 2012; Lappin et al. 2006).

Due to its dose proportionality, as well as to the lack of pharmacological effect, a midazolam microdose is an appealing tool for integrating into early clinical studies without influencing the examination of the experimental drug. In support of this potential application for midazolam microdosing, it has been shown that midazolam microdoses are able to detect inhibition of CYP3A by a perpetrator drug, without reports of any benzodiazepine effects being present or adverse events occurring (Eap et al. 2004; Hohmann et al. 2015). Furthermore, midazolam microdoses have been used both alone to detect CYP3A DDIs, as well as together with other substrates for DDI testing (Croft et al. 2012) and results when administered with perpetrators have been consistent with results for therapeutic doses (Croft et al. 2012; Eap et al. 2004; Hohmann et al. 2015). Thus, the assessment of the feasibility and appropriateness of applying the midazolam microdosing approach in clinical drug development is investigated as part of the work presented here.

1.3.4 Limited Sampling Approaches

As another tool to facilitate measurements in the clinic and to reduce inconvenience to subjects or patients, costs, and burden to site staff, limited sampling approaches have increasingly been investigated for various drug compounds (Egorin et al. 1989; Katzenmaier et al. 2010; Miyazaki et al. 1997; Ratain and Vogelzang 1987; Yang et al. 2018). Such approaches utilise between 1 to 4 plasma/blood samples to predict AUC and/or clearance of a drug, rather than taking the typical 6-15 samples over a 12 to 24 hour period. Limited sampling approaches have been successfully applied for multiple drugs, including multiple cancer drugs and some immunosuppressive medications.

Given the liability for DDIs with CYP3A and the use of midazolam as the typical phenotyping agent, various limited sampling strategies have been proposed for assessing midazolam exposure. As a single time point measurement to predict exposure is particularly appealing, multiple researchers have examined the ability of a single sample to predict midazolam AUC or clearance (Chaobal and Kharasch 2005; Krupka et al. 2006; Lee et al. 2006; Nguyen et al. 2016; Penzak et al. 2008; Rogers et al. 2002; Yang et al. 2018; Zadoyan et al. 2012). Although findings have often been favourable, at least for constitutive CYP3A conditions, the ideal time point differs between studies and the ability of a single time point to detect DDIs has been inconsistent. The most predictive single time point within studies ranges from anywhere between 2 and 6 h, with one group not finding any single time point to be predictive of midazolam exposure (Rogers et al. 2002). The group finding no predictive time points estimated metabolite exposures and/or the ratio of 1'-OH midazolam to midazolam exposure, rather than midazolam exposure/clearance itself; neither metabolite exposure nor metabolite ratios has been validated as a reliable phenotyping method, likely explaining the negative outcome compared to other groups. Additionally, metabolic ratios have generally not been found to be a good predictor of CYP3A activity (Lee et al. 2006).

With regards to DDI outcomes, only three studies examined a single time point for DDI prediction. In one study, only the single time point (6 h) in the absence of full profiles was used for assessment of a DDI, thus, it is unclear if the time point would be truly predictive or not (Zadoyan et al. 2012). In the other two studies examining DDIs, results were mixed; Penzak et al. (Penzak et al. 2008) found that different time points were needed to be able to predict midazolam AUC under different conditions, such that a 4 h time point was ideal for basal

conditions, while 2 or 8 h were ideal for conditions of induction, thereby limiting the usefulness of the approach for DDI predictions. In contrast, Chaobal et al. (Chaobal and Kharasch 2005) found that a 5 h time point could adequately predict midazolam exposure under conditions of inhibition and induction, as well as for basal conditions. Furthermore, geometric mean (gMean) ratios and 90% confidence intervals (CIs) for AUCs and for single time points were in the same magnitude as those found using full profiles for all conditions.

In order to avoid limitations noted with a single time sample, as well as to decrease the possibility of losing data when difficulties arise in obtaining or analysing the single sampling point, other groups have examined the predictability of 2 to 4 samples over different time intervals (e.g. (Katzenmaier et al. 2010; Katzenmaier et al. 2011; Kim et al. 2002; Masters et al. 2015; Nguyen et al. 2016)). The particular time points to use have generally been decided using linear regression models, comparing regression predicted outcomes to observed midazolam AUCs or clearance values (Katzenmaier et al. 2010; Katzenmaier et al. 2011; Lee et al. 2006), although a PopPK model has also been used to predict midazolam exposures (Nguyen et al. 2016). Constitutive CYP3A activity was generally well-predicted using multiple limited sampling schemes, including 5 min, 0.5 and 6 h (Kim et al. 2002), 0.5, 2 and 6 h (Lee et al. 2006), 2, 2.5, 3 and 4 h (Katzenmaier et al. 2010; Katzenmaier et al. 2011), 0.5, 1, 2 and 8 h (Mueller and Drewelow 2013), and 0.25, 2, 2.5, and 6 h (Nguyen et al. 2016). In contrast, Masters et al. (Masters et al. 2015), who examined multiple partial AUCs (AUC_{0-4} being the most predictive), found baseline activity to be poorly predicted, while Ma et al. (Ma et al. 2010) who examined the ability of 2 and 3 time point sampling schemes to predict CYP3A baseline activity, induction and inhibition, observed mixed results for baseline activity.

Induction could be well predicted in the schemes of Masters et al., Mueller and Drewelow, and Katzenmaier et al., although Ma et al. found induction was poorly predicted using their sampling scheme. Only the limited sampling scheme used by Katzenmaier et al. was able to accurately predict midazolam exposure following CYP3A inhibition, although inhibition of intestinal CYP3A activity was also accurately predicted by the sampling scheme used by Ma et al. Thus, limited sampling schemes for midazolam have displayed promising results, but could still benefit from further optimization to increase their predictability. Combining a limited sampling scheme with PopPK, as done by Nguyen et al. (Nguyen et al. 2016) for basal CYP3A activity, could provide the required optimization, thereby offering another tool for reducing

subject and patient burden, as well as development time and costs when assessing CYP3A DDIs. As such, the following sections will review the definition and theory behind PopPK modelling, model development and evaluation, and give an overview of the currently available midazolam PopPK models.

1.4 Overview of Population Pharmacokinetic Models

Models are a powerful tool to better understand a drug's characteristics and potential factors contributing to its pharmacokinetics and/or pharmacodynamics. There are multiple types of models used in pharmacology, ranging from simple mechanistic models to complex quantitative systems pharmacology (QSP) models. Each model has its advantages and disadvantages and different places where it is likely most useful within drug development or individualization of patient care. One of the more common modelling approaches in clinical pharmacology is PopPK modelling, which can provide important information and be used in numerous ways without being overly complex. Thus, for the purposes of the current dissertation, the focus here will solely be on PopPK models.

1.4.1 Definition and Theory

PopPK is a modelling approach which combines information from multiple trials and sources to achieve different aims. One important goal of PopPK is to identify and describe covariate relationships that impact exposure, as well as to describe the overall inter- and intra-individual variability for different pharmacokinetic parameters. This information can then be used to estimate exposures based on different dosing regimens, special populations, or other factors where direct empirical evidence has not necessarily been collected yet (Lalonde et al. 2007; Whiting et al. 1986). Thus, using all relevant information from different settings allows for predictions that can have important impact on drug development decisions, as well as on the label of a compound (Lalonde et al. 2007).

PopPK can be used with either sparse or dense sampling schemes and it is robust to differences in sampling and/or dosing schedules (Wade et al. 1994). As such, PopPK is becoming a regularly used tool in drug development to inform study design, dosing regimens, dose adjustments in special populations, as well as to provide richer information regarding the relationship between drug exposure and safety or efficacy outcomes (Atkinson Jr and Lalonde 2007; Mould and Upton 2012). PopPK is particularly useful, as it does not rely on

stringent criteria for timing of data collection and is helped, rather than hindered, by heterogeneous samples, as are usually seen in patient trials (Sheiner 1997).

Multiple methods have previously been used for PopPK, including the naïve-pooled approach, the two-step approach and, more recently, the nonlinear mixed effects approach (Mould and Upton 2012). The naïve pooled approach consists of fitting the pooled data from all individuals while ignoring differences between the individuals. The two-step approach first fits each individual's data and then uses the mean of the combined individuals' parameter estimates to determine population parameters. These two methods are less robust to deviations in sampling and/or dosing and have been found to result in biased estimates (Mould and Upton 2012). Biased estimates are those which are further from the actual values and, thus, do not fit the data as well. Nonlinear mixed effects modelling, originally introduced by Sheiner and colleagues for PopPK (Sheiner et al. 1972), is currently the most applicable and likely most commonly used method. Mixed effects refers to the fact that both fixed and random effects are accounted for in the model (Sun et al. 1999). Fixed effects are the aspects that are constant for the population, while random effects are the effects that differ for each individual without being able to be accounted for by a covariate effect. For inter-individual differences that are measurable (e.g. weight and age) and influential for model parameters, a covariate effect is built in for the model parameter's estimate, as the covariate should have a fixed effect for the population as a whole. On the other hand, an example of a random effect, i.e. an effect of something which is not directly measurable but which contributes to variability between individuals, would be the differing expression of CYP3A in each individual. This differing expression would affect an individual's exposure to CYP3A substrate drugs, as well as likely having an influence on the impact of CYP3A modulators on overall exposure of such substrates. Thus, although pharmacokinetic parameters are estimated at the population level, the individual's parameters are maintained through estimates of variability within the model. The process of developing the structure, including appropriate variability and identifying appropriate covariates will be described in the next sections, followed by a review of available midazolam PopPK models in order to give the background for development of the model which is the topic of this dissertation.

1.4.2 Model Development and Evaluation

The process associated with model development and evaluation consists of multiple steps, which are depicted in Figure 1, below. While not all aspects listed are necessarily needed for every model, each can play an important role in obtaining the most appropriate final model and/or simulation for the model’s final intended use.

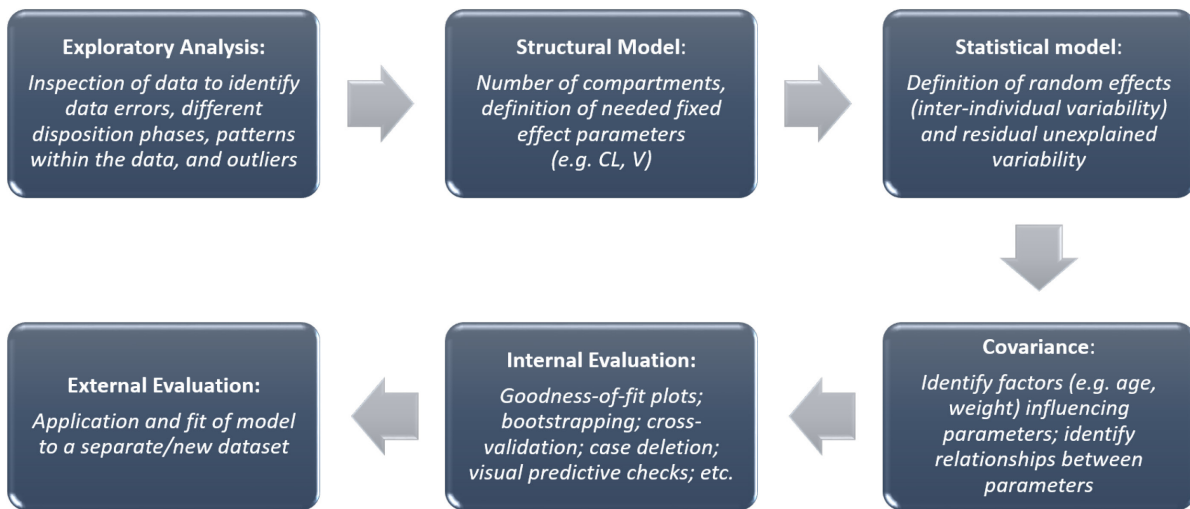


Fig. 1: Model development and evaluation overview

1.4.2.1 Model Development

Model development begins before the actual development itself. As an initial step, it is important to take an exploratory look at the available data. With this initial exploratory analysis, data errors can immediately be identified and corrected or omitted, different phases in the substance’s disposition may be apparent and can give an initial framework for the model structure, patterns in the data may be readily visible, variability in exposure can be assessed, and outliers can be identified. Extreme outliers may disproportionately affect the estimation of parameters and, thus, it may be best to leave them out during model development, although completely removing outliers requires reasonable justification (Sun et al. 1999).

Following the exploratory analysis and any needed steps which may have been implemented as a result of the analysis, the actual model development begins. Model development is a multi-stage process, consisting of three main elements: 1) the structural model, 2) the statistical model, and 3) the covariate model (Mould and Upton 2013). The structural model describes the important fixed effect parameters required to adequately describe the data.

INTRODUCTION

Compartments, which may be either theoretical in nature, or which may refer to an actual physiological “compartment”, such as blood, make up the main structure of the model. Parameters describing the typical (i.e. at a population level) movement of the dependent variable, usually concentration, through the compartments further make up the structure. In a simple 1-compartment model, these parameters would generally consist of clearance and volume of distribution. With the inclusion of more compartments, more parameters are needed to describe movement between compartments. For a typical PopPK analysis, 1-, 2-, and/or 3-compartment models are tested and included for any one particular analyte (with multiple analytes, there may be a series of 1-, 2-, or 3- compartment models combined), with at least one absorption/depot compartment generally incorporated for drugs administered via extravascular routes.

Model parameters describe the typical pharmacokinetic processes following drug administration and, thus, account for absorption, distribution, and metabolism/elimination. Absorption is customarily accounted for using zero-order absorption (e.g. administration directly into the compartment of interest) or first-order absorption, such as that typically seen following oral administration of a drug, while elimination is generally defined as linear, non-linear, or a combination thereof. Non-linear, or saturable elimination, is most commonly described for small molecule drugs via the Michaelis-Menten equation (Menten and Michaelis 1913), which describes saturable enzyme kinetics (Mould and Upton 2013):

$$CL_{int} = V_{max}/(K_m+C_p)$$

where CL_{int} is the intrinsic clearance, V_{max} is the maximum rate of metabolism at high substrate concentrations, C_p is the unbound concentration of the substrate, and K_m is the Michaelis-Menten constant, representing the unbound concentration where the half-maximal rate of metabolism is achieved.

Additionally, a lag time or one or more transit compartments may be added to the model to describe a delay between drug administration and appearance of drug within the blood (Savic et al. 2007). The advantage to transit compartments is that the drug concentrations appear more gradually within the central compartment, although finding the optimal number of transit compartments may be a question of trial and error.

Along with choosing the right structural model, it is important to appropriately describe the variability between and within individuals through selection of an appropriate statistical model. Variability in the dependent variable is described via the inter-individual variability (IIV), the inter-occasion variability (IOV), as well as the remaining/residual unexplained variance (RUV). IIV can be applied in different ways, although most commonly, due to the log-normal distribution of most biological data (Fisher and Shafer 2007), it is modelled exponentially:

$$P_i = \vartheta_{pop} \times e^{\eta_i},$$

where P_i is the individual pharmacokinetic parameter, ϑ_{pop} is the 'typical' (mean) population value for P , and η_i describes the random effect (making the variability) on P for the i th individual; η_i is assumed to be normally distributed with a mean of 0 and a variance of ω^2 . IOV is modelled using a similar approach, although the random effect is determined over numerous occasions, to account for fluctuations due to, for example, physiological processes and measurement errors, with the resulting formula being (Karlsson and Sheiner 1993):

$$P_{ij} = \vartheta_{pop} \times e^{\eta_i + \kappa_{ij}},$$

where κ_{ij} describes the random effect on P for the i th individual at the j th occasion. As with η_i , the κ_{ij} effect is assumed to be normally distributed with a mean of 0 and a variance of π^2 . RUV is added to the model to identify any remaining variability that cannot be accounted for using the available data (Fisher and Shafer 2007). This may be due to assay measurement errors, covariates for which one has no data, errors during study conduct, or may be due to model misspecification. Misspecification occurs when one or more components of the model are falsely characterised, such as a potentially inappropriate structural model, an incorrect variability structure, inappropriately defined parameter values (e.g. a local minimum during the minimization process rather than a true, global minimum for the value), or spurious covariate relationships within the model. The most common ways to account for RUV are through additive error, proportional error, or combined additive and proportional error, although other ways of accounting for the variance exist (e.g. Poisson distribution or log-normal error). The equations accounting for RUV are as follows (Fisher and Shafer 2007):

$$\text{Additive error: } Y_{ij} = C_{true,ij} + \varepsilon_{ij}$$

Proportional error: $Y_{ij} = C_{\text{true},ij} * (1 + \varepsilon_{ij})$

Combined additive and proportional error: $Y_{ij} = C_{\text{true},ij} * (1 + \varepsilon_{ij}) + \varepsilon_{ij}$

Poisson error: $Y_{ij} = C_{\text{true},ij} + \sqrt{C_{\text{true},ij}} * \varepsilon_{ij}$

where Y_{ij} represents the concentration value for the i th individual at time j , C_{true} represents the “true” concentration (if it could be known) for the i th individual at time j , and ε_{ij} represents the residual error associated with the observation.

A final consideration (though not necessarily the last step) for model development is the incorporation of any important covariates. Covariates pertain to subject characteristics and/or other known factors that may predictably account for variability in the pharmacokinetic parameters. Some common covariates include age, weight, body mass index, body surface area, sex, disease state, (e.g. renal or hepatic impairment; severe or mild disease), race, co-medications, and creatinine clearance. In PopPK models, these are often normalised (divided by the ‘typical’ value) or centered (‘typical’ value subtracted; should be used with caution) for better interpretability of the final parameters. Specifically, by normalising or centering covariates, then the resulting value is that of a ‘typical’ subject or patient (Mould and Upton 2013). Covariates may be entered into a model in a variety of ways. If a covariate is expected to have a direct, linear effect on the pharmacokinetics, then the following equation may be used:

$$P_i = (\vartheta_{\text{pop}} + \text{covariate}_i \times \vartheta_{\text{cov}}) \times e^{\eta_i},$$

where P_i is again the individual pharmacokinetic parameter for the i th subject, ϑ_{pop} is the mean population value for P , covariate_i is the individual’s value for the covariate being examined, ϑ_{cov} is the constant influence of the value in the population, and η_i describes the variability on P for the i th individual. More commonly, a power model with covariate normalisation is used to describe the relationship between a covariate and the parameter of interest:

$$P_i = (\vartheta_{\text{pop}} \times (\text{covariate}_i / \text{covariate}_{\text{pop}})^{\vartheta_{\text{cov}}}) \times e^{\eta_i}$$

The decision to include a covariate in a model is generally based on i) knowledge based on prior research that the covariate impacts the pharmacokinetics of the substance being modelled and/or ii) the covariate is identified during model development (usually using graphical analysis) as having an impact on any of the model’s parameters. In a graphical

analysis, covariates are plotted against model parameters and/or parameter variability values. This graphical analysis may or may not be combined with a statistical analysis, though the usefulness of statistical analysis may partly depend on the sample size examined (Mould and Upton 2013). Those covariates that appear to explain some of the model's variability are entered into the model and an evaluation to ascertain if there is an improvement in model fit is conducted.

1.4.2.2 *Model Evaluation*

Model evaluation is a topic of great interest and is conducted using various methods, including both internal and external evaluation methods. Although there appears to be some disagreement on the best methods to use (for example, see (Sherwin et al. 2012)), it is suggested that the method chosen to evaluate a model should be consistent with the purpose of the model (Ette et al. 2003). An initial evaluation of a model's acceptability may be based on the physiological plausibility of values obtained, as well as on the precision with which the parameters are estimated. The precision of a parameter estimate is based on its relative standard error (RSE) and is generally considered acceptable when it is <30% (CDC/National Center for Health Statistics 2010). The fit of a model is further assessed using multiple graphical tools, as well as through improvements in the objective function value (OFV). An OFV is a value that is being minimised to obtain the best model parameter estimations for the data and, thus, the smaller the OFV, the better the model fit (though one should beware of overfitting the model, such that it is no longer useful beyond the dataset used for development). Commonly, this value is minimised via maximum likelihood estimation and is expressed as $-2 \times \log\text{-likelihood}$ (-2LL)(Mould and Upton 2013). Multiple methods for maximum likelihood estimation exist, with first order conditional estimation (FOCE), Laplace estimation, importance sampling and stochastic approximation expectation-maximization (SAEM) as some of the more common estimation methods used (see (Bauer 2019) for a review of the different estimation methods). When examining the OFV, different initial estimates in the model should be examined, as minimisation may stop at what is referred to as a local minimum, rather than at the true minimum. A local minimum occurs because the slope of the function being evaluated has stopped decreasing for an increment, so the model evaluations stop and the current function parameters are considered the best fit (see Figure 2 for a graphical representation). In such cases, if different function values are used, a greater slope

decrease would be noted until the true (global) minimum is reached. Thus, the examination of different initial values may mean that one avoids the local minimum and the model continues to minimise to the true minimum OFV for the set of given parameters.

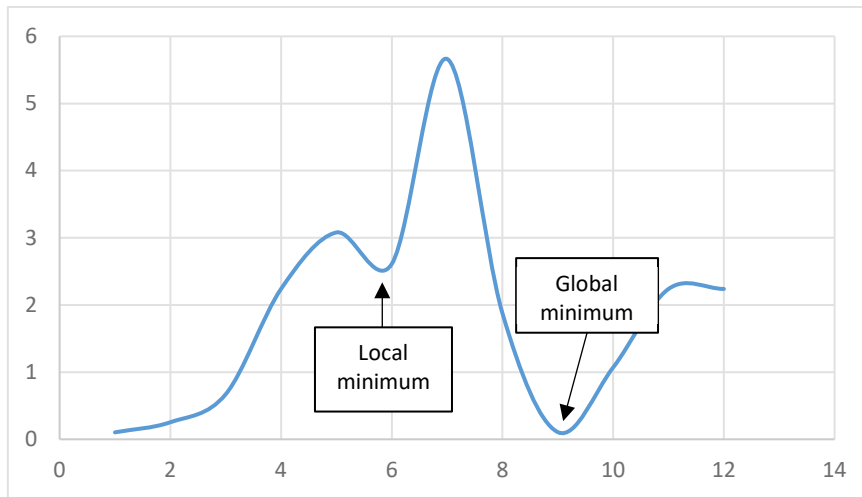


Fig. 2: Illustration of local and global minima. A local minimum is reached when there is a 'dip' in the slope which does not represent the lowest value, while the global minimum is the truly lowest (minimum) value.

With regards to the graphical analyses, a general set of plots that should be used in model evaluation has been proposed by the International Society of Pharmacometrics Model Evaluation Group, along with an assessment of the pros and cons of each evaluation type (Nguyen et al. 2017). Due to the different strengths and weaknesses of the different diagnostic tools, a best practice is to use a combination of methods. In this way, bias, precision, and predictability of the model can be better determined.

The plots used to evaluate the model are termed "goodness-of-fit" or diagnostic plots. Goodness-of-fit plots usually consist of a series of plots examining individual and/or population predictions against the observed data, against associated errors over time, and against associated errors over actual observations (Figure 3).

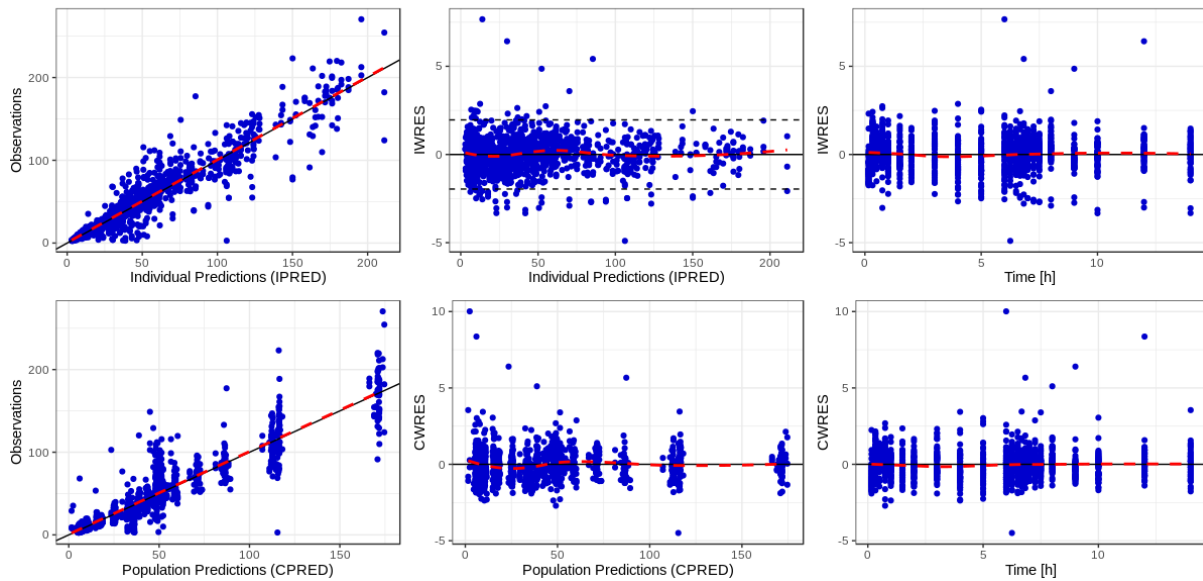


Fig. 3: “Goodness-of-fit”/diagnostic plots for model evaluation. The upper row displays individual model predictions, while the lower row displays population predictions. The predictions are plotted against actual concentrations (first panels), weighted errors over concentrations (second panels), and weighted errors over time (last panels). Blue dots represent actual concentrations, while the red-dashed lines represent smoothing functions using a linear regression (first panels) or a loess smooth (middle and last panels). The black solid lines represent the line of unity (first panels) or the 0 line (middle and last panels). Dashed black lines show the boundaries for ± 1.96 standard deviations. IWRES = individual weighted residuals; CWRES = conditional weighted residuals.

For individual predictions plotted against observations, a good model fit should result in a regression line similar to the line of unity (as in the first upper left panel of Figure 3); the same cannot necessarily be said of the population predictions against observations, as the level of direct association is dependent upon the nature of the processes involved and variability in the model (Karlsson and Savic 2007). The individual or population predictions plotted against the observations can help identify misspecifications in the structural model, although misspecification in the residual error model does not necessarily affect such plots (Nguyen et al. 2017). To evaluate an overall misspecification in structural or residual error model, predictions should be plotted against their weighted residual errors. Examination of these plots should not reveal any evident trends in error dispersion around the line of 0, but rather, errors should be relatively evenly distributed above and below when the model is correctly specified (as in Figure 3). Furthermore, the error associated with individual predictions should have approximately 95% of the data falling within ± 1.96 standard deviations, which indicates a normal distribution of error.

Examination of model estimations against their weighted residual errors should typically not reveal any non-symmetrical error dispersion, as a non-symmetrical dispersion may indicate structural, covariate or residual error misspecification. However, a non-symmetrical dispersion in the population conditional weighted error is not always indicative of a problem with the model, as it may also be an indication of highly nonlinear data or a particularly high inter-individual variability. With individual predictions, inter-individual variability is already accounted for and, therefore, does not influence error dispersion. One caution with using plots of individual predictions against weighted residuals, is that a covariate misspecification cannot be assessed, as it is considered part of the inter-individual variability; thus, both population predictions and individual predictions need to be examined together for a real understanding of potential deficiencies in the model (Nguyen et al. 2017).

The dispersion of errors over model predictions gives an indication of whether there are trends for certain concentrations to be less well fit by the model (e.g. maximum concentration values), but another valuable assessment for model fit is that of the dispersion of errors over time. A trend in deviation from the 0 line may indicate a structural misspecification (e.g. if later time points are systematically increased, it may indicate a missing compartment in the model). Diagnostic plots from a misspecified model (structural misspecification) are depicted in Figure 4. Here, although the regression line for the individual data overlaps with unity, it is clear by the two distinct spreads of the observations compared to the predictions that the data is not being adequately described by the model. Furthermore, in each of the plots of predictions against the weighted residuals, there are evident trends in the scatter of errors around the 0 line. Finally, when looking at the errors over time, there is a clear trend for errors to scatter considerably above the 0 line towards the end of the substance's terminal phase of elimination, suggesting that there may be a compartment missing in the model or that an important covariate has been missed.

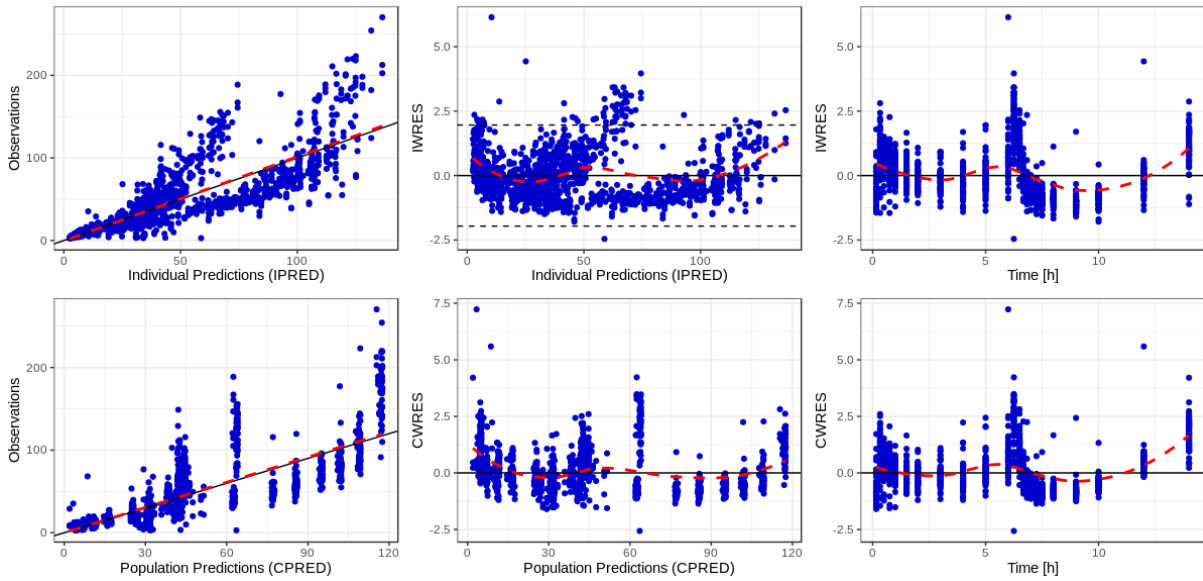


Fig. 4: “Goodness-of-fit”/diagnostic plots for a misspecified model. A clearly distinguishable trend for poor prediction of peak concentrations is noted in the first two panels and is particularly evident for the individual predictions. Predictions plotted against errors over time indicate that the terminal phase is not well captured by the model, as evidenced by the rising trend line. Blue dots represent actual concentrations, while the red-dashed lines represent smoothing functions using a linear regression (first panels) or a loess smooth (middle and last panels). The black solid lines represent the line of unity (first panels) or the 0 line (middle and last panels). Dashed black lines show the boundaries for ± 1.96 standard deviations. IWRES = individual weighted residuals; CWRES = conditional weighted residuals.

A final graphical method that is commonly used for the individual and/or population predictions is one whereby the concentration-time profiles based on model predictions are plotted together with the observed data points. This allows one to determine, for example, particularly problematic individuals for model predictions, as well as to get an overall impression of the fit of the model predictions to the data (see Figure 5). Furthermore, when a “typical” profile (i.e. the population predicted profile) is added, one can determine the extent to which individuals differ overall.

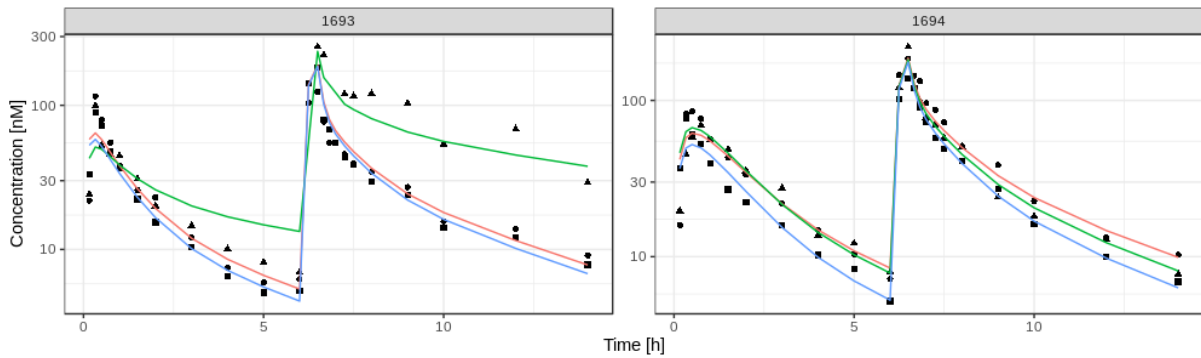


Fig. 5: Individual model predicted concentration-time profiles fit to actual observations. Lines represent the model predictions, while points are the actual observations. Different coloured lines and different shaped points represent different visits; each panel depicts a different subject.

In addition to assessing model misspecifications, graphical inspection can be used to aid in the decision of appropriate relationships to include for explaining inter-individual variability and in describing any relationships between model parameters. This graphical assessment can be carried out using plots of empirical Bayes estimates (EBEs), which are the resulting random effect values. A potential need for covariates in the model may be detected if the histogram of a particular EBE displays multiple peaks and/or if a plot of EBEs against each of the covariates gives an indication of any relationships (Figure 6). Those covariates that appear to be related to the random effects should be tested in the model to examine if an improvement of model fit is observed. With regards to the error model assessment, if the majority of EBEs cluster around the mean of the histogram, with very little spread overall, this may indicate that IIV on this parameter is not needed, as only limited information is apparent at the individual level. Such a phenomenon refers to the shrinkage of a parameter towards the population value, suggesting overfitting of the model. A plot of EBEs against one another allows one to assess the potential correlation between parameters, which should then be built into the model (Figure 6). Thus, these graphical assessments are quite beneficial in ascertaining the most appropriate IIV error models, as well as in identifying important covariates for inclusion in the model.

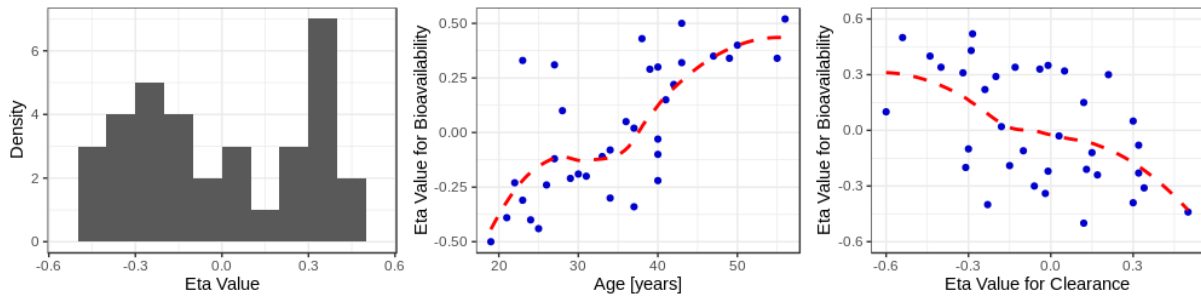


Fig. 6: EBE and covariate relationship plots. The double peak in the histogram suggests that a covariate (e.g. sex) should be added to the model to account for differences in variability. The next two plots display a relationship between age and bioavailability and between the variances for bioavailability and clearance.

Further common model evaluation methods include bootstrapping, cross-validation, case deletion, data-splitting, visual predictive checks (VPCs), and normalised prediction distribution errors (NPDEs). Data-splitting consists of using a portion of the available dataset for model development (usually about 2/3 of the data) and testing the resulting model on the remaining data. Although data-splitting is a commonly used method, when used with small datasets it generally results in biased, overly optimistic results (Steyerberg and Harrell 2016). A slightly more robust method is that of cross-validation, whereby the data are repeatedly split into “training” and “test” sets via resampling methods and an out-of-sample error is generated based on the average of all cross-validation runs (Sherwin et al. 2012). In case deletion, which is a form of cross-validation, each case (for example, an individual subject) is sequentially deleted (only one case deleted per evaluation) from the overall dataset and the influence of each case is then computed based on changes in parameter variables. This can help identify highly influential subjects/cases, as well as helping to determine how robust the model is in the face of potential outliers (Sherwin et al. 2012).

Bootstrapping, VPCs, and NPDEs are all examples of simulation-based tools which are used for internal qualification of a model. Using the original dataset, many simulations (e.g. 1000) are conducted with the final model and the results of the simulated datasets are then compared to the observed values or model-estimated parameters based on the original dataset. With bootstrapping, datasets are created by sampling the original dataset using replacement, with an approximately equal distribution of important characteristics (e.g. proportion of subjects in a particular treatment or of a specific covariate) compared to the original dataset. Confidence intervals (usually 95%) are then computed for each model parameter using the

results of each successfully minimised model run. VPCs provide a visual representation of how well the model describes the actual data used for developing the model (Figure 7).

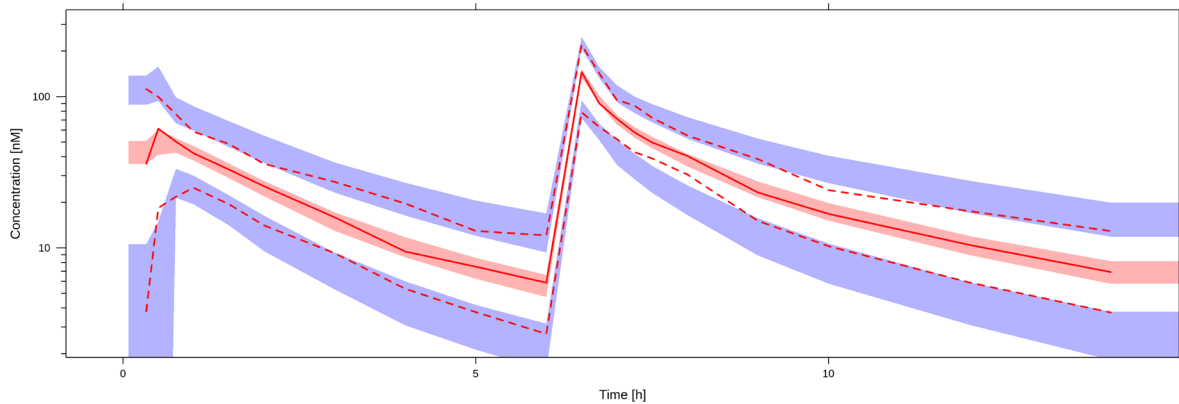


Fig. 7: Visual predictive check. The red solid line depicts the observed median, while the dashed red lines depict the observed 97.5th and 2.5th percentiles. The shaded blue areas represent the 90% confidence intervals for the 97.5th and 2.5th percentiles, based on a large number of simulations from the data, and the red shaded area depicts the 90% confidence intervals of the median.

Although there are a number of ways a VPC can be conducted, currently the more common approach is to use confidence interval VPCs (Nguyen et al. 2017). In this VPC approach, Monte Carlo simulations based on the final model and observed data are conducted and 95% confidence intervals over various relatively equally representative bins (usually binned over time) for the median and for the 97.5th and 2.5th percentiles (or other preferred percentiles) are calculated. If the model describes the data well, then the observed median, 97.5th and 2.5th percentiles of the data should fall within the respective 95% confidence intervals. When a dataset contains large heterogeneity in study design or unbalanced designs, it may be preferential to use a prediction-corrected VPC, which normalises the data to population median values at each of the independent variable (e.g. time) values (Bergstrand et al. 2011). An NPDE is based on the quantile of an observation within its predicted distribution (obtained in the same way as by a VPC); as observation errors are not independent within an individual, both the simulated and observed data are decorrelated (Brendel et al. 2006). When the model provides an adequate description of the data, a normal distribution of prediction discrepancies (i.e. observation quantiles), with a mean of 0 and standard deviation of 1, should emerge.

1.4.3 Review of Available Midazolam Population Pharmacokinetic Models

In order to develop the PopPK model for midazolam under constitutive, inhibitory, and inductive CYP3A conditions, a review of the currently available models will provide the initial framework from which to begin. Of the numerous midazolam PopPK models which have been published, a search of the literature revealed that all are currently based only on basal levels of CYP3A activity. The available PopPK models range from very simple 1- to 2-compartment models with midazolam only, to more complex PopPK-physiological model combinations including midazolam's main metabolite (Brill et al. 2014; Brussee et al. 2018; De Wildt et al. 2003; Nguyen et al. 2016; Tomalik-Scharte et al. 2014; van Rongen et al. 2015; Yang et al. 2018). Of the existing models, multiple were developed specifically for paediatric populations (Ahsman et al. 2010; Brussee et al. 2018; De Wildt et al. 2003; van Groen et al. 2019), where maturation processes may result in drugs impacting enzyme inhibition or induction differently than with adults. Furthermore, paediatric drug development is often limited by sparse sampling, thus, PopPK models are needed to better understand the pharmacokinetics (and pharmacodynamics) of drugs. Other models have been developed for other special populations (Brill et al. 2014; Seng et al. 2014; Swart et al. 2004; van Rongen et al. 2015), for special situations (Hostler et al. 2010; Tomalik-Scharte et al. 2014; Zomorodi et al. 1998), or in anticipation of future model application to DDIs (Nguyen et al. 2016; Yang et al. 2018).

As the majority of midazolam models have been developed for paediatrics, specifically in neonate populations, only a few paediatric models including differing paediatric age ranges will be described here (see Table 1 for an overview of each model).

INTRODUCTION

Tab. 1: Paediatric midazolam population pharmacokinetic models

| Model | Population | Structural model: MDZ | Structural model: metabolite(s) | Error model | Covariates |
|--------------------------|---|---|---|------------------------------------|--|
| (Ahsman et al. 2010) | 20 neonates receiving extracorporeal membrane oxygenation | 2-compartment | 1-compartment (1'-OH MDZ); 1-compartment (glucuronide) | Combined additive and proportional | Bodyweight with all parameters; postnatal age with 1'-OH MDZ clearance |
| (Brussee et al. 2018) | 264 patients, 1-18 years old | 3-compartment + physiological compartments (gut wall, liver, portal vein) | 1-compartment (1'-OH MDZ) + physiological compartments (gut wall, liver, portal vein) | Combined additive and proportional | Bodyweight with volume and intrinsic hepatic and gut wall clearance |
| (De Wildt et al. 2003) | 18 children in intensive care, 2 days - 17 years old | 2-compartment | --- | Combined additive and proportional | --- |
| (van Groen et al. 2019) | 15 children, preterm to 2 years in intensive care | 2-compartment | --- | Combined additive and proportional | Bodyweight with central volume |
| (van Rongen et al. 2015) | 19 overweight or obese 12.5-18.9 year olds | 2-compartment | 1-compartment (1'-OH MDZ); 2-compartment (glucuronide) | Proportional | Excess bodyweight with MDZ peripheral volume |

MDZ = midazolam

The main reasons for PopPK model development were to examine the covariates influencing midazolam exposure and to better understand CYP3A-related metabolism in paediatrics. In the majority of cases, a 2-compartment model was found to best describe midazolam concentrations (Ahsman et al. 2010; De Wildt et al. 2003; van Groen et al. 2019; van Rongen et al. 2015). Metabolite concentrations were best described using a 1-compartment model for 1'-OH midazolam (Ahsman et al. 2010; Brussee et al. 2018; van Rongen et al. 2015) and 1-compartment (Ahsman et al. 2010) or 2-compartment (van Rongen et al. 2015) model for the 1'-OH midazolam glucuronide. A combined additive and proportional error was largely found to be the best error model. Bodyweight was observed to be a significant covariate of volume of distribution (Ahsman et al. 2010; Brussee et al. 2018; van Groen et al. 2019) and/or of clearance and inter-compartmental clearances (Ahsman et al. 2010; Brussee et al. 2018).

Although van Rongen et al. did not find bodyweight in-and-of itself to be a significant covariate, excess bodyweight was a covariate of peripheral volume of distribution for midazolam (van Rongen et al. 2015). Thus, for paediatrics, midazolam models were relatively consistent across populations, with a 2-compartment model for midazolam, a 1-compartment model for the 1'-OH midazolam metabolite, a combined error model, and bodyweight as a covariate of volume of distribution and potentially also clearance.

In adult populations, midazolam PopPK models have also been developed for various purposes, including to better understand CYP3A activity, to examine how certain clinical practices may impact CYP3A substrate pharmacokinetics, to better characterise sources of inter-individual variability in CYP3A activity, and for anticipated use in predicting DDIs. Due to the nature of the populations examined, some of the covariate models which have been used are not applicable for the healthy population being examined in the model under development (e.g. examination of disease status). As such, only potentially relevant factors for a healthy population will be summarised here. The PopPK models of midazolam developed in adults appear to be less consistent than those for children. The structural models best suited to the midazolam data have contained 1-compartment (Tomalik-Scharte et al. 2014), 2-compartment (Hostler et al. 2010; Nguyen et al. 2016; Seng et al. 2014; Swart et al. 2004; Yang et al. 2018), or 3-compartment (Brill et al. 2014; Zomorodi et al. 1998), while those for the 1'-OH midazolam and 1'-OH midazolam glucuronide metabolites have consistently contained 1-compartment (Nguyen et al. 2016; Seng et al. 2014; Tomalik-Scharte et al. 2014). The proportional residual error model has most often been shown to be the most suitable (Brill et al. 2014; Hostler et al. 2010; Tomalik-Scharte et al. 2014; Yang et al. 2018; Zomorodi et al. 1998), although additive (Seng et al. 2014) and combined error models (Nguyen et al. 2016; Swart et al. 2004) have also been used. Multiple covariates have been examined and the influence of these covariates have been mixed. None of Nguyen et al. (Nguyen et al. 2016), Tomalik-Scharte et al. (Tomalik-Scharte et al. 2014), or Zomorodi et al. (Zomorodi et al. 1998) found any covariate effects for the parameters in their models. In contrast, two groups found weight to be a covariate in their models, with Seng et al. finding it to be a covariate of 1'-OH midazolam clearance and volume of distribution (Seng et al. 2014), and Brill et al. finding weight to be a significant covariate of midazolam central and peripheral volumes of distribution (Brill et al. 2014). Only one model found sex to be a significant covariate (Yang et al. 2018), while age was found to be significant covariate of central volume (Yang et al. 2018)

or clearance parameters (Swart et al. 2004). Finally, Seng et al. also examined genotypes and found the CYP3A5*3 to be a significant covariate of midazolam clearance (Seng et al. 2014).

A number of limitations are present within the models reviewed here. First, in the majority of published models, relatively small sample sizes (6 to 32 subjects/patients) have been used (Brill et al. 2014; Nguyen et al. 2016; Seng et al. 2014; Swart et al. 2004; Tomalik-Scharte et al. 2014), although at least two groups used 63 or more subjects during model development (Yang et al. 2018; Zomorodi et al. 1998). Additionally, the population models found in the literature do not include inter-occasion variability, as samples were only taken during one dosing interval. Given the large variability seen with CYP3A activity, it is especially important to account for inter-occasion variability when examining profiles of midazolam given multiple times, as this variability could partly confound the results when examining potential effects of different conditions on midazolam exposure. Given the purposes that most other models have been developed for until now, this second point is likely not too critical and the models have suited the purpose they were designed for. Despite the limitations noted here, the published models provide a starting point for developing a midazolam model to examine DDI liabilities.

1.5 Aim of Thesis

The aim of this thesis project is to establish a midazolam microdosing approach for assessing CYP3A DDI liability in early clinical development, which reduces burden to subjects and/or patients while simultaneously giving an earlier assessment of true DDI liability. To further increase the feasibility of the approach, a limited sampling scheme is examined to determine the performance and robustness of this method in predicting the presence of DDIs. Finally, the ability of a PopPK model to assess the presence of a CYP3A-related drug-drug interaction is evaluated, both with full PK profiles and with limited sampling, and specific cut-points for exposure parameters are assessed for identification of the presence of inhibition and/or induction of CYP3A.

2. MATERIALS AND METHODS

2.1 Implementation of Midazolam Microdosing

Three monocenter early clinical studies in healthy male volunteers, all sponsored by Boehringer Ingelheim Pharma GmbH & Co. KG, Germany, were conducted for potential drug

candidates that displayed CYP3A liability signals *in vitro*. Specifically, the three compounds were all potential perpetrators of CYP3A4 induction and two of the compounds showed potential for CYP3A4 inactivation. CYP3A4 liability thresholds, as determined in *in vitro* assessments, are listed in Table 2, along with the constants used to calculate the respective thresholds. If the maximum concentrations of the test substances exceeded these thresholds, a DDI was expected. In the case of inactivation, an increase in midazolam concentrations would be expected following multiple dosing of the test substance, while induction would be expected to result in lower midazolam concentrations following multiple dosing of the test substance. When both inactivation and induction were detected *in vitro*, until both thresholds were exceeded, the process with the lower threshold (in this case it was always inactivation) would be expected to influence the midazolam concentrations; however, once both thresholds were exceeded, it would be expected that both processes would influence CYP3A activity. Thus, it is possible that the combination of processes would negate each other *in vivo*, but this is difficult to determine based on *in vitro* data. Furthermore, the authority guidelines specifically state that the mechanistic models given are to be used separately for reversible inhibition, irreversible inhibition, and induction, thus, regardless of the expected combined influence on CYP3A activity, clinical studies would need to be conducted. Finally, for Compound C, the ability to assess inhibition *in vitro* was limited by the compound's poor solubility, as well as for a propensity to bind to certain materials. Thus, CYP3A inhibition potential was also assessed *in vivo*, with the expectation that if Compound C was an inhibitor, an increase in midazolam exposure would be seen following a single dose of active substance.

IMPLEMENTATION OF MIDAZOLAM MICRODOSING

Tab. 2: CYP3A4 Drug-Drug Interaction Thresholds Based on *In Vitro* Experiments, and Achieved Concentrations *In Vivo*

| | EC ₅₀ [nM] | E _{max} [fold] | CYP3A4 Induction [nM] | k _{inact} /K _i [min ⁻¹ ·nM ⁻¹] | CYP3A4 Inactivation [nM] | gMean C _{max,ss} [nM] |
|------------|--------------------------|----------------------------|-------------------------------------|--|--------------------------------|--|
| Compound A | 7100 | 14 | C _{max} ≥ 130 | 0.0130/3210 = 4.05x10 ⁻⁶ | C _{max} ≥ 4.60 | 1840 ^{a,b} , 2260 ^{a,b} |
| Metabolite | 34800 | 11 | C _{max} ≥ 110 | 0.00666/4010 = 1.66x10 ⁻⁶ | C _{max} ≥ 2.70 | 513 ^{a,b} , 680 ^{a,b} |
| Compound B | 230 | 2.26 | C _{max} ≥ 12.0 | 0.140/28800 = 4.85x10 ⁻⁶ | C _{max} ≥ 2.95 | 19.8 ^{a,b} , 41.8 ^{a,b} , 43.4 ^{a,b} , 52.6 ^{a,b} |
| Compound C | 140 | 8.3 | C _{max} ^c ≥ 448 | | | 138, 225, 383, 843 ^a , 1150 ^a |

^aConcentrations exceeded the *in vitro* determined thresholds for producing CYP3A induction, thus, a decrease in midazolam concentrations when combined with the active substance would be expected;

^bConcentrations exceeded the *in vitro* determined thresholds for producing CYP3A inactivation, thus, an increase in midazolam concentrations when combined with the active substance would be expected

^cBased on ≥2-fold increase in mRNA criteria (EMA-CHMP 2012 Jun)

Induction potential was determined using FDA guidelines from 2012(US-FDA 2012 Feb), where R₃<0.9 rather than <0.8 was required for a DDI study to be conducted.

In order to avoid conducting dedicated DDI studies, microdosing was seen as a promising tool for combining with early clinical studies. Thus, to assess the CYP3A DDI liability *in vivo*, midazolam microdosing was incorporated in studies that were primarily designed to assess multiple rising doses (MRD) of the test compounds. As microdoses should result in concentrations below pharmacologically active levels, it was not expected to interfere with the regular investigation of the test compounds.

The studies were carried out at CTC North GmbH & Co. KG, Hamburg, Germany (Compound A) and at CRS Clinical Research Services Mannheim GmbH, Germany (Compounds B & C). All procedures were performed in compliance with the respective clinical trial protocols, and in accordance with the principles of the Declaration of Helsinki, the International Conference on Harmonization Good Clinical Practice (as defined in the International Conference on Harmonization E6 Guideline for Good Clinical Practice), and in accordance with applicable regulatory requirements. Approval by the appropriate Ethics Committees (CTC North: Ethics Committee of the Medical Council [Ethikkommission bei der Ärztekammer], Hamburg, Germany; CRS: Ethics Committee of the State Medical Council of Baden-Württemberg

[Ethikkommission bei der Landesärztekammer Baden-Württemberg], Stuttgart, Germany) and the Federal Institute of Drugs and Medical Devices (BfArM, Bonn, Germany) was obtained prior to conducting any of the trials.

2.1.1 Subjects

The studies consisted of 24 (Study 1), 40 (Study 2), and 50 (Study 3) healthy male subjects. All subjects provided written informed consent prior to participation in the studies. For inclusion in the studies, subjects were required to be both mentally and physically healthy, as ascertained by a complete medical history, physical examination, vital signs (blood pressure, pulse rate), 12-lead ECG, and clinical laboratory tests. Subjects were between the ages of 18 and 50 and within a healthy Body Mass Index range of 18.5 to 29.9 kg/m².

2.1.2 Study Design

All three studies were multiple rising dose studies that were placebo controlled and randomised within dose group (i.e. dose levels were known, but not if it was active drug or placebo). A 75 ug dose of midazolam was administered orally as a solution in a fixed sequence: alone (baseline/reference treatment; R) and in the presence of single and/or multiple doses of each of the test compounds (test treatment; T). The days on which midazolam profiles were obtained in the presence of active compounds were based on the liability signals obtained *in vitro* or on uncertainties due to limitations in the ability to assess *in vitro*. All test compounds had reached steady state before Day 14/17. Further details for each study are given below:

Study 1 (ct.gov: NCT03279978; EudraCT: 2017-001653-14): For Compound A, midazolam profiles were obtained on Days -1, 3 and 14 for the two highest doses in the study. In total, 6 subjects received midazolam+placebo (3 per dose group) and 18 subjects received midazolam+Compound A (9 per dose group).

Study 2 (ct.gov: NCT03325712; EudraCT: 2017-003269-85): For Compound B, midazolam profiles were obtained on Days -1 and 17 for the 4 highest tested doses. In total, 8 subjects received midazolam+placebo (2 per dose group) and 32 received midazolam+Compound B (8 per dose group).

Study 3 (ct.gov: NCT03754959; EudraCT: 2018-000389-12): For Compound C, midazolam and 1'-OH midazolam profiles were obtained on Days -1, 1, and 14 for all 5 tested dose groups. The additional characterisation of the metabolite 1'-OH midazolam was implemented both due to the development of an assay which measured both midazolam and 1'-OH midazolam analytes, as well as to obtain further information regarding the metabolism of midazolam. A total of 10 subjects received midazolam+placebo (2 per dose group) and 40 received midazolam+Compound C (8 per dose group).

2.1.3 Study Conduct

2.1.3.1 Preparation of Study Medication

All midazolam microdoses were prepared from commercially available intravenous formulations containing 5 mg midazolam per 5 mL (Midazolam-ratiopharm® 5 mg/ 5 ml Injektionslösung). The oral solutions were prepared by transferring 1 mL of Midazolam-ratiopharm® via a 2 mL syringe into a glass beaker; thereafter, 19 mL of 0.9% isotonic saline solution (Fresenius, Germany) was also transferred into the glass beaker via a 20 mL syringe. The resulting solution was gently swirled in the beaker for 1 minute; the final concentration of the diluted midazolam solution was 50 µg/mL. Any potential loss of substance due to adsorption was excluded beforehand and chemical stability of the compound over 24 hours was assessed in experiments prior to study conduct.

Test compounds and placebo treatments were administered as tablets according to the available dose strengths.

2.1.3.2 Drug Administration and Blood Sampling

Subjects were orally administered 1.5 mL (75 µg) of the diluted midazolam solution via the syringe used for drawing up the solution, along with 240 mL of water, following a standard continental breakfast. Midazolam administration occurred at approximately the same time each day (between 7:30 and 9:30 AM). The continental breakfast was served 30 min before midazolam administration and was to be completely consumed prior to drug administration. On test treatment days, midazolam and the test compound or midazolam and placebo were administered together.

Subjects were not to lie down (except during medical examination) or sleep for the first 2 h following dose administration and no food was allowed for 4 h following dosing. Meals on study days consisted of standardised meals provided by the study center. Alcoholic beverages were not allowed starting at least 7 days prior to study participation up until after the last PK sample of the trial. Methylxanthine-containing beverages were not allowed from 4 h before until 4 h following trial drug (midazolam and/or test substance) administration.

Concomitant medications, as well as foods and herbal supplements known to modulate CYP3A activity (e.g. St. John's Wort, grapefruit, Seville oranges, etc.) were not allowed for the duration of the trials.

For each midazolam plasma concentration-time profile, 4.0 mL of blood was drawn from an antecubital or forearm vein. Samples were drawn at each of the following time points:

Study 1: Day -1, Day 3 and Day 14; pre-dose, 0.25, 0.5, 1, 2, 2.5, 3, 4, 6, 8 h

Study 2: Day -1, Day 17; pre-dose, 0.25, 0.5, 1, 1.5, 2, 2.5, 3, 4, 6, 8 h

Study 3: Day -1, Day 1, Day 14; pre-dose, 0.17, 0.5, 1, 2, 2.5, 3, 4, 6, 8 h

The EDTA-anticoagulated blood samples were centrifuged for about 10 minutes at 2000 g to 4000 g and at 4 to 8°C. Plasma was stored at -20°C or lower until bioanalysis.

As Katzenmaier et al. (Katzenmaier et al. 2010; Katzenmaier et al. 2011) have previously found a 4 time point sampling scheme (2, 2.5, 3, and 4 h post-dose) to be highly predictive of overall CYP3A activity, these time points were included in all three studies. As such, the predictability and robustness of the limited sampling schedule during induction and/or inhibition or inactivation of CYP3A could be examined.

2.1.3.3 Analytical Assays

Studies 1 and 2: Midazolam plasma concentrations were quantified in the Department for Drug Metabolism and Pharmacokinetics at Boehringer-Ingelheim (Biberach, Germany) using a validated high performance liquid chromatography-tandem mass spectrometry (HPLC-MS/MS) assay. The lower limit of quantification for the assay was 3.00 pmol/L (0.00097731 ng/mL), with two calibration ranges tested (3.00-300 pmol/L and 3.00-3000 pmol/L).

Study 3: Midazolam and 1'-OH midazolam concentrations were quantified at Nuvisan (Neu-Ulm, Germany) using a validated LC-MS/MS assay. The lower limit of quantification for the assay was 9.21 pmol/L (0.003 ng/mL) for midazolam, with a calibration range of 9.21-9210 pmol/L, and 8.78 pmol/L (0.003 ng/mL) for 1'-OH midazolam, with a calibration range of 8.78-8780 pmol/L.

2.1.3.4 Pharmacokinetic Analysis and Statistical Evaluation

Pharmacokinetic parameters were calculated using Phoenix WinNonlin version 6.3 or later (Certara USA Inc., Princeton, NJ, USA) and the PKNCA package for R (Buckeridge et al. 2015). The parameters used for the assessment of a drug-drug interaction with midazolam were area under the concentration-time curve (AUC) from 0 extrapolated to infinity ($AUC_{0-\infty}$), derived using a linear up, log down method and maximum measured concentration (C_{max}), with apparent clearance (CL/F) included as an exploratory DDI assessment measure. AUC from 0 to the last quantifiable time point (AUC_{0-tz}) was assessed descriptively. AUC from time 2 h to 4 h (AUC_{2-4}) and time to maximum concentration (t_{max}) were also calculated and provided descriptively. Geometric means (gMeans) and geometric coefficients of variation (gCVs) were calculated for all parameters.

Statistical analyses were conducted using SAS version 9.4 (SAS Institute Inc., Cary, NC, USA) and R 3.5.2 (R Core Team 2018). The potential effect of each of the test compounds on midazolam was assessed using an analysis of variance (ANOVA) model on the logarithmic scale. Estimates were back-transformed following analysis. For each study, 'Time Point' was a fixed effect and 'Subjects' was a random effect. Potential DDI effects were estimated by the gMean ratios of $AUC_{0-\infty}$ and C_{max} when given with the BI compound compared to the reference (midazolam alone); for Compound A and Compound C, this was done separately for Day 1/3 and Day 14; two-sided 90% confidence intervals (CIs) were calculated based on residual error. Analyses were conducted separately for each individual dose group. A DDI result was considered positive if, based on FDA and EMA cutoffs, point estimates indicated at least an increase to 125% from baseline/reference (inhibition/inactivation) or a decrease to 80% or less of the baseline/reference concentrations (induction) (EMA-CHMP 2012 Jun; US-FDA 2020a). A descriptive assessment of the number of subjects exceeding the thresholds per parameter was also provided.

For the exploratory analyses comparing AUC_{2-4} and $AUC_{0-\infty}$ test-to-reference ratios, i.e. comparing the ratio of $(AUC_{2-4, \text{Day } 1/3 \text{ or } 14/17}) / (AUC_{2-4, \text{Baseline}})$ to $(AUC_{0-\infty, \text{Day } 1/3 \text{ or } 14/17}) / (AUC_{0-\infty, \text{Baseline}})$, a linear mixed effects model was performed on log-transformed AUC values for each study and overall. 'AUC-type', 'Time Point' (Baseline and Day 1/3 or Day 14/17) and the interaction thereof were fixed effects and 'Subjects' was a random effect. When applicable, test treatment days (Day 1/3 or Day 14) were assessed separately.

The two-sided 90% CI was constructed using standard errors and degrees of freedom from the model. The back-transformed point estimates and confidence intervals represent the estimate of comparability. Perfect comparability holds true if the point estimate equals one.

2.2 Midazolam and Metabolite Population PK Model Development

Non-linear mixed-effects modeling was employed for the development of a parent-metabolite population PK model for midazolam (metabolite: 1'-OH midazolam). The purpose of the model was to determine which factors may be most relevant for DDI predictability and to allow for estimation of PK parameters/presence of DDIs using a sparse/limited sampling method. Model development was conducted in a stepwise manner, whereby separate base models were first developed for midazolam and for 1'-OH midazolam. The adopted base models were then combined into one composite model and the resulting model was further refined. During initial development, only the first midazolam baseline profile per subject was used. For the midazolam only model and for the composite model, the remaining profiles were included and the inter-occasion variability (IOV) was estimated. Once the appropriate structural and statistical models were ascertained, the covariates of age, weight, and sex were examined for influence on any of the model parameters. Finally, covariance between model parameters was examined and any relationships were incorporated into the model.

Previously gathered data regarding midazolam and 1'-OH midazolam concentrations (when administered alone versus in the presence of a CYP3A modulator) were used together with data from the prospective studies described in Section 2.1 to qualify and refine the midazolam and metabolite models. All data were anonymised prior to data analysis.

2.2.1 Datasets

Midazolam and 1'-OH midazolam data were available from 11 previously conducted trials. Of the 11 studies, 7 which included full midazolam profiles were used for model development (development set), while the remaining 4 were used as an external validation set, particularly for examination of the model's ability to detect DDIs based on limited sampling. The studies had various purposes, including examining CYP3A activity following different doses of midazolam alone, as well as in the presence of known inhibitors or inducers of CYP3A. A description of the available conditions, doses, and profile types for each of the studies is displayed in Table 3. Plasma profiles were obtained following both oral and iv administration of midazolam. Plasma concentrations were measured using validated ultra (Burhenne et al. 2012) or high (Quintela et al. 2004) performance liquid chromatography–tandem mass spectrometry methods. The lower limits of quantification ranged from 50 fg/mL to 0.525 ng/mL for midazolam and from 250 fg/mL to 0.550 ng/mL for 1'-OH midazolam.

Tab. 3: Model Dataset Characteristics

| Study | MDZ Alone | MDZ + Inhibitor | MDZ + Inducer | MDZ Doses | Route(s) | Profile Type | Reference |
|--------------|------------------|------------------------|----------------------|----------------------------------|-----------------|---|--|
| K119* | X | X (RTV) | | 4 mg + 2 mg | po+iv | Full: 25 samples/subject per treatment arm | (Hafner et al. 2010) |
| K155* | X | | X (EFV) | 3 mg | po | Full: 12 samples/subject per treatment arm | (Bayer et al. 2009) |
| K169* | X | | | 4 mg + 2 mg | po+iv | Full: 23 samples/subject per treatment arm | (Fetzner et al. 2011) |
| K257* | X | X (VCZ/RTV) | | 3 mg | po | Full: 13 samples/subject per treatment arm + Limited sampling | (Katzenmaier et al. 2011) |
| K380* | X | X (VCZ) | | 1 ug, 1 mg (iv); 3 ug, 3 mg (po) | iv&po | Full: 15 samples per subject/iv treatment arm; 14 samples per | (Hohmann et al. 2015; Hohmann et al. 2016) |

MODEL DEVELOPMENT

| | | | | | subject/po treatment arm | |
|-------|---|----------|---|-------|--|----------------------------|
| K194* | X | | 4 mg + 2 mg | po+iv | Full: 23 samples/subject per treatment arm | (Mikus et al. 2017) |
| K345* | X | X (keto) | 1 ug, 100 ug, 1 mg, 3 ug, 30 ug, 3 mg | po | Full: 14 samples/subject per treatment arm | (Halama et al. 2013) |
| K292 | X | X (keto) | 3 mg | po | Limited = 4 samples per subject/treatme nt arm | (Ziesenitz et al. 2015) |
| K293 | X | X (SJW) | 3 mg | po | Limited = 4 samples per subject/treatme nt arm | (Fuchs et al. 2013) |
| K342 | X | X (RTV) | 3 mg | po | Limited = 4 samples per subject/treatme nt arm | (Eichbaum et al. 2013) |
| K363 | X | X (RTV) | 100 ug | po | Limited = 4 samples per subject/treatme nt arm | (Stoll et al. 2013) |

*Used for model development

EFV = efavirenz; keto = ketoconazole; MDZ = midazolam; RTV = ritonavir; SJW = St. John's Wort; VCZ = voriconazole; iv = intravenous dosing; po = *per os* (oral) dosing.

2.2.2 Software

Models were developed using NONMEM 7.3 (ICON Development Solutions, Ellicott City, MD). The ADVAN6 subroutine was used and models were fit using the first-order conditional estimation with interaction between inter- and intra-individual error (FOCE-I) method. NONMEM outputs and plot generation were processed in RStudio using R version 3.5.2 ((R Core Team 2018) and Pearl-speaks-NONMEM (PsN; psn.sourceforge.net). The 'mrgsolve' package for R (Baron et al. 2015) was used for simulating profiles based on limited sampling strategies.

2.2.3 Base Midazolam Model Development

Concentrations used in the midazolam datasets for model development were expressed in nmol/L, while doses were converted to nmol doses. The molecular weight of midazolam (325.77 g/mol) was used in the transformation of concentrations and doses. Doses ranged from 1 ug (3.0697 nmol) to 4 mg (12279 nmol) and were administered both orally and via iv infusion.

As previous midazolam models have described midazolam using 1-, 2- and 3-compartment models, all were tested during model development. Models were examined using a first-order absorption process (oral administration) with linear elimination. Given the rapid absorption time of midazolam, no lag time or transit compartments were assessed. Bioavailability, absorption rate constant (k_a), compartment volumes, inter-compartmental clearance, and total midazolam clearance were all estimated in the models.

Appropriateness of the models was evaluated based on physiological plausibility, the OFV, and goodness-of-fit plots; a final evaluation of the chosen model was assessed employing a VPC.

2.2.4 Base 1'-OH Midazolam Model Development

As with midazolam, concentrations in the dataset for 1'-OH midazolam model development were expressed in nmol/L and doses in nmol. Since 1'-OH midazolam was not given directly, nmol doses were based on the molecular weight of midazolam, while concentrations of 1'-OH midazolam were converted based on its own molecular weight (341.77 g/mol).

As the majority of previously developed midazolam models have described 1'-OH midazolam data with a 1-compartment model, the initial assessment of the base 1'-OH midazolam model included use of a 1-compartment model, followed by assessment of 2-compartment and 3-compartment models, as appropriate. A dual first-order absorption model was evaluated, with one 'absorption' compartment representing the pre-systemic and systemic metabolism following oral administration, and the second 'absorption' compartment representing systemic metabolism following iv infusion of midazolam. In order to account for any potential lag in the presence of metabolite (due to the need for midazolam to first be absorbed/present in systemic circulation and then metabolised), models were also tested with a lag time on the second 'absorption' compartment or with transit compartments between the second

'absorption' compartment and the central metabolite compartment. Linear elimination was assumed for all models tested.

Parameters for availability of metabolite, rate of metabolism, compartment volumes, inter-compartmental clearance, and metabolic clearance were estimated. Model evaluation was based on the same criteria previously described.

2.2.5 Statistical Models

A log-normal distribution was assumed for all pharmacokinetic parameters. Random effects for inter-individual variability (IIV) were modeled exponentially. Initially, random effects for all parameters were examined and any effects smaller than 0.001 or leading to the model not minimising were removed from the model.

Residual unexplained variance (RUV) was assessed in the separate midazolam and 1'-OH midazolam base models using additive, proportional, and combined additive and proportional error models. Additionally, as more noise tends to be apparent in earlier sampling time points compared to later time points, residual error was further examined by splitting the error term into early/late time points, referred to by Karlsson, Beal and Sheiner as a 'Two-Step' error model (Karlsson et al. 1995). As suggested, the split was chosen such that the 'early' error term described the majority of the main absorption phase for both midazolam and 1'-OH midazolam, while the 'late' error term was meant to describe the disposition of the profiles. The error model that best described the data (based on estimated values, OFVs and goodness-of-fit plots) was retained for use in the composite model.

2.2.6 Composite Model

The adopted base structural and statistical models for midazolam and 1'-OH midazolam were combined and fraction of midazolam metabolised (f_m) to 1'-OH midazolam was added to the model. As midazolam is eliminated almost entirely by metabolism, the f_m was fixed to 1. The composite model was then evaluated based upon the same criteria as for each of the base models. Once the structural and statistical models were obtained, a covariate analysis for the model was investigated, followed by an examination of covariance within the model parameters.

Information was available for all subjects regarding age, weight and sex. Potential relationships with these covariates were first examined graphically; if correlations between any of the covariates and the model parameters were apparent, p-values were calculated and any covariate correlated with a $p < .01$ was added individually to the model. In order to be retained in the model, a drop in OFV of at least 3.84 points (corresponding to $p < .05$) was required, along with adequate precision in the estimation of the effect, the disappearance of a correlation between errors for the covariate and affected model parameter, along with a noticeable improvement in model fit based on model diagnostics.

The covariance of model parameters was assessed by plotting IIVs against each other and assessing statistical significance of any apparent correlations. As for the covariates, a $p < .01$ was required for inclusion in the model, along with a decrease in OFV and adequate precision ($RSE < 50\%$) for the estimation of the covariance. The final model was considered well-described if the values were physiologically plausible, if residual standard errors were $< 30\%$ for all model parameters, if individual and population predicted vs. observed values were relatively evenly dispersed around the unity line, if weighted residual errors (both individual and population) were generally evenly distributed around 0, and if there were no trends (e.g. considerable increase in errors for elimination phase) for inadequate description of the model based on weighted residuals over time. The final model was subsequently assessed using a visual predictive check, ensuring that the median, 2.5th and 97.5th percentiles based on the model were within or close to the 95% CIs predicted by the model following 1000 samplings of the original dataset.

2.2.7 Model Testing for Drug-Drug Interactions

Both the final adopted midazolam model and the final adopted composite model were evaluated for their ability to describe CYP3A drug-drug interaction presence through the addition of the inhibition and induction treatment arms into the dataset. Model parameters were fixed and treatment was added as a covariate on F (bioavailability), clearance (CL for midazolam only model; Q_{met} and CL_{met} for the composite model), and k_{met} (rate of pre-systemic metabolism; only present in composite model). If the resulting model did not provide an adequate description of the inhibition and induction data, further plausible parameters were examined for changes due to treatment effect.

2.2.7.1 *Assessment of Cut-points*

If the inhibition and/or induction data were well-described by the composite model and/or the midazolam only model, a further evaluation of the model parameters was undertaken. In this evaluation, the R package 'OneR' was used to determine the parameter that was best able to distinguish between treatment conditions (induction, inhibition, midazolam alone). The 'OneR' package applies a simple rule based on the One Rule Machine Learning classification algorithm (Holte 1993) (also described as a 1-level decision tree) to determine parameter cut-points to distinguish each treatment category for each of the various model parameters. The percent of values assigned to the correct treatment, based on the cut-points, are output, along with a more detailed breakdown of the predicted versus observed category for the parameter with the highest accuracy.

2.2.8 **Limited Sampling Testing**

As a final assessment of the adopted composite model and the final midazolam model, limited profiles from both midazolam alone and midazolam administered with an inhibitor or an inducer were simulated. This was done both by using the full profile data and removing all but the appropriate time points (e.g. 2, 2.5, 3, and 4 h), and by using the data in studies where only a limited number of samples were obtained. Predictions were then compared to actual observations through a visual predictive check.

3. **RESULTS**

3.1 **Midazolam Microdosing Implementation**

Midazolam microdosing was accepted by health authorities and successfully employed in all three early clinical studies. Administration instructions were adapted following the first study completed, as some difficulty was encountered with drawing up the midazolam solution for administration to the subjects. Consequently, a blunt steel-tipped needle was used to help with drawing the solution into the syringe for all subsequent studies. All post-dose concentrations of midazolam following microdosing were quantifiable and, thus, AUC and C_{\max} values could be accurately determined. For 1'-OH midazolam (Study 3 only), concentrations were quantifiable by no later than 30 min post-dose (the second post-dose sampling time) and remained quantifiable for the remainder of the sampling interval. The results of the

individual midazolam assessments from the three clinical studies are presented in the following sections.

3.1.1 Study 1

In Study 1, midazolam was administered at baseline, as well as on two separate days to assess potential inactivation of CYP3A (Day 3) or induction of CYP3A (Day 14) by Compound A. Twenty-four healthy male subjects, aged 19 to 43 years (2 Asian, 2 Black/African American), underwent midazolam microdosing during the two highest dose groups (12 per dose group). All subjects completed the study. On the baseline day and on Day 3 of Compound A/placebo dosing, all midazolam pre-dose concentrations were below the lower limit of quantification (BLQ). On Day 14 of Compound A/placebo dosing, 3 subjects (1 in placebo group, 2 in 400 mg Compound A dose group) had pre-dose concentrations above BLQ. However, these concentrations were still <5% of the individual C_{max} values and, thus, were included as-is in all analyses.

Geometric mean midazolam plasma concentration-time profiles at baseline and in the presence of the test compound (combined over all dose groups) or placebo are depicted in Figure 8. Descriptive statistics are presented in Appendix Table A1.

The $C_{max,ss}$ values of the test compound were above the potentially clinically relevant DDI thresholds (predicted AUC ratio ≥ 1.25 for inactivation or predicted AUC ratio ≤ 0.80 for induction) determined *in vitro* for the dose groups tested with midazolam microdosing, both for parent substance and metabolite (see Table 2). Thus, both inactivation and induction of CYP3A were expected, with inactivation expected to be most apparent at Day 3, while induction would likely have reduced the influence of inactivation by Day 14.

A minor increase in concentrations following treatment on Days 3 and 14 can be seen in the concentration-time profiles (Figure 8), as well as in the PK parameters (Appendix Table A1). This same trend was not observed for subjects receiving placebo. Median time to maximum concentrations was 0.75-1.00 h post-dose. Inter-individual variability in parameters was in a similar range for subjects treated with Compound A and those treated with placebo.

Statistical analyses of the adjusted geometric mean ratios of midazolam administered following 3 days of dosing of Compound A compared with administration alone, as well as for

MIDAZOLAM MICRODOSING RESULTS

administration following 14 days of Compound A dosing compared with administration alone are displayed in Table 5. Point estimates of the $AUC_{0-\infty}$ gMean ratios ranged from 108.3%-127.1%, while those for C_{max} ranged from 110.2%-123.9%. The 90% CIs for C_{max} were mostly above 100%, except for on Day 3 of dosing in the 400 mg dose group, where CIs for C_{max} minimally exceeded 125% at the upper limit. For the 200 mg dose group, $AUC_{0-\infty}$ 90% CIs were completely above 100%, while for the 400 mg dose group, the 90% CIs included 100%. Point estimates for CL/F ranged from 79.5%-99.7%. The 90% CIs for CL/F contained 100% for both the placebo and 400 mg dose groups, although for the 200 mg dose groups, the range lay completely below 100%; this minor decrease in clearance is consistent with the minor increase in exposure seen for $AUC_{0-\infty}$. As only one parameter for on treatment arm exceeded the cut-off of 1.25 (127.1% for $AUC_{0-\infty}$) for a weak inactivator, Compound A was not considered to relevantly modulate CYP3A activity.

Looking at the individual subjects, it is noteworthy that based on the often used cut-offs of 1.25 and 0.80, even in the placebo group individual subjects would still be classified as having a DDI (33.3%-50% of subjects). Specifically, the C_{max} parameter consistently resulted in the highest number of subjects being classified as having inhibition of CYP3A, while $AUC_{0-\infty}$ and CL/F tended to have fewer subjects classified as having a DDI, at least on Day 3. When subjects exceeded the thresholds, the direction of DDI was inconsistent for $AUC_{0-\infty}$ and CL/F.

MIDAZOLAM MICRODOSING RESULTS

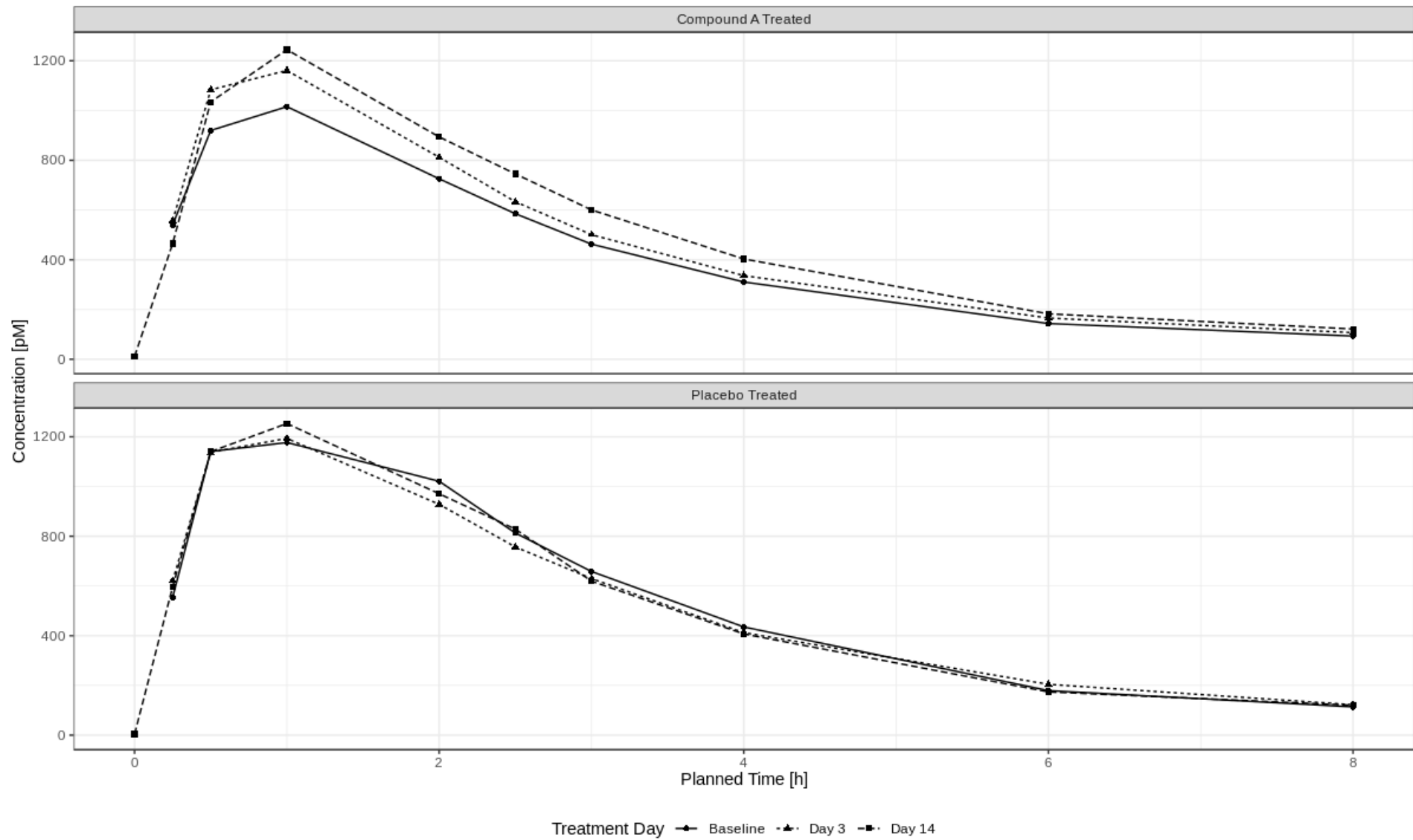


Fig. 8: Geometric mean midazolam concentration-time profiles for Baseline, Day 3, and Day 14 with either Compound A or placebo.

MIDAZOLAM MICRODOSING RESULTS

Tab. 5: Adjusted by-treatment geometric mean ratios of a single dose of midazolam administered alone (R) compared with administration following multiple dosing (Days 3 and 14) of Compound A (T) – Study 1

| PK parameter | MDZ + Compound A/Placebo Test (T) | | | MDZ alone Reference (R) | | 90% Confidence interval (%) | | | Number of subjects with DDI classification (INH,IND) |
|------------------------------|-----------------------------------|---|-------|-------------------------|-------|-----------------------------|-------------|-------------|--|
| | N | n | gMean | n | gMean | Ratio T/R (%) | Lower limit | Upper limit | |
| Placebo (T0) | | | | | | | | | |
| AUC _{0-∞,3} [pM·h] | 6 | 6 | 4605 | 6 | 4550 | 101.2 | 90.4 | 113.3 | 0,0 |
| C _{max,3} [pM] | 6 | 6 | 1315 | 6 | 1234 | 106.5 | 87.5 | 129.6 | 2,1 |
| CL/F ₃ [L/h] | 6 | 6 | 50.4 | 6 | 51.0 | 98.7 | 88.4 | 110.3 | 0,0 |
| AUC _{0-∞,14} [pM·h] | 6 | 6 | 4598 | 6 | 4550 | 101.1 | 83.5 | 122.3 | 1,1 |
| C _{max,14} [pM] | 6 | 6 | 1393 | 6 | 1234 | 112.9 | 96.8 | 131.5 | 2,0 |
| CL/F ₁₄ [L/h] | 6 | 6 | 50.9 | 6 | 51.0 | 99.7 | 82.2 | 120.8 | 1,1 |
| 200 mg Compound A (T1) | | | | | | | | | |
| AUC _{0-∞,3} [pM·h] | 9 | 9 | 4322 | 9 | 3717 | 116.3 | 107.7 | 125.5 | 2,0 |
| C _{max,3} [pM] | 9 | 9 | 1313 | 9 | 1060 | 123.9 | 106.9 | 143.5 | 4,0 |
| CL/F ₃ [L/h] | 9 | 9 | 54.2 | 9 | 62.7 | 86.4 | 80.0 | 93.4 | 1,0 |
| AUC _{0-∞,14} [pM·h] | 9 | 9 | 4726 | 9 | 3717 | 127.1 | 113.8 | 142.0 | 3,0 |
| C _{max,14} [pM] | 9 | 9 | 1265 | 9 | 1060 | 119.4 | 108.5 | 131.3 | 3,0 |
| CL/F ₁₄ [L/h] | 9 | 9 | 49.9 | 9 | 62.7 | 79.5 | 70.9 | 89.2 | 3,0 |
| 400 mg Compound A (T2) | | | | | | | | | |
| AUC _{0-∞,3} [pM·h] | 9 | 9 | 3887 | 9 | 3588 | 108.3 | 97.4 | 120.6 | 2,1 |
| C _{max,3} [pM] | 9 | 9 | 1238 | 9 | 1123 | 110.2 | 95.3 | 127.6 | 3,1 |
| CL/F ₃ [L/h] | 9 | 9 | 59.8 | 9 | 64.9 | 92.1 | 82.8 | 102.3 | 1,1 |
| AUC _{0-∞,14} [pM·h] | 9 | 9 | 4270 | 9 | 3588 | 119.0 | 99.9 | 141.8 | 4,0 |
| C _{max,14} [pM] | 9 | 9 | 1372 | 9 | 1123 | 122.2 | 101.4 | 147.2 | 4,0 |
| CL/F ₁₄ [L/h] | 9 | 9 | 54.6 | 9 | 64.9 | 84.1 | 70.8 | 100.0 | 4,0 |

MDZ = midazolam; AUC_{0-∞} = area under the curve extrapolated to infinity; C_{max} = maximum measured concentration; CL/F = apparent clearance; INH = inhibition; IND = induction; N = number of subjects in analysis set; n = number of observations included in the analysis

Subscript '3' refers to Day 3 parameter comparison and subscript '14' refers to Day 14 parameter comparison

Safety and tolerability

Only a few drug-related (as evaluated by the investigator) AEs were reported. Specifically, two drug-related events were reported close to a midazolam administration: dyshidrotic eczema and mild headache. Both adverse events were reported more than 24 h following the last midazolam microdose; given the short half-life of midazolam, these AEs were most likely related to the test compound or study conditions only. All drug-related AEs were of mild or moderate intensity. No AEs were reported on the midazolam only baseline day.

3.1.2 Study 2

In Study 2, 40 healthy male subjects, aged 21 to 51 years (2 Black/African American), participated in the midazolam microdosing cohorts of the study. Two subjects in the 40 mg

MIDAZOLAM MICRODOSING RESULTS

dose group did not have PK samples for midazolam following multiple dosing of Compound B (one discontinued due to an AE; one was discontinued due to a refusal to comply with the study protocol), thus, only baseline PK profiles are available for these subjects. Prior to single doses of midazolam, plasma concentrations were BLQ for all subjects in all dose groups.

Geometric mean midazolam plasma concentration-time profiles at baseline and in the presence of the test compound or placebo are depicted in Figure 9. Descriptive statistics are presented in Appendix Table A2.

$C_{max,ss}$ values were above the CYP3A inactivation thresholds at all dose groups and above the threshold for induction as of the highest dose group tested. Thus, increased midazolam concentrations following dosing of Compound B were expected for the lower dose groups; the expectation for the combined influence of inactivation and induction on midazolam concentrations was unclear. Following treatment with Compound B (20 to 80 mg) or placebo, no differences in exposure to midazolam were apparent and plasma-concentration time profiles were similar in shape to that seen for the placebo subjects. Similarly, midazolam C_{max} and AUC values were similar both when dosed alone or in the presence of Compound B/placebo (Table 6). Median t_{max} was achieved at approximately the same time (1-1.5 h), regardless of treatment. Inter-individual variability in PK parameters was low-to-moderate.

MIDAZOLAM MICRODOSING RESULTS

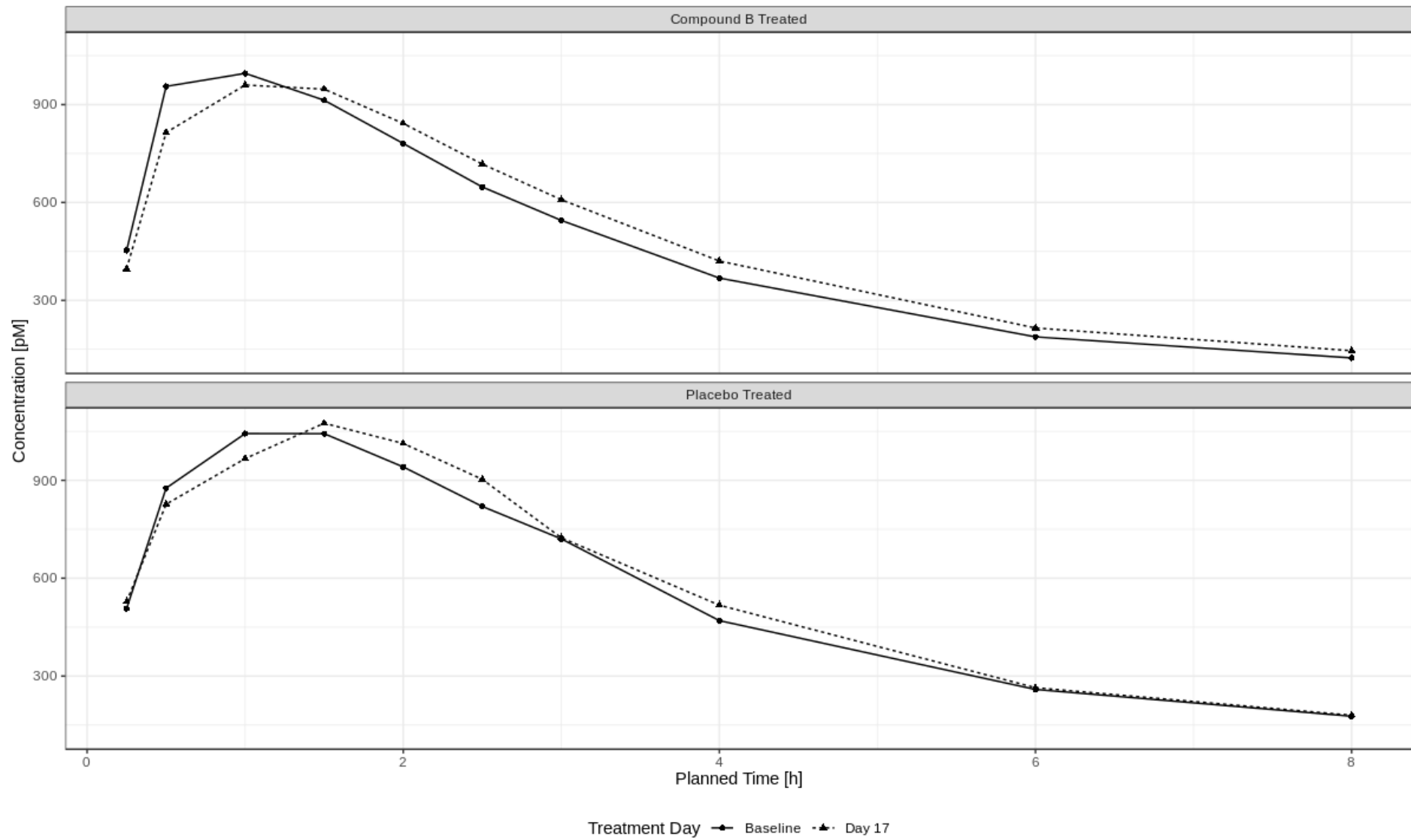


Fig. 9: Geometric mean midazolam concentration-time profiles for Baseline and Day 17 with either Compound B or placebo.

MIDAZOLAM MICRODOSING RESULTS

Results of the inferential analyses of the adjusted gMean ratios for $AUC_{0-\infty}$, C_{max} , and CL/F are displayed in Table 6. Point estimates of the $AUC_{0-\infty}$ gMean ratios for midazolam in the presence of Compound B versus midazolam alone ranged from 93.3%-114.5%, for C_{max} from 84.4%-109.4%, and for CL/F from 88.2%-106.1%. The majority of 90% CIs contained 100%. In cases where 100% was not included (C_{max} , 20 mg dose group, and CL/F and $AUC_{0-\infty}$, 40 mg dose group), the upper and/or lower limits of the 90% CIs only minimally exceeded 80-125%, thus, no DDI via CYP3A was observed.

As with Study 1, examination of individual subject ratios revealed that even in the placebo group, a number of subjects (25%-62.5%) would have been classified as having DDIs based on the limits of 1.25 and 0.8. In most groups tested, there was no clear direction for classification of DDI.

Tab. 6: Adjusted by-treatment geometric mean ratios of a single dose of midazolam administered alone (R) compared with administration following multiple dosing of Compound B – Study 2

| PK parameter | MDZ + Compound B/Placebo Test (T) | | MDZ alone Reference (R) | | Ratio T/R (%) | 90% Confidence interval (%) | | Number of subjects with DDI classification (INH,IND) | |
|-------------------------|-----------------------------------|---|-------------------------|---|---------------|-----------------------------|-------------|--|-------------|
| | N | n | gMean | n | | gMean | Lower limit | | Upper limit |
| Placebo (T0) | | | | | | | | | |
| $AUC_{0-\infty}$ [pM·h] | 8 | 8 | 4479 | 8 | 4356 | 102.8 | 87.2 | 121.3 | 2,2 |
| C_{max} [pM] | 8 | 8 | 1198 | 8 | 1197 | 100.1 | 84.0 | 119.3 | 1,1 |
| CL/F [L/h] | 8 | 8 | 45.1 | 8 | 45.7 | 98.8 | 82.0 | 119.0 | 3,2 |
| 20mg Compound B (T1) | | | | | | | | | |
| $AUC_{0-\infty}$ [pM·h] | 8 | 8 | 3961 | 8 | 4246 | 93.3 | 77.9 | 111.7 | 1,2 |
| C_{max} [pM] | 8 | 8 | 1040 | 8 | 1232 | 84.4 | 72.3 | 98.6 | 0,3 |
| CL/F [L/h] | 8 | 8 | 58.5 | 8 | 55.1 | 106.1 | 88.7 | 127.0 | 1,3 |
| 40mg Compound B (T2) | | | | | | | | | |
| $AUC_{0-\infty}$ [pM·h] | 8 | 6 | 5659 | 8 | 4945 | 114.5 | 104.5 | 125.4 | 1,0 |
| C_{max} [pM] | 8 | 6 | 1255 | 8 | 1147 | 109.4 | 94.3 | 126.9 | 2,0 |
| CL/F [L/h] | 8 | 6 | 41.8 | 8 | 47.0 | 88.9 | 82.9 | 95.2 | 0,0 |
| 60mg Compound B (T3) | | | | | | | | | |
| $AUC_{0-\infty}$ [pM·h] | 8 | 8 | 4343 | 8 | 3842 | 113.1 | 93.1 | 137.3 | 3,1 |
| C_{max} [pM] | 8 | 8 | 984 | 8 | 1031 | 95.4 | 79.8 | 114.2 | 1,1 |
| CL/F [L/h] | 8 | 8 | 53.8 | 8 | 61.0 | 88.2 | 72.8 | 106.8 | 3,1 |
| 80mg Compound B (T4) | | | | | | | | | |
| $AUC_{0-\infty}$ [pM·h] | 8 | 8 | 3894 | 8 | 3619 | 107.6 | 90.7 | 127.6 | 4,2 |
| C_{max} [pM] | 8 | 8 | 1058 | 8 | 1175 | 90.0 | 70.8 | 114.6 | 2,3 |
| CL/F [L/h] | 8 | 8 | 60.4 | 8 | 64.8 | 93.2 | 78.2 | 111.1 | 4,2 |

MDZ = midazolam; $AUC_{0-\infty}$ = area under the curve extrapolated to infinity; C_{max} = maximum measured concentration; CL/F = apparent clearance; INH = inhibition; IND = induction; N = number of subjects in analysis set; n = number of observations included in the analysis

Safety and tolerability

Five instances of drug-related AEs were reported on days of midazolam administration: Two participants (5%) reported drug-related events on the midazolam alone baseline day and three participants (7.5%) reported drug-related events on Day 17 (test compound/placebo and midazolam administered together). Mild fatigue and headache were each reported by single participants on the baseline day and fatigue, dizziness, and petechiae were each reported by single participants on Day 17. Day 17 AEs were reported in the placebo (fatigue) and 60mg dose groups. Similar AEs were reported for days with and without midazolam administration.

3.1.3 Study 3

Fifty healthy male subjects, aged 18 to 45 years (1 Black/African American), received midazolam microdoses in the study. One subject withdrew from participation due to an AE prior to administration of midazolam with the multiple dose of Compound C, thus, only baseline and single dose PK profiles are available for this subject. One further subject withdrew due to an AE following 6 hours on the first Compound C administration day; this subject, thus, contributed baseline midazolam and 1'-OH midazolam profiles, as well as AUC₂₋₄ following a single Compound C dose.

Prior to single doses of midazolam on Days -1 and 14, plasma concentrations of midazolam and 1'-OH midazolam were BLQ for all subjects in all dose groups. On Day 1, 18 subjects receiving the active test compound with midazolam and 3 subjects receiving placebo with midazolam still had measureable concentrations of midazolam at the pre-dose sample; however, all pre-dose concentrations were <5% C_{max} and were included as-is in all analyses.

Plasma concentration-time profiles (geometric means) of midazolam and 1'-OH midazolam are depicted graphically in Figures 10 and 11. Greater differences were seen for the 1'-OH midazolam profiles between treatment days than for midazolam itself and this was evident both for Compound C and placebo treated patients, suggesting greater inter-occasion variability, rather than a true effect. C_{max} and AUC values of both midazolam and 1'-OH midazolam were similar when midazolam was dosed alone or in the presence of Compound C or placebo (Appendix Table A3). Inter-individual variability in midazolam PK parameters was moderate-to-high; inter-individual variability for 1'-OH midazolam was moderate.

MIDAZOLAM MICRODOSING RESULTS

Following oral administration of midazolam with or without Compound C, adjusted gMean ratios for $AUC_{0-\infty}$, C_{max} , and CL/F ranged from 88.7%-101.0%, from 94.5%-117.5%, and from 101.1%-113.4%, respectively, following a single Compound C dose, and from 87.9%-117.5%, 83.9%-116.3%, and 81.1%-115.0%, respectively, following multiple dosing of Compound C (Table 7). Following a single dose of Compound C with midazolam, the 90% CIs for C_{max} contained 100% for all but the 25 mg dose group, while 90% CIs for CL/F and $AUC_{0-\infty}$ contained 100% for all but the 100 mg and 200 mg dose groups; upper and lower limits were either within or only marginally exceeded the standard bioequivalence acceptance range (80-125%). Following administration of midazolam in the presence of Compound C at steady state, 90% CIs contained 100% for all CL/F and $AUC_{0-\infty}$ gMean ratios except for in the 10 mg and 25 mg dose groups; for C_{max} , 90% CIs included 100% for all but the 100 mg dose group. Upper and lower limits of the 90% CIs were either within or only marginally exceeded 80-125%, indicating no relevant drug-drug interaction.

Examination of ratios for individual subjects again indicated that up to 50% of subjects in the placebo group would have been classified as having a DDI. Again, there was no clear direction for the DDI classification, such that multiple subjects would have been classified as experiencing CYP3A inhibition, while others in the same dose group would have been classified as having CYP3A induction.

MIDAZOLAM MICRODOSING RESULTS

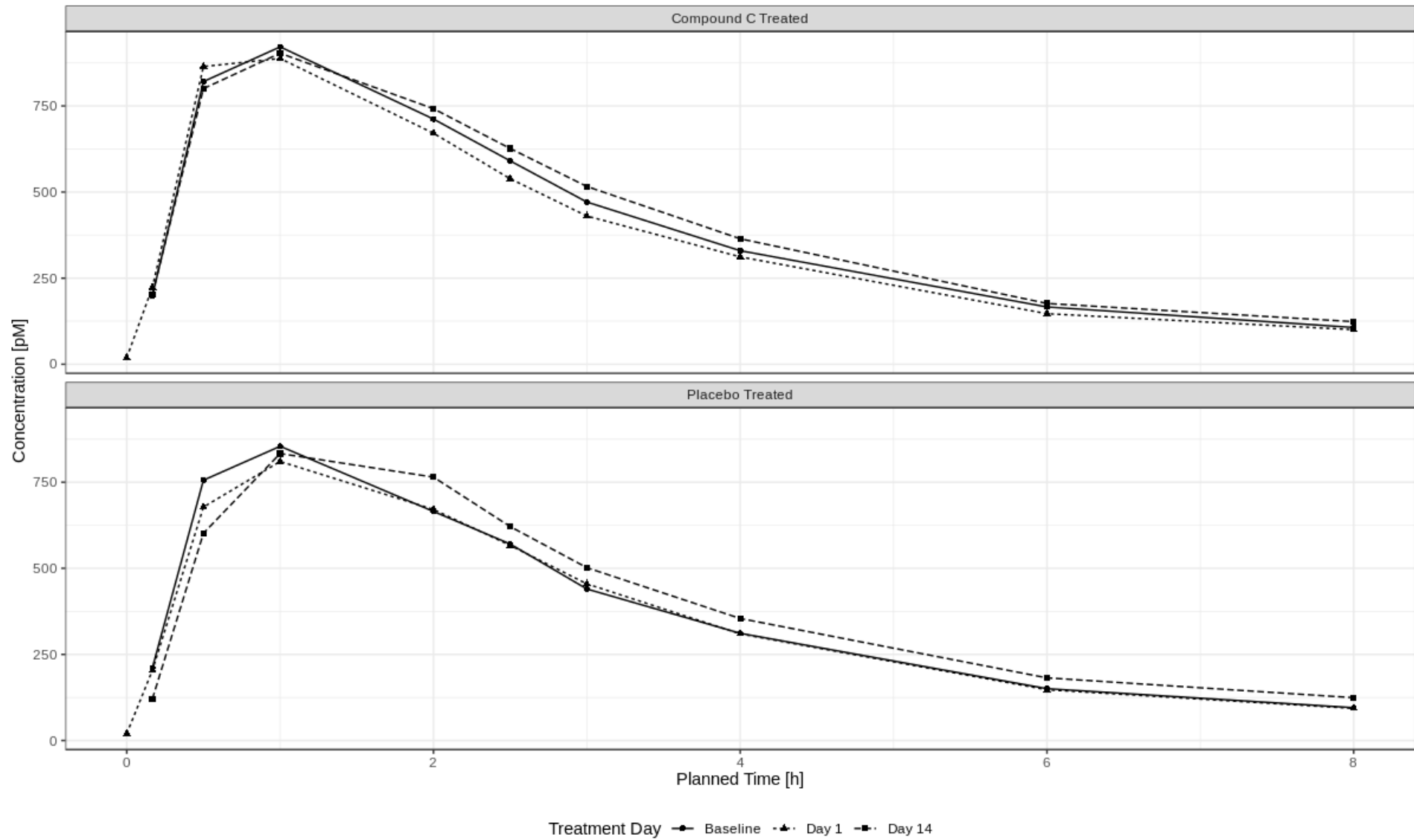


Fig. 10: Geometric mean midazolam concentration-time profiles for Baseline, Day 1, and Day 14 with either Compound C or placebo.

MIDAZOLAM MICRODOSING RESULTS

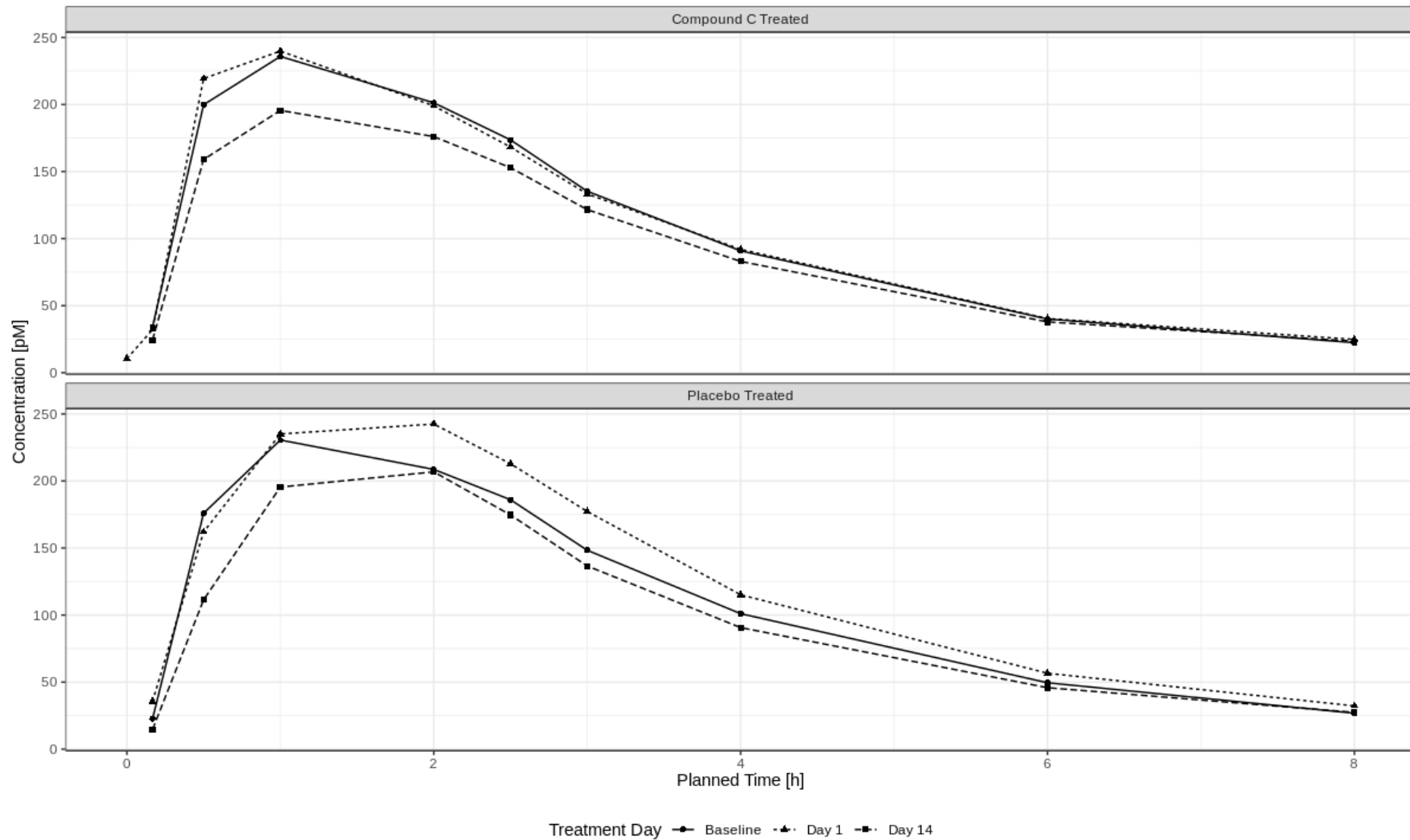


Fig. 11: Geometric mean 1'-OH midazolam concentration-time profiles for Baseline, Day 1, and Day 14 with either Compound C or placebo.

MODEL DEVELOPMENT RESULTS

Tab. 7: Adjusted by-treatment geometric mean ratios of a single dose of midazolam administered alone (R) compared with single or multiple dose administration of Compound C or placebo dosing (T) – Study 3

| PK parameter | MDZ + Compound C /Placebo Test (T) | | | MDZ alone Reference (R) | | Ratio T/R (%) | 90% Confidence interval (%) | | Number of subjects with DDI classification (INH,IND) |
|------------------------------|--|----|-------|----------------------------|-------|------------------|--------------------------------|----------------|--|
| | N | n | gMean | n | gMean | | Lower limit | Upper limit | |
| Placebo (T0) | | | | | | | | | |
| AUC _{0-∞,1} [pM·h] | 10 | 10 | 3280 | 10 | 3374 | 97.2 | 90.2 | 104.8 | 0,1 |
| C _{max,1} [pM] | 10 | 10 | 913 | 10 | 929 | 98.3 | 84.2 | 114.8 | 2,3 |
| CL/F ₁ [L/h] | 10 | 10 | 71.2 | 10 | 68.5 | 104.0 | 96.4 | 112.2 | 0,1 |
| AUC _{0-∞,14} [pM·h] | 10 | 10 | 3689 | 10 | 3374 | 109.3 | 98.3 | 121.7 | 2,1 |
| C _{max,14} [pM] | 10 | 10 | 887 | 10 | 929 | 95.5 | 81.3 | 112.1 | 2,3 |
| CL/F ₁₄ [L/h] | 10 | 10 | 63.5 | 10 | 68.5 | 92.7 | 83.4 | 103.1 | 2,1 |
| 10mg Compound C (T1) | | | | | | | | | |
| AUC _{0-∞,1} [pM·h] | 8 | 8 | 4048 | 8 | 4230 | 95.7 | 89.0 | 102.8 | 0,0 |
| C _{max,1} [pM] | 8 | 8 | 1095 | 8 | 1117 | 98.0 | 87.9 | 109.3 | 1,1 |
| CL/F ₁ [L/h] | 8 | 8 | 58.0 | 8 | 55.2 | 105.0 | 97.9 | 112.6 | 0,0 |
| AUC _{0-∞,14} [pM·h] | 8 | 8 | 5204 | 8 | 4230 | 123.0 | 109.9 | 137.7 | 3,0 |
| C _{max,14} [pM] | 8 | 8 | 1180 | 8 | 1117 | 105.7 | 91.5 | 122.0 | 1,1 |
| CL/F ₁₄ [L/h] | 8 | 8 | 44.8 | 8 | 55.2 | 81.1 | 72.0 | 91.4 | 3,0 |
| 25mg Compound C (T2) | | | | | | | | | |
| AUC _{0-∞,1} [pM·h] | 8 | 8 | 3600 | 8 | 3564 | 101.0 | 97.7 | 104.4 | 0,0 |
| C _{max,1} [pM] | 8 | 8 | 1132 | 8 | 963 | 117.5 | 102.6 | 134.6 | 4,0 |
| CL/F ₁ [L/h] | 8 | 8 | 65.8 | 8 | 65.0 | 101.1 | 97.3 | 105.1 | 0,0 |
| AUC _{0-∞,14} [pM·h] | 8 | 7 | 4188 | 8 | 3564 | 117.5 | 105.1 | 131.3 | 2,0 |
| C _{max,14} [pM] | 8 | 7 | 1120 | 8 | 963 | 116.3 | 90.9 | 148.7 | 3,0 |
| CL/F ₁₄ [L/h] | 8 | 7 | 56.3 | 8 | 65.0 | 86.6 | 77.3 | 96.9 | 2,0 |
| 50mg Compound C (T3) | | | | | | | | | |
| AUC _{0-∞,1} [pM·h] | 8 | 8 | 3097 | 8 | 3366 | 92.0 | 84.1 | 100.7 | 0,1 |
| C _{max,1} [pM] | 8 | 8 | 920 | 8 | 974 | 94.5 | 85.5 | 104.4 | 0,0 |
| CL/F ₁ [L/h] | 8 | 8 | 75.2 | 8 | 69.6 | 108.1 | 99.2 | 117.7 | 0,0 |
| AUC _{0-∞,14} [pM·h] | 8 | 7 | 3740 | 8 | 3366 | 111.1 | 86.6 | 142.5 | 2,1 |
| C _{max,14} [pM] | 8 | 7 | 1040 | 8 | 974 | 106.8 | 92.4 | 123.4 | 1,1 |
| CL/F ₁₄ [L/h] | 8 | 7 | 63.1 | 8 | 69.6 | 90.6 | 72.0 | 114.1 | 2,1 |
| 100mg Compound C (T4) | | | | | | | | | |
| AUC _{0-∞,1} [pM·h] | 8 | 8 | 3746 | 8 | 4074 | 92.0 | 86.1 | 98.2 | 0,0 |
| C _{max,1} [pM] | 8 | 8 | 1153 | 8 | 1175 | 98.2 | 87.3 | 110.4 | 1,1 |
| CL/F ₁ [L/h] | 8 | 8 | 61.8 | 8 | 57.0 | 108.4 | 101.9 | 115.3 | 0,0 |
| AUC _{0-∞,14} [pM·h] | 8 | 8 | 3941 | 8 | 4074 | 96.7 | 83.3 | 112.4 | 0,2 |
| C _{max,14} [pM] | 8 | 8 | 985 | 8 | 1175 | 83.9 | 71.2 | 98.9 | 0,3 |
| CL/F ₁₄ [L/h] | 8 | 8 | 59.5 | 8 | 57.0 | 104.3 | 90.2 | 120.7 | 0,2 |

MODEL DEVELOPMENT RESULTS

| PK parameter | MDZ + Compound C /Placebo Test (T) | | MDZ alone Reference (R) | | Ratio T/R (%) | 90% Confidence interval (%) | | Number of subjects with DDI classification (INH,IND) | |
|------------------------------|--|---|----------------------------|---|------------------|--------------------------------|-------------|--|----------------|
| | N | n | gMean | n | | gMean | Lower limit | | Upper limit |
| 200mg Compound C (T5) | | | | | | | | | |
| AUC _{0-∞,1} [pM·h] | 8 | 8 | 2721 | 8 | 3069 | 88.7 | 80.4 | 97.7 | 0,2 |
| C _{max,1} [pM] | 8 | 8 | 812 | 8 | 828 | 98.0 | 84.3 | 114.0 | 1,1 |
| CL/F _{,1} [L/h] | 8 | 8 | 85.2 | 8 | 75.1 | 113.4 | 102.3 | 125.5 | 0,2 |
| AUC _{0-∞,14} [pM·h] | 8 | 8 | 2699 | 8 | 3069 | 87.9 | 70.1 | 110.3 | 1,3 |
| C _{max,14} [pM] | 8 | 8 | 722 | 8 | 828 | 87.2 | 73.5 | 103.5 | 0,3 |
| CL/F _{,14} [L/h] | 8 | 8 | 86.4 | 8 | 75.1 | 115.0 | 91.6 | 144.3 | 1,3 |

MDZ = midazolam; AUC_{0-∞} = area under the curve extrapolated to infinity; C_{max} = maximum measured concentration; CL/F = apparent clearance; INH = inhibition; IND = induction; N = number of subjects in analysis set; n = number of observations included in the analysis

Subscript '1' refers to Day 1 parameter comparison and subscript '14' refers to Day 14 parameter comparison

Safety and tolerability

Twenty-one (42%) participants reported drug-related AEs on days when midazolam was administered. Most commonly reported AEs were headache and orthostatic intolerance, and were similarly reported on days with and without midazolam administration, suggesting relation to the test compound, rather than midazolam itself. All drug-related AEs were of mild or moderate intensity. No drug-related AEs were reported following midazolam administration alone at baseline.

3.1.4 Exploratory Analysis of Partial AUC

An exploratory analysis of AUC₂₋₄ compared to AUC_{0-∞} was conducted for each study separately and over all three studies combined. The results of the comparison of AUC₂₋₄ ratios and AUC_{0-∞} ratios are displayed in Table 8. The gMean point estimates were close to one for all three studies and overall. Furthermore, the 90% CI included one for all three studies, as well as for the pooled data, indicating that the ratios based on either AUC type were comparable.

MODEL DEVELOPMENT RESULTS

Tab. 8: Comparison of AUC₂₋₄ and AUC_{0-∞} test-to-reference gMean ratios, with point estimates and 90% confidence intervals

| | Day 1 or 3 | | | Day 14 or 17 | | |
|---------|------------|----------------|------------|--------------|----------------|------------|
| | n | Point estimate | 90% CI | n | Point estimate | 90% CI |
| Study 1 | 24 | 0.960 | 0.885-1.04 | 24 | 1.02 | 0.921-1.14 |
| Study 2 | --- | --- | --- | 38 | 1.04 | 0.962-1.13 |
| Study 3 | 50 | 0.996 | 0.954-1.04 | 48 | 1.02 | 0.947-1.09 |
| Pooled | 74 | 0.989 | 0.953-1.03 | 110 | 1.03 | 0.978-1.08 |

n = number of observations included in the analysis; CI = confidence interval

3.2 Model Development Results

Information regarding sex, age, and weight for each of the subjects was available for covariate analysis. Population characteristics for each of the studies and over both the model development and external validation datasets are given in Table 9. The proportion of males to females, as well as the ranges of values, were adequate for assessing covariate relationships, although all subjects were still young to middle-aged adults within a healthy range of weights.

Tab. 9: Population characteristics

| | N | Age (years) | | Sex | Weight (kg) | |
|----------------------|------------|-------------|--------------|--------------|-------------|---------------|
| | | Mean | Range | M:F | Mean | Range |
| K119* | 12 | 26.0 | 22-33 | 8:4 | 74.9 | 51-103 |
| K155* | 12 | 26.4 | 21-45 | 8:4 | 75.9 | 53.5-101 |
| K169* | 20 | 24.6 | 21-34 | 10:10 | 67.0 | 47-91 |
| K257* | 16 | 28.5 | 22-34 | 9:7 | 71.2 | 57-88 |
| K380* | 16 | 30.0 | 22-52 | 12:4 | 72.4 | 55.1-96.3 |
| K194* | 12 | 25.3 | 21-34 | 6:6 | 73.4 | 55-109 |
| K345* | 11 | 27.4 | 19-36 | 6:5 | 70.0 | 53.1-111 |
| Total* | 99 | 26.9 | 19-52 | 59:40 | 71.7 | 47-111 |
| K292 | 16 | 32.7 | 22-49 | 12:4 | 73.4 | 61-92 |
| K293 | 12 | 31.0 | 22-49 | 12:0 | 70.6 | 61-97 |
| K342 | 12 | 29.8 | 19-50 | 8:4 | 74.7 | 50.0-94.1 |
| K363 | 18 | 33.7 | 24-50 | 7:11 | 67.9 | 52.8-88.9 |
| Total Overall | 157 | 28.8 | 19-52 | 98:59 | 71.6 | 47-111 |

*Used for model development

3.2.1 Midazolam Model

Ninety-nine subjects contributed data to the base midazolam model development, providing a total of 2652 evaluable midazolam concentrations. Measurements were below the lower limit of quantification (BLQ) for 29 samples and were, thus, omitted from data analysis. The midazolam concentrations were best described using a 3-compartment drug disposition model with first-order absorption and linear elimination. The proportional error model, using an early/late cut-point at 0.5 h, best fit the data. Although a potential relationship was found for weight and V_{p1} , addition of weight as a covariate to the model did not improve the overall

fit nor did it reduce the amount of residual variability or the IIV for V_{p1} . A number of correlations between EBEs were observed and were sequentially added to the model from largest correlation to smallest; only the correlation between the EBE for clearance and bioavailability (the largest correlation) was estimated with reasonable precision ($RSE < 50\%$), thus, only this relationship was added to the model.

A comparison of a 2-compartment model with the 3-compartment model over time is shown in Figure 12 and goodness-of-fit plots for the final adopted model are displayed in Figure 13. As seen by the considerably higher distribution of errors at the later time points using the 2-compartment model compared to the even distribution of errors over time for the 3-compartment model, the 2-compartment model clearly did not describe the elimination phase of midazolam as well as the 3-compartment model. Inspection of the predicted concentrations compared to observed concentrations showed that both individual and population predictions coincided well with the observed data, as noted by the trend lines, which mostly overlapped with the lines of unity. When examining the individual and population predictions plotted against their weighted residual errors, IWRES and CWRES, respectively, no trends were observed, showing an even distribution of errors. Furthermore, the majority of individual weighted residual errors (other than for the lowest concentrations) fell within the range of ± 1.96 standard deviations, indicating a normal distribution of errors and a good model fit.

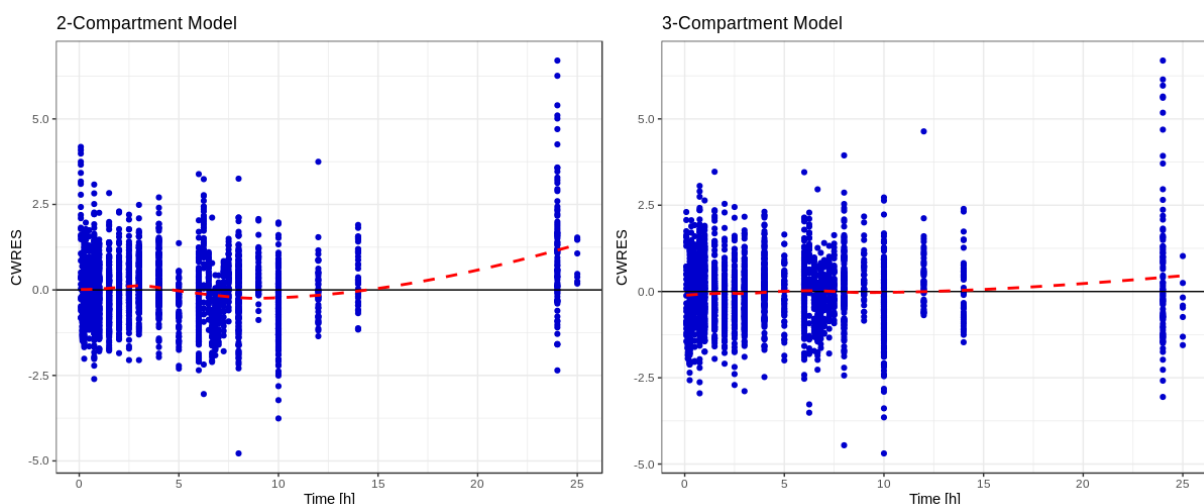


Fig. 12: Comparison of 2-compartment and 3-compartment structural models for midazolam using conditional weighted residuals for the predictions over time. CWRES = conditional weighted residual error.

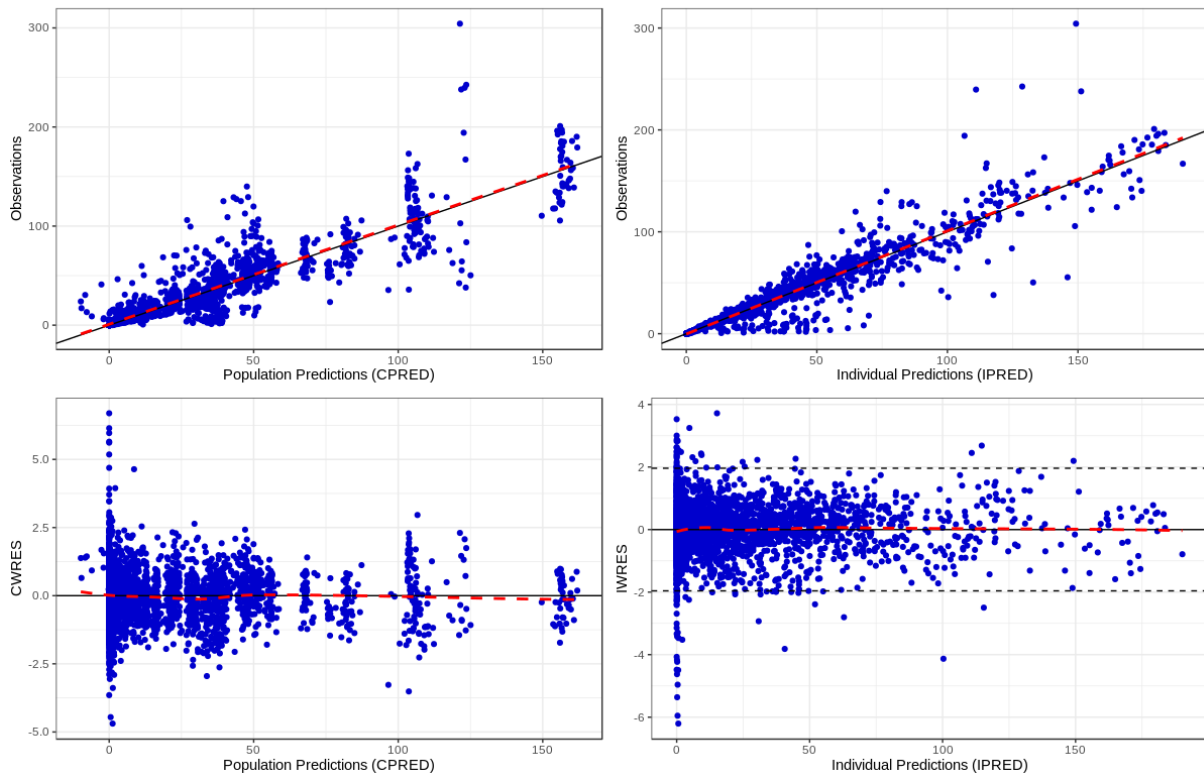


Fig. 13: Goodness-of-fit plots for final adopted midazolam model. Blue points denote individual values; black solid lines represent unity (top panels); red-dashed line is a linear smoothing function (top panels) or a loess smoothing function (bottom panels); black dashed lines represent ± 1.96 standard deviations (bottom right panel). CPRED = conditional population predictions; IPRED = individual predictions; CWRES = conditional weighted residual error; IWRES = individual weighted residual error.

Population PK parameter values, RSEs and shrinkage for the final model are given in Table 10. Random effects (IIV) were applied to all parameters except inter-compartmental clearance for peripheral compartment 2, where IIV was found to be close to 0 and, thus, was removed from the model. Inter-occasion variability was added and could be estimated with good precision for apparent clearance and bioavailability. Eta-shrinkage was generally below 30%, although for apparent volume of the 2nd peripheral compartment and for clearance, shrinkage was 39.0% and 31.5% for IIV, respectively, which was still considered acceptable; the IOV for clearance was 48.6%, suggesting that the variance of this parameter may be biased (i.e. is not accurately describing the true variance).

The population parameters as estimated by the model were in-line with expected values. For example, bioavailability was expected to be ~30% (Heizmann et al. 1983) and the model estimated the bioavailability of the population to be 27.8%; clearance was expected to be around 18-30 L/h (Heizmann et al. 1983) and the population estimated parameter was 24.1 L/h. Inter-individual variability as estimated by the model was also found to be in the range of

MODEL DEVELOPMENT RESULTS

low-to-moderate, which is consistent with findings in other midazolam studies. Thus, the final estimated parameters were considered physiologically plausible.

For the addition of the data from the prospective studies, all pre-determined values from model development were fixed. Additionally, as the prospective studies all gave midazolam with a standard continental breakfast, fed status was added as a covariate. Specifically, an interaction effect of food was added on V_c , k_a , and F_1 , and a separate late residual error term was added to account for a later t_{max} following fed administration. Goodness-of-fit plots looked very similar when examining both the original model alone and the original model with addition of the prospective studies, indicating that the model structure was appropriate for both sets of data.

Tab. 10: Population parameter values for the final adopted midazolam model.

| Parameter | Model Development (N=99 (2652 obs)) | | | w/Prospective Studies (N=213 (3718 obs)) | |
|-------------------------------------|--|---------|---------------|---|---------|
| | Value | RSE [%] | Shrinkage [%] | Value | RSE [%] |
| V_c [L] | 20.7 | 6.24 | | FIXED | |
| V_{p1} [L] | 44.0 | 7.25 | | FIXED | |
| V_{p2} [L] | 23.7 | 4.49 | | FIXED | |
| Q_{p1} [h^{-1}] | 8.03 | 7.08 | | FIXED | |
| Q_{p2} [h^{-1}] | 45.7 | 7.76 | | FIXED | |
| CL [$L \cdot h^{-1}$] | 24.1 | 1.87 | | FIXED | |
| k_a [h^{-1}] | 2.33 | 3.81 | | FIXED | |
| F_1 [%] | 27.8 | 3.28 | | FIXED | |
| $V_{c, fed}$ [L] | --- | --- | | 11.3 | 11.8 |
| $k_{a, fed}$ [h^{-1}] | --- | --- | | -1.08 | 3.33 |
| $F_{1, fed}$ | --- | --- | | 0.178 | 9.06 |
| Early _{MDZ, prop} | 0.473 | 3.60 | | FIXED | |
| Late _{MDZ, prop} | -0.156 | 5.18 | | FIXED | |
| Late _{MDZ, prop, fed} | --- | --- | | -0.0728 | 4.24 |
| Inter-Individual Variability | | | | | |
| $\omega^2_{V_c}$ | 0.323 | 9.71 | 25.1 | FIXED | |
| $\omega^2_{V_{p1}}$ | 0.430 | 12.2 | 29.9 | FIXED | |
| $\omega^2_{V_{p2}}$ | 0.184 | 23.6 | 39.0 | FIXED | |
| $\omega^2_{Q_{p1}}$ | 0.470 | 12.6 | 12.2 | FIXED | |
| $\omega^2_{k_a}$ | 0.301 | 17.6 | 27.6 | FIXED | |
| ω^2_{CL} | 0.0851 | 36.9 | 31.5 | FIXED | |
| ω^2_F | 0.239 | 12.6 | 14.4 | FIXED | |
| $\omega^2_F \sim \omega^2_{CL}$ | -0.624 | 21.3 | --- | FIXED | |
| Inter-Occasion Variability | | | | | |
| ω^2_{CL} | 0.138 | 16.5 | 48.6 | FIXED | |
| ω^2_F | 0.143 | 15.0 | 15.9 | FIXED | |

MODEL DEVELOPMENT RESULTS

| | | |
|-------------|-----|-------|
| OFV* | 241 | -3639 |
|-------------|-----|-------|

*Due to different datasets, OFVs are not comparable, however, both OFVs are given for reference; relative standard errors for inter-individual variability are given on the approximate standard deviation scale (standard error/variance estimate)/2; obs = observations; OFV = Objective function value; prop. = proportional; RSE = Relative Standard Error; w/ = with

As a final check of the model's ability to describe the data, a VPC was conducted, split by dosing regimen (a single midazolam dose over the dosing interval vs. semi-simultaneous administration of oral plus iv midazolam) and dataset source, with 1000 simulations conducted. The resulting VPC (Figure 14) showed good concurrence with the data, with the median, 97.5th and 2.5th percentiles of the observed data mostly encompassed within the 95% CIs for the model predicted median, 97.5th and 2.5th percentiles. For the prospective studies, the 2.5th percentile for the early time points was under-predicted, but otherwise the model proved to be able to describe the data well. Thus, the final adopted midazolam alone model was a 3-compartment model with first-order absorption (following oral dosing) and linear elimination, as depicted in Figure 15.

MODEL DEVELOPMENT RESULTS

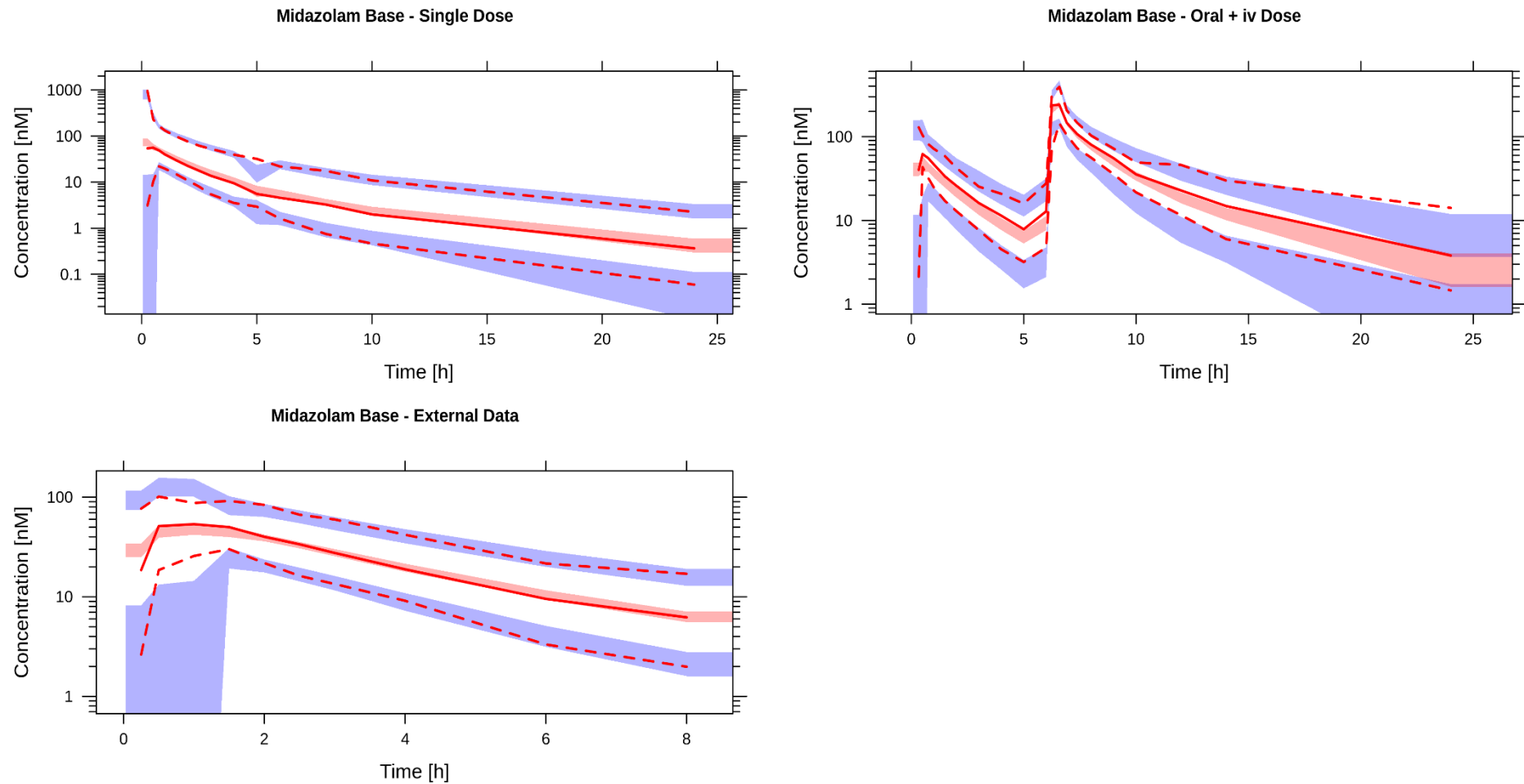


Fig. 14: Visual predictive checks for the adopted midazolam model. 1000 simulations were used and data are displayed on a semi-log scale. The top two panels are run on the dataset used to build the model, while the bottom panel includes only data from the prospective studies. The solid red line depicts the observed median concentrations, while the dotted lines depict the observed 97.5th and 2.5th percentiles. The shaded red area pertains to the 90% confidence interval for the predicted medians, while the shaded blue areas pertain to the 90% confidence interval for the 97.5th and 2.5th percentile predictions. Data are normalised to a midazolam dose of 4 mg. nM = nanomolar; h = hours.

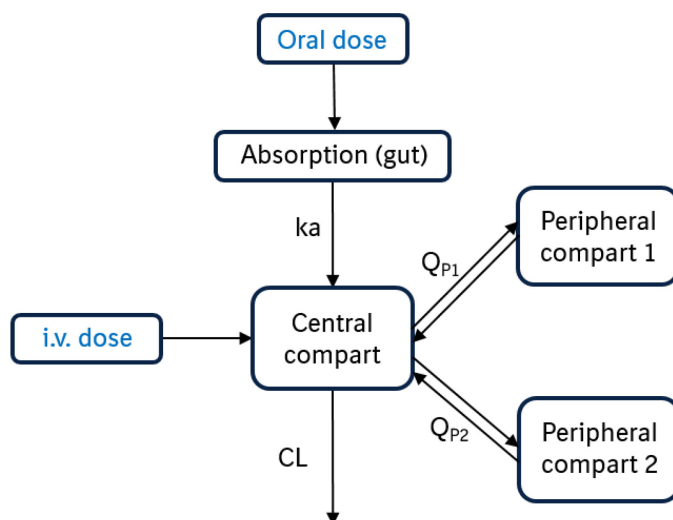


Fig. 15: Adopted base midazolam model: 3 compartment model with absorption compartment, first-order absorption and linear elimination; k_a = absorption rate; Q_{P1}/Q_{P2} = inter-compartmental clearance; CL = clearance.

3.2.2 1'-OH Midazolam Model

The same 99 subjects from the midazolam model development also contributed data to the base 1'-OH midazolam model development. Due to difficulties in modelling 1'-OH midazolam concentrations following a 1 μg dose of midazolam, 1'-OH midazolam profiles following this dose were excluded. Subjects contributed a total of 1571 concentrations that were above the lower limit of quantification, with an additional 190 samples omitted from analyses as they were BLQ. As with the midazolam model, 1'-OH midazolam concentrations were best described using a 3-compartment drug disposition model with first-order absorption and linear elimination. The two-step proportional error model was again the best error model. An early/late cut-point was applied at 0.75 h. Inclusion of a transit compartment resulted in the model not converging. Although inclusion of lag time resulted in an improvement of OFV by 10 points, numerous large correlations between model parameters resulted and the model became unstable. Therefore, no lag time was included in the model.

The plot examining residual errors over time (Figure 16) indicated that the 3-compartment model best described the data, as no trends were evident for the errors over time, while with the 2-compartment model, a clear increase in error distribution was seen during the terminal phase.

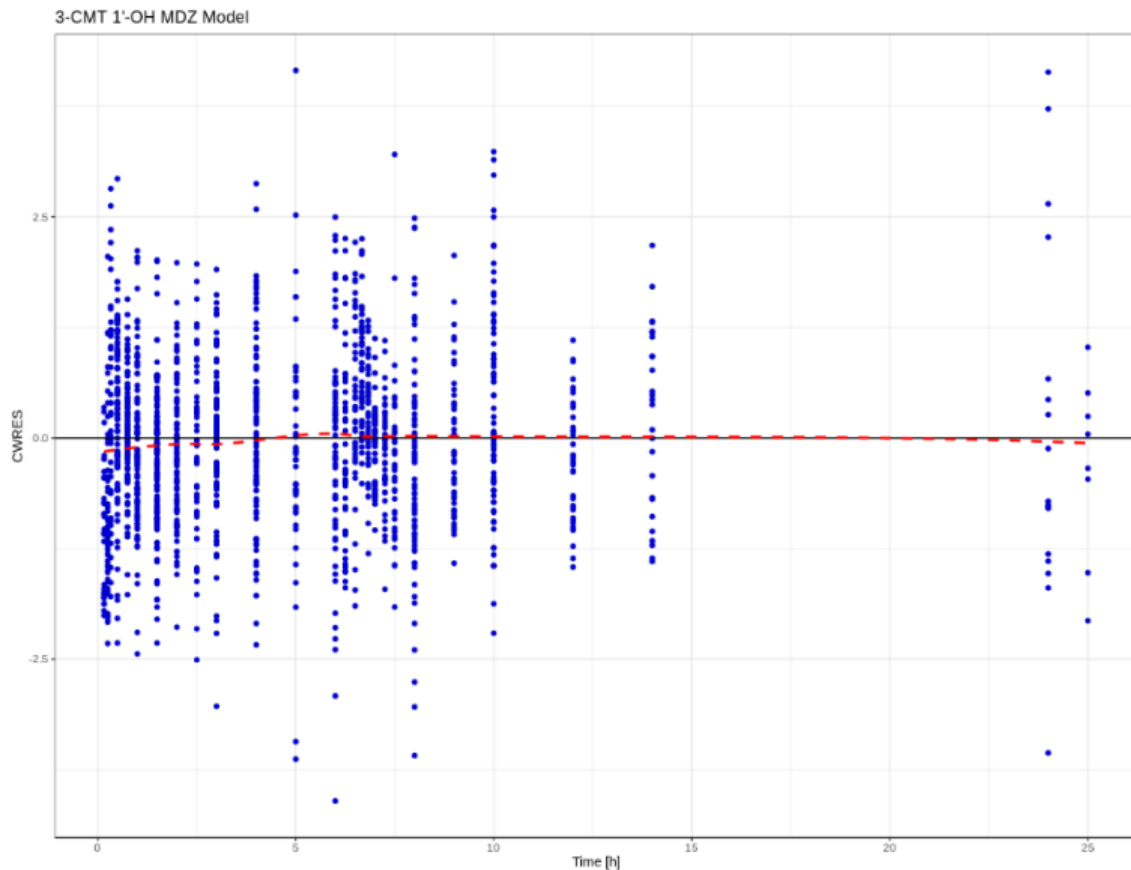


Fig. 16: Goodness-of-fit for 1'-OH midazolam 3-compartment model using conditional weighted residuals for the predictions over time. 3-CMT = 3-compartment; 1'-OH MDZ = 1-hydroxymidazolam; CWRES = conditional weighted residual error; h = hours.

Goodness-of-fit plots (Figure 17) showed that both population and individual values were under-predicted at higher concentrations, but that residual errors for the predictions were still within an acceptable range (the majority of errors within ± 1.96 standard deviations). Furthermore, VPCs (Figure 18) indicated that the model was able to describe the data well, although the maximum concentrations and the 2.5th percentile were still under-predicted by the model when midazolam was administered first as an oral dose, then as an iv dose. The model predictions for 1'-OH midazolam data from the prospective study (Study 3) also indicated a good fit of the model to the data.

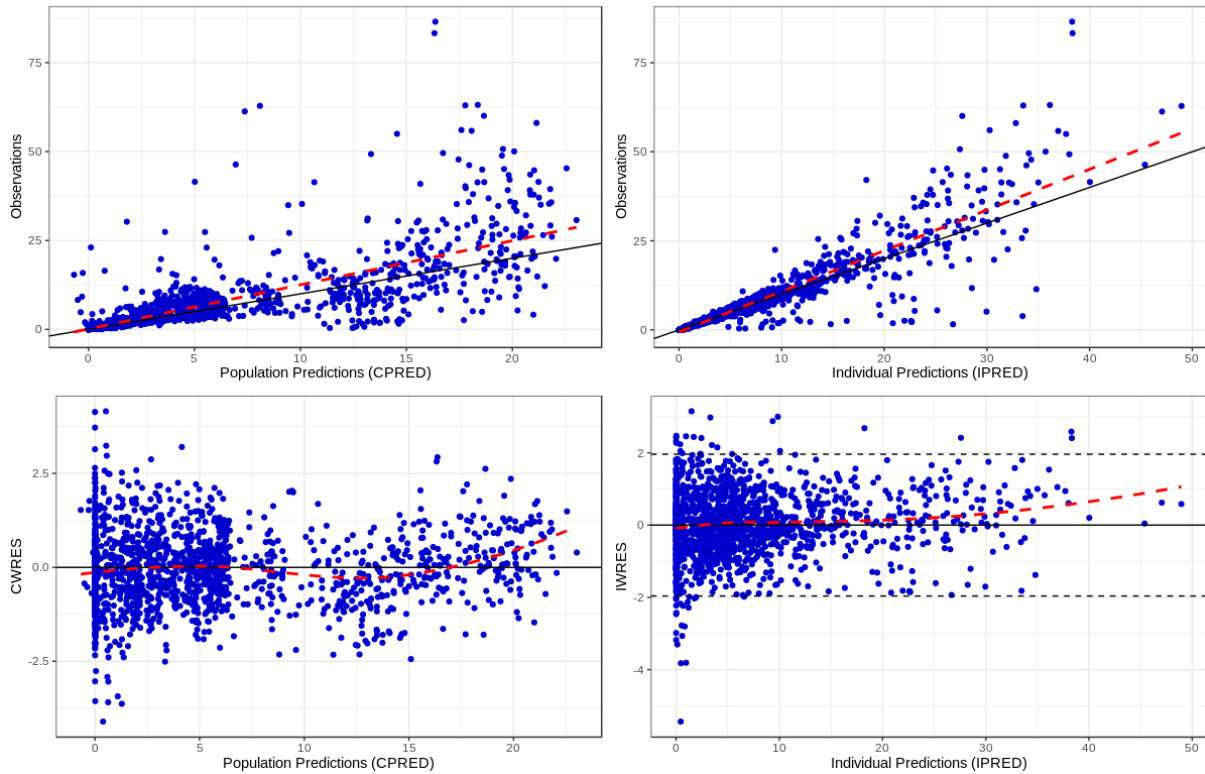


Fig. 17: Goodness-of-fit plots for final adopted 1'-OH midazolam model. Blue points denote individual values; black solid lines represent unity (top panels); red-dashed line is a linear smoothing function (top panels) or a loess smoothing function (bottom panels); black dashed lines represent ± 1.96 standard deviations (bottom right panel). CPRED = conditional population predictions; IPRED = individual predictions; CWRES = conditional weighted residual error; IWRES = individual weighted residual error.

MODEL DEVELOPMENT RESULTS

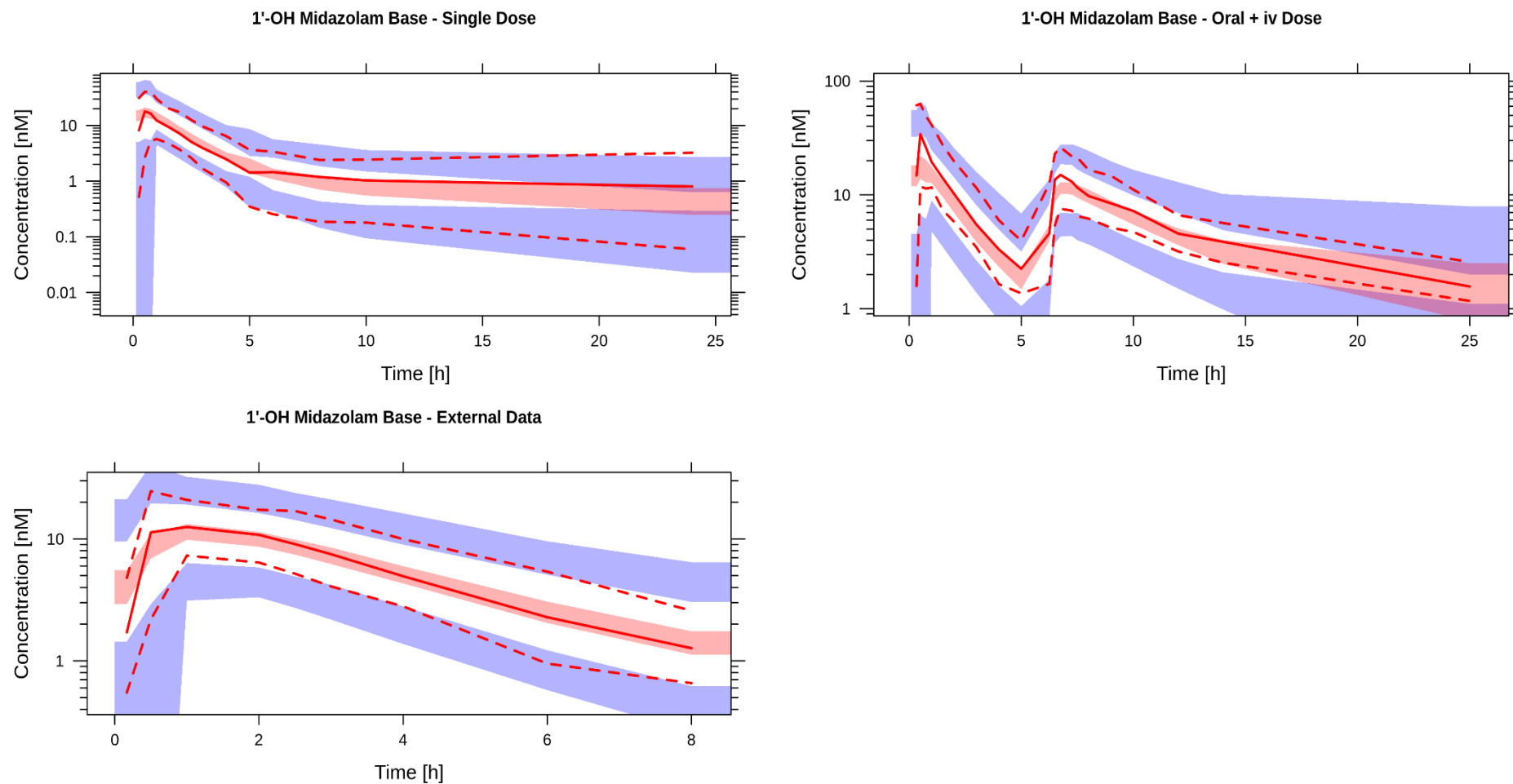


Fig. 18: Visual predictive checks for the adopted 1'-OH midazolam model. 1000 simulations were used and data are displayed on a semi-log scale. The top panels are run on the dataset used to build the model, while the bottom panel includes only data from the prospective studies. The solid red line depicts the observed median concentrations, while the dotted lines depict the observed 97.5th and 2.5th percentiles. The shaded red area pertains to the 90% confidence interval for the predicted medians, while the shaded blue areas pertain to the 90% confidence interval for the 97.5th and 2.5th percentile predictions. Data are normalised to a midazolam dose of 4 mg. nM = nanomolar; h = hours.

MODEL DEVELOPMENT RESULTS

Table 13 lists the population PK parameter values, RSEs and shrinkage for the final 1'-OH midazolam model. Random effects (IIV) were tested on all parameters. IIV was not included on Q_{MP2} (inter-compartmental clearance for peripheral compartment 2) and k_a (rate of metabolism following an oral dose) for the final model, as including IIV on these parameters resulted in imprecise parameter estimation for the full model. Eta-shrinkage was below 30% for V_{met} , Q_{MP} , $F1$ and CL_{met} , while shrinkage for $F5$, k_{met} , V_{MP} (metabolic peripheral compartment 1 volume) and V_{MP2} (metabolic peripheral compartment 2 volume) was generally high. Removal of the IIV on these parameters resulted in worse parameter estimate precision (many RSEs >30%). Thus, it should be noted that the estimates for the high shrinkage parameters may be biased. This was not considered a concern for the composite model, as at least the values represented by $F5$ and k_{met} were expected to be more accurately estimated with the inclusion of the actual midazolam concentrations. Assessment of the different error models revealed that the early/late split proportional error, with an additive error fixed at 0.00001 was best suited to the data. Finally, the correlation between EBEs was examined and a covariance term between ω^2_{F1} and $\omega^2_{CL_{met}}$ was added to the model. The resulting correlation was -1.00, which improved the fit and stability of the model, but which suggests that in the 1'-OH midazolam base model, no additional information is given by including both bioavailability and clearance parameters.

Tab. 13: Population parameter values for the final adopted 1'-OH midazolam model.

| Parameter | Model Development (N=99 (1571 obs)) | | | w/Prospective Studies (N=149 (2009 obs)) | |
|---------------------------------|--|---------|---------------|---|---------|
| | Value | RSE [%] | Shrinkage [%] | Value | RSE [%] |
| V_{met} [L] | 59.2 | 1.36 | | FIXED | |
| V_{MP} [L] | 2491 | 10.8 | | FIXED | |
| V_{MP2} [L] | 56.9 | 9.61 | | FIXED | |
| Q_{MP} [h^{-1}] | 114.5 | 1.58 | | FIXED | |
| Q_{MP2} [h^{-1}] | 24.7 | 0.916 | | FIXED | |
| CL_{met} [$L \cdot h^{-1}$] | 129.5 | 1.53 | | FIXED | |
| k_{met} [h^{-1}] | 0.803 | 1.44 | | FIXED | |
| k_a [h^{-1}] | 0.427 | 5.26 | | FIXED | |
| $F1$ [%] | 81.1 | 1.73 | | FIXED | |
| $F5$ [%] | 79.7 | 2.83 | | FIXED | |
| $V_{met, fed}$ [L] | --- | --- | | 118.9 | 12.1 |
| $k_{met, fed}$ [h^{-1}] | --- | --- | | -0.228 | 10.6 |
| $Q_{MP, fed}$ [h^{-1}] | --- | --- | | -41.8 | 16.0 |
| Early $1'$ -OHMDZ $_{prop}$ | -0.487 | 3.65 | | FIXED | |
| Late $1'$ -OHMDZ $_{prop}$ | 0.182 | 3.93 | | FIXED | |

MODEL DEVELOPMENT RESULTS

| Inter-Individual Variability | | | | |
|--|-------------|------|------|--------------|
| $\omega^2_{V_{met}}$ | 0.660 | 13.7 | 16.7 | FIXED |
| $\omega^2_{V_{MP}}$ | 0.611 | 14.7 | 39.8 | FIXED |
| $\omega^2_{V_{MP2}}$ | 0.915 | 16.7 | 55.2 | FIXED |
| $\omega^2_{Q_{MP}}$ | 0.643 | 10.4 | 14.9 | FIXED |
| $\omega^2_{k_{met}}$ | 0.0929 | 22.5 | 46.0 | FIXED |
| $\omega^2_{CL_{met}}$ | 0.315 | 22.2 | 11.5 | FIXED |
| ω^2_{F1} | 0.113 | 39.7 | 11.5 | FIXED |
| ω^2_{F5} | 0.112 | 12.2 | 42.5 | FIXED |
| $\omega^2_{F1} \sim \omega^2_{CL_{met}}$ | -1.00 | 12.3 | --- | FIXED |
| OFV* | -376 | | | -3061 |

*Due to different datasets, OFVs are not comparable, however, both OFVs are given for reference; relative standard errors for inter-individual variability are given on the approximate standard deviation scale (standard error/variance estimate)/2; obs = observations; OFV = Objective function value; prop. = proportional; RSE = Relative Standard Error; w/ = with

Model-predicted CL values for 1'-OH midazolam were similar to the clearance values obtained in the midazolam microdosing Study 3 and the high fraction of metabolite available is in-line with the extensive metabolism of midazolam, suggesting physiological plausibility to the parameter estimates.

To test the model with the prospective data, fed status was added as a covariate on V_{met} (metabolic central compartment volume), k_{met} (rate of metabolism following oral administration), and Q_{MP} (inter-compartmental clearance for peripheral compartment 1); a separate late residual error term for fed administration was not required, as t_{max} remained similar for both fed and fasted conditions. Goodness-of-fit plots indicated similarly well fit data for both the original model alone and the original model with addition of the prospective studies. Thus, the 1'-OH midazolam base model showed both internal and external validity and was adopted for incorporation in the composite model. The graphical representation of the final model is depicted in Figure 19.

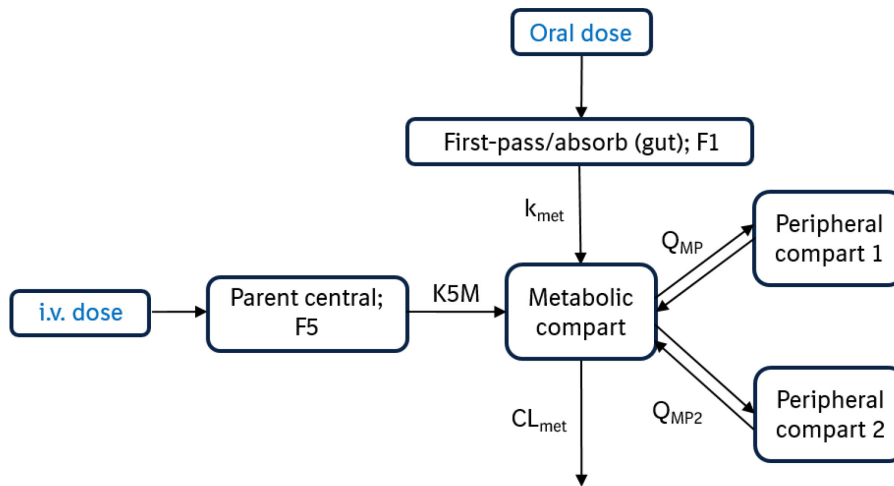


Fig. 19: Adopted base 1'-OH midazolam model: 3 compartment model with dual absorption compartments, first-order absorption and linear elimination; F1 = 1'-OH midazolam availability following oral dosing of midazolam; F5 = 1'-OH midazolam availability following iv dosing of midazolam; k_{met} = pre-systemic+systemic metabolism following oral administration of midazolam; K5M = systemic metabolism following iv administration of midazolam; Q_{MP}/Q_{MP2} = inter-compartmental clearance; CL_{met} = apparent metabolic clearance.

3.2.3 Composite Model

The adopted midazolam and 1'-OH midazolam models were combined to form the composite model, with CL for midazolam being replaced by Q_{met} to represent the clearance of midazolam via metabolism to 1'-OH midazolam; the midazolam base model replaced parameters designed to account for metabolism following iv administration that had been added to the 1'-OH midazolam model. Final estimates from the base models were used as the initial values for estimating final model parameters. The combination of both models as they were adopted resulted in model instability and various parameters could not be precisely estimated. Thus, IIVs were removed one by one, based on worst precision, until all parameters could be adequately estimated. As well, to further simplify the model, the late/early split for the proportional error term was set to 0.5 h for both midazolam and 1'-OH midazolam. The resulting model had IIV removed for the apparent volume of both metabolite peripheral compartments and for midazolam's peripheral compartment 2. The IOV on F and CL (now Q_{met}) was retained from the midazolam model, with the addition of IOV on CL_{met} . All three IOVs could be precisely estimated, as seen in Table 13. Inspection of covariates revealed relationships between weight and Q_{MP} , as well as between age and k_{met} . Therefore, these covariates were normalised to 70 kg and 26.5 years (approximate mean values), respectively, and added to the model using the power functions:

$$Q_{MP,i} = (\vartheta_{QMP} * (\text{weight},i/70 \text{ kg})^{\vartheta_{weight}}) * e^{\eta_i}$$

$$k_{met,i} = (\vartheta_{kmet} * (\text{age},i/26.5 \text{ years})^{\vartheta_{age}}) * e^{\eta_i}$$

MODEL DEVELOPMENT RESULTS

where i refers to the individual values, $\theta_{Q_{MP}}$ and $\theta_{k_{met}}$ refer to the population values, ϑ_{weight} and ϑ_{age} refer to the population level effects of weight and age, respectively, and e^{η^i} refers to the IIV for the parameter. Following addition of these parameters, the OFV was significantly decreased and variability on Q_{MP} was reduced, although no differences were noted for the variability of k_{met} . Re-assessment of the errors following covariate addition revealed that the initially present relationships had disappeared, indicating that the covariates had indeed contributed to inter-individual differences in parameter values. However, as no improvement of fit was seen for the addition of age, only the effect of weight was left in the final model. Next, EBEs were examined for covariance and it was noted that the EBEs for central compartment volumes for both midazolam and 1'-OH midazolam were related, as well as the EBEs for inter-compartmental clearance and volume of midazolam's peripheral compartment 1. Inclusion of the relationship between compartment volume errors resulted in a better model fit, as well as adequate precision for parameter estimation. Further inclusion of a covariance between inter-compartmental clearance and volume of peripheral compartment 1 resulted in a large increase in the OFV and, thus, was not included in the final model.

Final parameter estimates, RSEs, and shrinkage are presented in Table 13. Parameters were estimated with good precision, with all RSEs for fixed effects <30%. Parameter estimates for midazolam were mostly similar to those determined in the base model, although F was increased, as it now accounted for both the availability of midazolam and 1'-OH midazolam combined, and k_a was decreased. 1'-OH midazolam parameters showed greater changes, although CL_{met} remained similar to the base model estimate. Thus, the parameters continued to show physiological plausibility. Eta-shrinkage was mostly acceptable, although Q_{met} , CL_{met} and the IOV for F had shrinkage greater than 30%, suggesting a potential bias to the estimated values. Given the good precision (RSEs between 1.96% to 4.75%) of estimation, combined with the coincidence with physiological plausible values, the potential bias was not considered problematic.

For the prospective study data, the fed effects as they were added to the base models were included in the composite model. The fed effect could no longer be well estimated for bioavailability, likely because it no longer just represented the bioavailability of midazolam, or for V_{met} , likely due to the correlation between V_{met} and V_c . Thus, these effects were removed from the model, but all others remained and could again be relatively precisely estimated (see Table 14).

MODEL DEVELOPMENT RESULTS

Tab. 14: Population parameter values for the final composite midazolam model.

| Model Parameters | Parameter Name | Final Model (N=99 (4568 obs)) | | | w/Prospective Studies (N=213 (6072 obs)) | |
|--|---|----------------------------------|---------|------------------|--|---------|
| | | Value | RSE [%] | Shrinkage [%] | Value | RSE [%] |
| Structural & Covariate Parameters | | | | | | |
| V_c [L] | MDZ central volume | 19.5 | 5.93 | | FIXED | |
| V_{p1} [L] | MDZ peripheral 1 volume | 41.3 | 6.77 | | FIXED | |
| V_{p2} [L] | MDZ peripheral 2 volume | 23.6 | 4.43 | | FIXED | |
| Q_{p1} [h^{-1}] | MDZ inter-compartment clearance 1 | 8.13 | 7.33 | | FIXED | |
| Q_{p2} [h^{-1}] | MDZ inter-compartment clearance 2 | 45.4 | 7.42 | | FIXED | |
| k_a parent [h^{-1}] | Absorption rate constant | 0.682 | 5.48 | | FIXED | |
| F | Combined bioavailability | 0.933 | 3.39 | | FIXED | |
| k_{met} [h^{-1}] | Pre-systemic metabolism rate | 1.60 | 4.84 | | FIXED | |
| Q_{met} [$L \cdot h^{-1}$] | MDZ clearance via metabolism | 24.2 | 2.00 | | FIXED | |
| V_{met} [L] | Metabolic central volume | 179.6 | 6.37 | | FIXED | |
| V_{MP} [L] | Metabolic peripheral 1 volume | 694.6 | 15.1 | | FIXED | |
| V_{MP2} [L] | Metabolic peripheral 2 volume | 64.6 | 11.1 | | FIXED | |
| Q_{MP} [h^{-1}] | Metabolic inter-compartment clearance 1 | 60.3 | 8.80 | | FIXED | |
| $Q_{MP,WT}$ [$h^{-1}/70$ kg] | Power of weight on Q_{MP} | 1.18 | 26.7 | | FIXED | |
| Q_{MP2} [h^{-1}] | Metabolic inter-compartment clearance 2 | 127.7 | 11.6 | | FIXED | |
| CL_{met} [$L \cdot h^{-1}$] | Metabolic clearance | 199.6 | 4.15 | | FIXED | |
| $V_{c, fed}$ [L] | Effect of food on central volume | | | | 9.20 | 13.8 |
| $k_{a, fed}$ [h^{-1}] | Effect of food on absorption rate | | | | -0.117 | 17.7 |
| $k_{met, fed}$ [h^{-1}] | Effect of food on pre-systemic metabolic rate | | | | -1.01 | 2.20 |
| $Q_{MP, fed}$ [h^{-1}] | Effect of food on metabolic inter-compartment clearance 1 | | | | -48.3 | 6.02 |
| Early _{MDZ,prop} | Early proportional error for MDZ (split: 0.5 h) | 0.500 | 3.36 | | FIXED | |
| Late _{MDZ,prop} | Late proportional error for MDZ (split: 0.5 h) | 0.147 | 4.12 | | FIXED | |
| Late _{MDZ,prop, fed} | Late fed proportional error for MDZ (split: 1.5 h) | --- | --- | | -0.0760 | 4.08 |
| Early _{1'-OHMDZ,prop} | Early proportional error for 1'-OH MDZ (split: 0.5 h) | 0.543 | 3.25 | | FIXED | |
| Late _{1'-OHMDZ,prop} | Late proportional error for 1'-OH MDZ (split: 0.5 h) | -0.215 | 3.91 | | FIXED | |

MODEL DEVELOPMENT RESULTS

| Inter-Individual Variability | | | | | |
|--------------------------------------|---|--------|------|-------|-------|
| ω^2_{Vc} | Variance of MDZ central volume | 0.368 | 9.34 | 16.5 | FIXED |
| ω^2_{Vp1} | Variance of MDZ peripheral 1 volume | 0.416 | 12.6 | 25.8 | FIXED |
| ω^2_{Qp1} | Variance of MDZ inter-compartment clearance 1 | 0.499 | 12.0 | 9.6 | FIXED |
| ω^2_F | Variance of bioavailability | 0.214 | 12.9 | 24.1 | FIXED |
| ω^2_{kmet} | Variance of pre-systemic metabolism rate | 0.309 | 11.6 | 11.1 | FIXED |
| ω^2_{Qmet} | Variance of MDZ clearance via metabolism | 0.0832 | 46.3 | 53.4 | FIXED |
| ω^2_{Vmet} | Variance of metabolic central volume | 0.349 | 9.34 | 18.1 | FIXED |
| ω^2_{QMP} | Variance of metabolic inter-compartment clearance 1 | 0.551 | 12.4 | 17.2 | FIXED |
| ω^2_{CLmet} | Variance of metabolic clearance | 0.155 | 29.2 | 50.8 | FIXED |
| $\omega^2_{Vmet} \sim \omega^2_{Vc}$ | Covariance of MDZ central volume and 1'-OH MDZ central volume | 0.615 | 14.0 | --- | FIXED |
| Inter-Occasion Variability | | | | | |
| ω^2_F | Inter-occasion variability for bioavailability | 0.161 | 13.3 | 40.1 | FIXED |
| ω^2_{Qmet} | Inter-occasion variability for MDZ clearance via metabolism | 0.152 | 15.1 | 17.3 | FIXED |
| ω^2_{CLmet} | Inter-occasion variability for metabolic clearance | 0.300 | 18.9 | 3.1 | FIXED |
| OFV* | | 2358 | | -4100 | |

*Due to different datasets, OFVs are not comparable, however, both OFVs are given for reference; relative standard errors for inter-individual variability are given on the approximate standard deviation scale (standard error/variance estimate)/2; obs = observations; OFV = Objective function value; prop. = proportional; RSE = Relative Standard Error; w/ = with

Examination of the diagnostic plots (Appendix Figure A1) indicated similar results to those seen with the individual models, in that midazolam concentrations were well described and 1'-OH midazolam concentrations were generally well described, although they were still under-predicted at higher concentrations. The majority of individual weighted residuals for both analytes were between ± 1.96 standard deviations, and no real trends were noted for error distribution. Furthermore, VPCs conducted for both the original dataset and for the prospective dataset indicated the model described both sets of data well, although the maximum concentrations and 2.5th percentile of 1'-OH midazolam concentrations continued to be under-predicted for the oral + iv administration of midazolam (Appendix Figure A2). The resulting final model is illustrated in Figure 20.

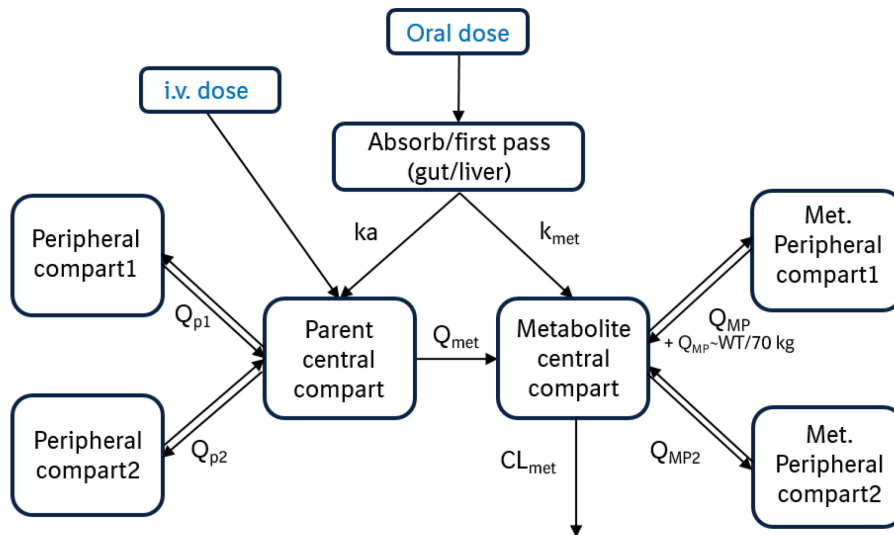


Fig. 20: Adopted composite parent-metabolite midazolam model: 3-compartment model for each substance, first-order absorption and linear elimination; k_{met} = pre-systemic metabolism rate; k_a = absorption rate constant; $Q_{p1}/Q_{p2}/Q_{MP1}/Q_{MP2}$ = inter-compartmental clearance; Q_{met} = midazolam clearance via metabolism; CL_{met} = metabolic clearance; WT = weight.

3.2.4 Model Assessment of Drug-Drug Interaction

To assess the adopted midazolam and composite models' ability to predict drug-drug interactions, final model parameter and variance values were fixed (Tables 10 and 14) and CYP3A modulation (inhibition or induction) was added as a covariate of F_1 and CL for the adopted midazolam model, and of F , Q_{met} , k_{met} , and CL_{met} for the composite model. Based on visual inspection of concentration-time profiles, a differential influence of reversible compared to irreversible inhibitors was present for the exposure of both midazolam and 1'-OH midazolam. Thus, for the midazolam model and the composite model, the inhibitory treatment effect was split into two components – one representing reversible inhibition and one representing irreversible inhibition - for V_c and for CL_{met} . For V_c , only an effect of irreversible inhibition was added, as adding the other treatment effects resulted in a worse fit to the data. Applying this same split for inhibition to the other parameters did not improve the model fit.

Including treatment effects in the midazolam model resulted in an increase in bioavailability of 0.529 (i.e. an additional 52.9%; RSE: 10.0%) and a decrease in clearance of 15.1 L/h (RSE: 2.45%) following inhibition, with an additional increase in central compartment volume of 16.6 L (RSE: 15.6%) following irreversible inhibition. Induction of CYP3A resulted in a decrease in bioavailability of 0.199 (i.e. a deduction of 19.9%; RSE: 6.09%) and an increased clearance of 39.8 L/h (RSE: 22.3%). The proportional residual error term added for inhibition was -0.195

MODEL DEVELOPMENT RESULTS

(RSE: 12.9%). For the composite model, addition of treatment effects resulted in the changes listed in Table 15. The effects of induction on the model parameters were generally estimated with less precision than for inhibition, likely due to the limited data available for estimating the effects. Furthermore, the increase in metabolic clearance following irreversible inhibition appeared rather high and, thus, was likely overestimated. As a whole, however, the effects appeared plausible and were estimated with reasonable precision.

Tab. 15: Interaction parameter values for the final adopted composite model.

| Effect Parameter | Parameter Meaning | Value | RSE [%] |
|----------------------------|---|--------|---------|
| Inhibition | | | |
| $V_{c,INH2}$ [L] | Irreversible inhibition effect on V_c | 23.2 | 24.2 |
| $k_{met,INH}$ [h^{-1}] | Overall inhibition effect on k_{met} | -1.04 | 15.4 |
| F_{INH} [%] | Overall inhibition effect on bioavailability | 77.7 | 16.3 |
| $Q_{met,INH}$ [h^{-1}] | Overall inhibition effect on midazolam clearance | -14.1 | 3.37 |
| $CL_{met,INH1}$ [L/h] | Reversible inhibition effect on metabolic clearance | -78.7 | 15.0 |
| $CL_{met,INH2}$ [L/h] | Irreversible inhibition effect on metabolic clearance | 1159 | 10.1 |
| $Early_{prop,INH}$ | Early proportional error for inhibition | 0.532 | 4.20 |
| $Late_{prop,INH}$ | Later proportional error for inhibition | -0.309 | 5.95 |
| Induction | | | |
| $k_{met,IND}$ [h^{-1}] | Induction effect on k_{met} | 1.56 | 46.0 |
| F_{IND} [%] | Induction effect on bioavailability | -39.1 | 16.3 |
| $Q_{met,IND}$ [h^{-1}] | Induction effect on midazolam clearance | 38.7 | 22.1 |
| $CL_{met,IND}$ [L/h] | Induction effect on metabolic clearance | -47.3 | 23.6 |

Inspection of the diagnostic plots revealed a generally good fit to the data for both the midazolam model and the composite model. Plotting the individual model estimated concentration-time profiles against the observed concentrations also showed good concordance between the model and the actual data (see Appendix Figures A3 and A4). Examination of the VPC for the midazolam model showed that the 2.5th and 97.5th percentiles, and the median values for all treatments were mostly contained within the respective 95% CIs. The exception to this was for the single dose with inhibition, where the model over-predicted the 2.5th percentile and under-predicted the 97.5th percentile during the elimination phase; the median was mostly contained within the 95% CI over the full dosing interval. For the interaction model, observed data were again relatively well described (Figure 21), although a worse fit was noted for 1'-OH midazolam following inhibition when administered orally first, followed by iv administration. Given that the data for that regimen were particularly scarce, with only 6 subjects contributing to the set, it was not considered representative of the overall model fit. The VPCs for the midazolam model with interaction

MODEL DEVELOPMENT RESULTS

are displayed in Appendix Figure A5. Due to limited data, confidence intervals for the inhibition and induction data were relatively wide.

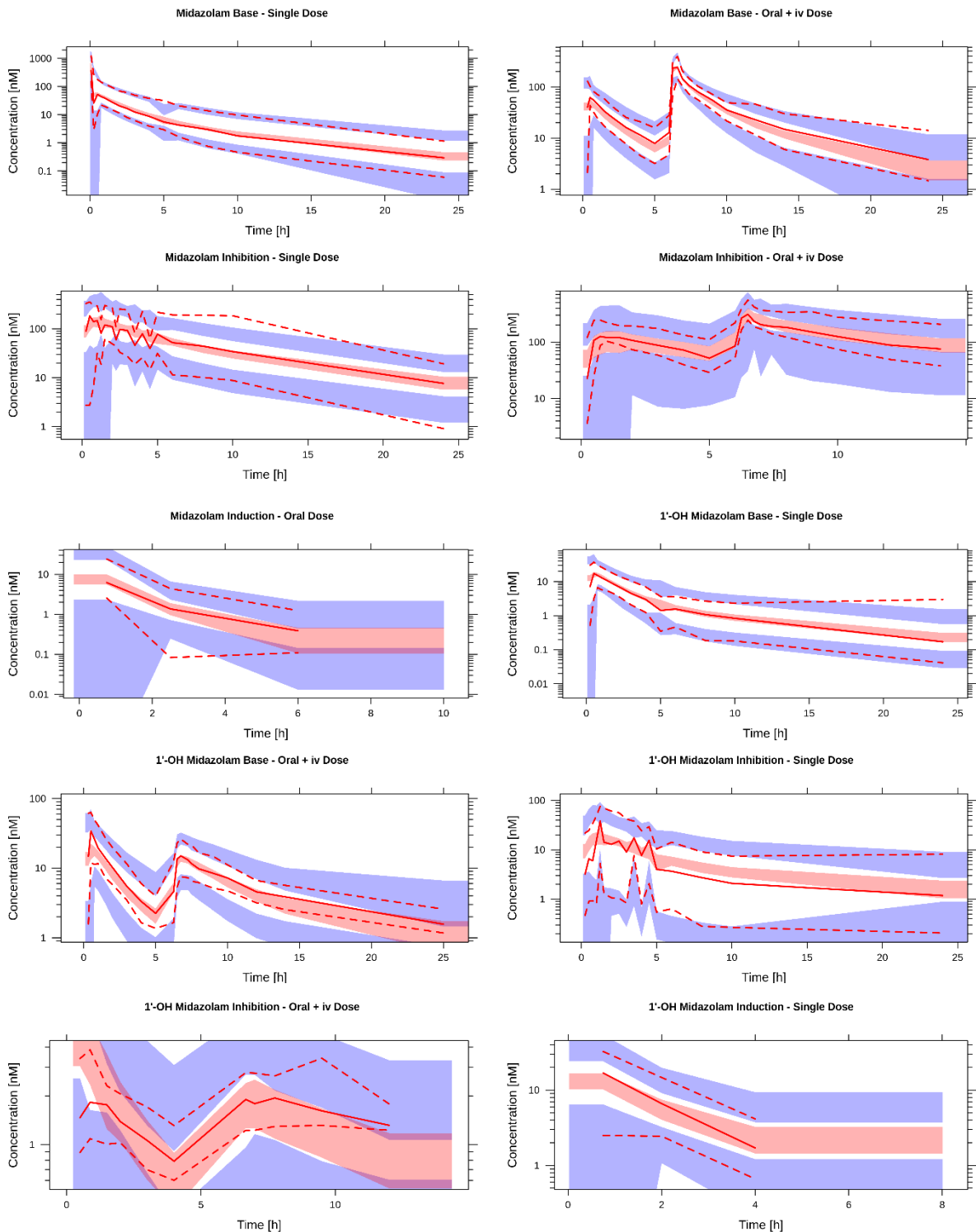


Fig. 21: Visual predictive checks for the final interaction model. 1000 simulations were used and data are displayed on a semi-log scale. The solid red line depicts the observed median concentrations, while the dotted lines depict the observed 97.5th and 2.5th percentiles. The shaded red area pertains to the 90% confidence interval for the predicted medians, while the shaded blue areas pertain to the 90% confidence interval for the 97.5th and 2.5th percentile predictions. Data are normalised to a midazolam dose of 4 mg. nM = nanomolar; h = hours.

3.2.4.1 *Cut-points*

Using model estimated parameters, an assessment of potential cut-points to use for identifying the different CYP3A modulation categories (inhibition, no modulation, induction) was conducted for the adopted midazolam model and for the final composite model. For the midazolam model, the parameter with the highest accuracy identifying modulation categories was clearance (CL). The applied cut-points, 4.85-13.2 L/h (inhibition), 13.2-39.6 L/h (no modulation), and 39.6-80.4 L/h (induction), correctly identified 100% of cases in the model development dataset. The cut-points were then applied to the estimated parameters from the prospective study data and 100% of cases were again correctly classified. Although upper and lower limits were given for the cut-points, cases falling below the lowest identified value (4.85 L/h) and those falling above the highest value (80.4 L/h) should be categorised as inhibition and induction, respectively. Thus, for the datasets tested, both specificity and sensitivity of the determined cut-offs was 100% using the midazolam only model.

The model estimated parameter with the highest accuracy in identifying modulation categories in the composite model was also midazolam clearance (Q_{met} ; i.e. the clearance of midazolam via metabolism). Cases were correctly identified 98.21% of the time, with cut-points of 6.81-16.8 L/h (inhibition), 16.8-43.3 L/h (no modulation), and 43.3-86.6 L/h (induction). Of the incorrectly classified cases, 2/148 (1.35%) cases with no modulation of CYP3A were classified as inhibition, and 2/63 (3.17%) of inhibition cases were classified as having no modulation. None of the induction cases was incorrectly classified. Applying these cut-offs to the prospective study data, 99.33% of cases were correctly categorised and for the values estimated from the external validation set (limited sampling only), 100% of cases were correctly classified. The 2 incorrectly categorised cases from the prospective studies were no modulation cases that were classified as inhibition. Thus, over all datasets, a specificity of 500/504 (99.2%) was achieved, with a sensitivity of 148/150 (98.7%) for inhibition and of 24/24 (100%) for induction. These outcomes support the use of the cut-points determined from the model development set to identify DDIs based on midazolam clearance.

3.2.5 **Limited Sampling**

In order to test if the model would still adequately estimate concentrations with a limited sampling scheme, simulations based on the final midazolam and composite models were

performed. These were conducted using the limited sampling scheme of 2, 2.5, 3, and 4 hours (Katzenmaier et al. 2010; Katzenmaier et al. 2011), as these were the sampling times from the external validation set (see Tables 3 and 9 for more details), as well as being times that have previously been shown to be predictive of midazolam clearance. Results from the simulations using the midazolam only interaction model were congruent with the actual data for all conditions from the original dataset and from the prospective studies (Figure 21). For the external validation set, the data were well predicted for baseline conditions and inhibition, as well as for the induction condition with 1'-OH midazolam. However, the midazolam concentrations in the induction condition were under-predicted for this dataset. Interestingly, the slope of the median induction observations was relatively parallel to the slope of the predicted elimination phase, even if the estimated concentrations were lower than the actual observations. Figures 22 and 23 depict the simulation results for the midazolam model based on the limited sampling. High overlap between the observed concentrations and medians with the 90% prediction intervals are apparent for all but the previously noted induction condition. The simulations for the composite interaction model also showed good congruence with the observed data, with the majority of observed points falling within the 90% prediction intervals (Appendix Figures A6 and A7).

MODEL DEVELOPMENT RESULTS

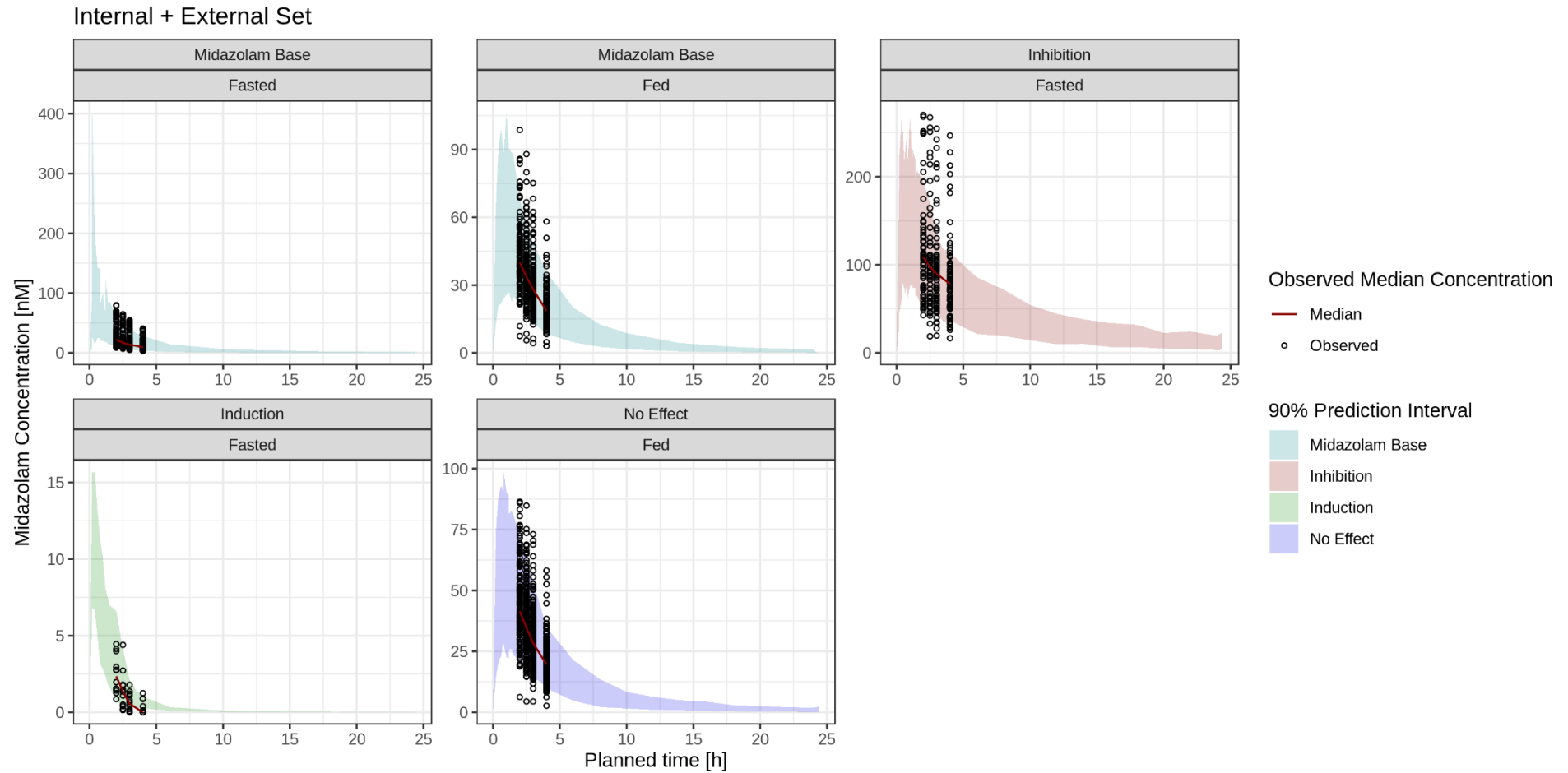


Fig. 22: Observed versus predicted midazolam concentrations, based on limiting sampling and the final adopted midazolam interaction model. Samples were taken at 2, 2.5, 3, and 4 h. Fasted conditions are simulated based on the original dataset, while fed conditions are simulated based on the prospective study dataset.

MODEL DEVELOPMENT RESULTS

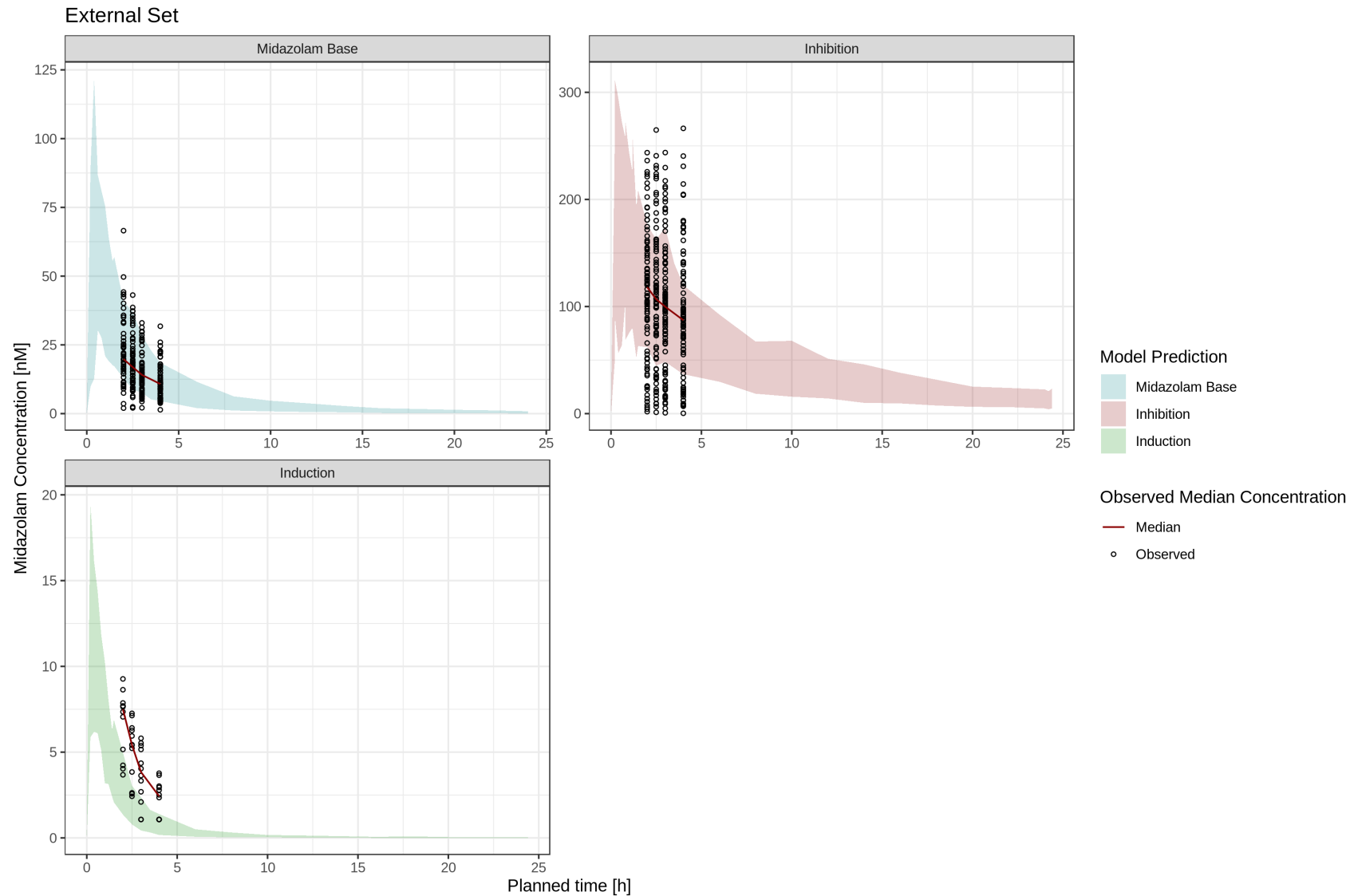


Fig. 23: Observed versus predicted midazolam concentrations, based on limiting sampling and the final adopted midazolam interaction model. Simulations are based on the external validation set and samples were taken at 2, 2.5, 3, and 4 h.

4. DISCUSSION

The current dissertation aimed to examine the feasibility of implementing and developing potential tools for more efficient determination of CYP3A DDIs. Specifically, the feasibility of implementing midazolam microdosing in early clinical studies was assessed, along with an exploratory comparison of AUC_{2-4} for test-to-reference ratios compared to $AUC_{0-\infty}$ ratios, given that AUC_{2-4} has previously been shown to be predictive of midazolam clearance for both baseline and DDI conditions (Katzenmaier et al. 2010; Katzenmaier et al. 2011). To complement microdosing and limited sampling, midazolam and composite midazolam + 1'-OH midazolam PopPK models were developed, together with proposed cut-points for clearance of midazolam via metabolism to potentially identify the presence of DDIs with a single profile. Various benefits could arise through the use of such tools, such as reduction of time and resources used during drug development, the reduction of subject and patient burden, as well as facilitation of DDI detection in clinical practice. The outcomes of the examinations are discussed below.

4.1 Midazolam Microdosing Implementation

Midazolam microdosing was successfully incorporated into three multiple rising dose studies for test compounds having given positive signals *in vitro* as perpetrators for CYP3A modulation. Specifically, Compounds A and B gave signals that they were both inactivators and inducers of CYP3A, while Compound C was found to be an inducer of CYP3A. Based on static mechanistic modelling of the *in vitro* results using the expected therapeutic exposure for Compound A, an overall increase in exposure of ~1.8-fold for midazolam was expected following multiple administration of Compound A. However, the C_{max} of Compound A was approximately 400-500 times higher than the concentration required for inactivation and ~14-17 times greater than that required to achieve an induction effect. These exposures were also much higher than the originally predicted therapeutic exposures, thus, larger effects of CYP3A modulation would have been expected. In particular, the effect of inactivation would have been expected to be particularly strong at Day 3, although by Day 14, the influence of induction may have reduced the overall impact of CYP3A modulation. For Compound B, C_{max} levels were ~7-18 and ~1.7-4.4 times higher than the thresholds for inactivation and induction determined *in vitro*, respectively. Based on experiments performed by others examining

DISCUSSION

simultaneous effects of induction and inactivation, it would be expected that the inactivation effect of the compound should dominate over the induction effect (Hafner et al. 2010). This may be particularly true, given that the inactivation effect was reached at a much lower threshold for Compound B than induction. Thus, it was expected that midazolam exposure would be increased following combined Compound B and midazolam treatment. However, even though the expectation was that midazolam exposure would be higher, it was still possible that the induction effect could negate any relevant inactivation effect, given that both exposure thresholds were exceeded. Finally, for Compound C, as of the second highest dose group, the achieved C_{max} concentrations were ~2-3 times higher than the induction thresholds determined *in vitro*. Furthermore, based on static mechanistic modelling, it was determined that an AUC ratio for midazolam of 0.122 should be expected (i.e. midazolam exposure at Day 14 should have been ~12% of that at baseline).

Midazolam concentrations and 1'-OH midazolam concentrations, when measured, were quantifiable over the entire sampling periods for all three studies. Concentration-time profiles for subjects receiving placebo plus midazolam showed that concentrations were consistent from one treatment period to the next, as evidenced by the overlapping gMean plots and similar C_{max} and AUC values, signifying that dosing was consistent between treatment arms. Geometric mean plasma concentration-time profiles for midazolam administered alone or in the presence of test treatment (combined over all dose groups) showed a minor increase in exposure for midazolam following treatment with Compound A, while no differences in concentration-time profiles for baseline and test treatment were evident following treatment with Compounds B or C (Figures 8 to 10). The concentration-time profiles for 1'-OH midazolam in Study 3, while showing greater variability between treatment arms, also did not indicate any relevant differences between treatments. Consistent with the concentration-time profiles from the three studies, analysis of C_{max} and $AUC_{0-\infty}$ showed midazolam ratios of 108-127% following dosing of Compound A, while point estimates of midazolam C_{max} and $AUC_{0-\infty}$ following administration together with Compound C or with Compound B were all close to 100%. Geometric mean ratios for CL/F showed similar results to those of $AUC_{0-\infty}$, albeit in the opposite direction, as a decreased clearance would result in increased exposure and vice versa. The 90% CIs of C_{max} and $AUC_{0-\infty}$ for midazolam in the presence of Compound A were mostly above 100%, although only the highest point estimate of 127.1% (for $AUC_{0-\infty}$ following 14 days of 200 mg Compound A dosing) would fall within the classification given by the FDA

of a weak inhibitor (1.25 to 2-fold increase of AUC) (US-FDA 2020a). Upon examination of individual test-to-reference ratios, the proportion of placebo subjects having point estimates in the range of a weak inhibitor or weak inducer in Study 1 was the same as the proportion of subjects in the 200 mg Compound A dose group (both 33.3% of subjects) whose point estimates would have classified them as having a DDI. This suggests that even the finding of one point estimate exceeding 125% was likely due in part to intra-individual variability in CYP3A activity, which has been found to vary by 5.25-21.8% (median: 9.75%) between occasions (Kashuba et al. 1998). For Compounds B and C, 90% CIs were mostly within or barely exceeded the range of 80 to 125%. Thus, despite all three compounds exceeding the thresholds defined from *in vitro* analyses, none of the compounds resulted in a relevant CYP3A DDI.

The lack of clinically relevant DDIs seen in these studies is consistent with findings showing higher false positive results for time-dependent inhibition (i.e. inactivation)(Vieira et al. 2014). Furthermore, the observation that substances with positive signals for both time-dependent inhibition and induction tend to overestimate inactivation potential (Einolf et al. 2014) is supported by the results of these studies, as 2 out of the 3 studies indeed had positive *in vitro* signals for both induction and inactivation. However, in contrast to the findings of Einolf et al. (Einolf et al. 2014), where induction was found to be well predicted *in vitro*, no relevant induction effect was observed in Study 3, where *in vitro* findings indicated that only induction potential was present. This discrepancy may come from the poor solubility of the test compound along with the propensity of the substance to bind to various plastic surfaces and microsomal proteins, thereby limiting the concentrations which could be tested *in vitro*; thus, potential inhibition effects in combination may have been missed. Additionally, the thresholds given by the authorities are designed to avoid false negatives to ensure the safety of patients, which consequently results in a higher number of false positive results. One may be tempted to hypothesize that the lack of evident DDI effect is due to a deficient sensitivity of the midazolam microdosing method itself. However, due to the linearity of midazolam over such a large range (Halama et al. 2013; Hohmann et al. 2015), as well as the finding from several researchers that DDI effects on midazolam microdoses scale well to those for therapeutic doses of midazolam (Croft et al. 2012; Halama et al. 2013; Prueksaritanont et al. 2016), this is considered an unlikely explanation.

DISCUSSION

Through the incorporation of midazolam microdosing in the early clinical studies described here, three dedicated DDI studies were avoided. This is particularly important given the nature of the DDIs being examined. Both inactivation and induction take multiple days for full effects to be seen and, thus, dedicated studies using the therapeutic dose of midazolam would have required a minimum of 1.5-2 weeks. Combined with the fact that such studies traditionally include a minimum of 12 subjects each, considerable time and resources were saved. Furthermore, subject burden was avoided for the at least 36 additional healthy subjects who would have been needlessly exposed to the test substances. Due to its linearity over a 30,000-fold dose range, midazolam microdosing is in-line with health authority guidelines, which state that for a victim drug, any dose within the linear range may be used to assess DDIs (US-FDA 2020a). Thus, microdosing incorporated with early clinical development can be a useful tool to avoid dedicated DDIs following positive results from *in vitro* examinations.

As microdosing is just one tool with which subject burden can be reduced in clinical trials, further methods have been proposed which may compliment the use of microdosing. Specifically, numerous researchers have proposed that a limited sampling scheme with midazolam may be adequate for determining CYP3A activity (Katzenmaier et al. 2010; Katzenmaier et al. 2011; Lee et al. 2006; Yang et al. 2018). Based on the time points found by Katzenmaier et al. (2, 2.5, 3, and 4 h) to be particularly predictive of the clearance of midazolam via metabolism both during constitutive and modulated CYP3A activity (Katzenmaier et al. 2010; Katzenmaier et al. 2011), an explorative analysis using AUC_{2-4} was conducted. Results of the analysis revealed that for all three studies, the ratios between treatment arms obtained using the partial AUC were consistent with those obtained using $AUC_{0-\infty}$. These results lend further support to the findings of Katzenmaier et al. regarding the ability to assess the presence of DDIs using just AUC_{2-4} . Additionally, in the three studies reported here, midazolam was given following a continental breakfast, suggesting that the limited sampling is robust to conditions such as food effects. Therefore, the limited sampling scheme proposed by Katzenmaier et al. appears to be an effective tool for assessing DDIs while reducing subject burden.

In the early clinical studies presented here, only a few drug-related AEs were reported during administration of midazolam with or without active substance and all that were reported were of mild or moderate intensity. The reported AEs were all in-line with those reported on days

when no midazolam was administered, suggesting that AEs were likely attributable to the test conditions or the test compounds themselves. This is supported by other studies which have shown that no adverse events or benzodiazepine effects are seen following midazolam microdosing (Eap et al. 2004). However, due to the presence of AEs at baseline in one of the three studies and the presence of AEs during placebo administration, as well as due to the design of the studies, the contribution of midazolam to the AEs reported here cannot be completely ruled out.

4.1.1 Limitations

Although midazolam microdosing has been shown to be a feasible and potentially useful tool for early clinical development, several limitations of the methodology are still present. First, there are currently no existing microdose formulations on the market; thus, dilutions are done on-site no more than 24 hours prior to dosing. This means that for each pharmacokinetic profile day, a new dilution must be prepared, potentially resulting in variability between doses administered on one day compared to another. However, the dilution procedure was designed to be quite simple, with only a limited number of steps involved. Therefore, it is expected that any variations in dose would be negligible, with little impact on the DDI assessment. Furthermore, subjects receiving placebo instead of active test compounds also received midazolam, so any differences in exposure due to different midazolam doses administered rather than due to modulation by the test substances would be seen for the placebo subjects, too. In Study 3, 1'-OH midazolam was also measured, which provides further assessment of the nature of midazolam concentration changes. If concentrations of both substances are impacted in similar ways over treatment conditions, then this implies that exposure differences are due to inter-occasion variability, a difference in dose, or a combination thereof. If the concentrations are impacted in opposite directions or to a different magnitude, this suggests that differences in midazolam concentrations are due to modulation of CYP3A activity. Thus, the additional measurement of 1'-OH midazolam would be desirable to obtain when conducting midazolam microdosing studies. Finally, for future studies it may be possible to obtain microdose formulations, as such preparations are currently under investigation for more regular use (PMID: 31102650) (Kiene et al. 2019).

Another limitation to the midazolam microdosing strategy proposed here is that AEs cannot be unambiguously assigned to the test substance versus midazolam. However, as mentioned before, other studies using midazolam microdosing alone have found that neither AEs nor pharmacodynamic effects, such as drowsiness or other sedative effects, have been noted (Eap et al. 2004; Halama et al. 2013; Hohmann et al. 2015), suggesting that the microdose indeed results in sub-pharmacological levels.

Finally, a limitation for the current dissertation is the lack of actual DDI effect observed for the test substances presented here. Although midazolam microdoses have previously been shown to result in the same levels of inhibition and induction effects as those produced with therapeutic doses (Croft et al. 2012; Halama et al. 2013; Prueksaritanont et al. 2016), examination of a substance with a clear DDI effect would provide unequivocal support for the sensitivity of the method for detecting DDIs in early clinical studies.

4.1.2 Midazolam microdosing conclusion

The studies presented here support the implementation of midazolam microdosing in early clinical studies, as they show that such an approach can be successfully implemented in the clinic with fully quantifiable profiles. Results of the presented studies provide confirmation that the signals for potential DDI liability determined *in vitro* do not necessarily translate into similar results *in vivo*. In all three studies, liabilities for induction and/or inactivation of CYP3A were observed *in vitro*, but no DDIs were detected *in vivo*, despite the fact that the C_{max} values for all three substances exceeded the predicted thresholds required for seeing clinically relevant DDIs. Midazolam microdosing was shown to be a safe and feasible tool for reducing the need for unnecessary dedicated drug-drug interaction studies during drug development, which may be complimented through the use of limited sampling designs. The results obtained from the microdosing implemented here allowed for earlier acquirement of information pertaining to the actual CYP3A DDI liability of the drug compounds under development, thereby supporting the selection of allowed medications for Phase II and III trials. Thus, by incorporating midazolam microdosing in early clinical studies, three further dedicated studies were avoided, thereby reducing the number of healthy subjects needlessly exposed to test substances, as well as reducing costs, time, and needed resources, while

gaining valuable information regarding CYP3A DDI liability for the future development of the test compounds.

4.2 Model Development

The microdosing approach employed in the preceding studies is one of several tools that may be implemented for more efficient assessment of DDI liability. An exploratory examination of a limited sampling scheme showed results similar to those obtained with $AUC_{0-\infty}$ assessments, suggesting this may be another method for improving DDI assessment through reduced subject burden. Modelling is a complementary technique for these proposed tools, as it may be used to increase the accuracy with which limited sampling techniques can detect DDIs. Thus, the aim of the model presented here was to describe the pharmacokinetics of midazolam and 1'-OH midazolam under various conditions of CYP3A activity (constitutive, inhibition, and induction) in healthy adult subjects, examining both extensive and sparse sampling designs. Numerous midazolam PopPK models have been developed previously (Brill et al. 2016; Brill et al. 2014; Brussee et al. 2018; Tomalik-Scharte et al. 2014; van Rongen et al. 2015; Yang et al. 2018), although none have assessed midazolam under conditions of CYP3A inhibition or induction. The composite model developed here was best described with 3-compartments for both analytes, first-order absorption and linear elimination. A two-step proportional error model was used to describe the residual variability. Addition of treatment effects to F , Q_{met} , k_{met} and CL_{met} , as well as a proportional error term for the delayed t_{max} by inhibition allowed for adequate description of the midazolam and 1'-OH midazolam concentrations under conditions of inhibition and induction. As an exploratory objective, potential cut-points were examined for identifying potential CYP3A activity conditions using a single profile. The outcome of the development, followed by the overall assessment of appropriateness and use for DDIs are discussed in the following sections.

4.2.1 Structural models

The structural model resulting in the best diagnostics and best overall fit to the data was the 3-compartment model for midazolam, combined with a 3-compartment model for 1'-OH midazolam. The 3-compartment model used to describe midazolam was in agreement with models by Brill et al. (Brill et al. 2014), Zomorodi et al. (Zomorodi et al. 1998), and by Brussee et al. (Brussee et al. 2018). In contrast, the model reported by Tomalik-Scharte et al. best

described midazolam pharmacokinetics with a 1-compartment model (Tomalik-Scharte et al. 2014), while multiple other groups found a 2-compartment model to be a better fit for midazolam (Hostler et al. 2010; Nguyen et al. 2016; Seng et al. 2014; Swart et al. 2004; van Rongen et al. 2015; Yang et al. 2018). As noted earlier, in the majority of the published models, data were obtained from a relatively small sample size (6-32 subjects), limiting the number of compartments and/or parameters which can be estimated by the models. The sample size for the current model development was much larger, with 99 subjects contributing to both midazolam and to 1'-OH midazolam concentration profiles. Furthermore, multiple subjects in the model development dataset contributed two or more profiles, as opposed to the single profiles modelled in the previous models, thereby increasing the number of observations going into the model development. Note that in the model by Tomalik-Scharte et al., not only was a small sample size used, but also the design consisted of hourly samples during a continuous infusion of midazolam; samples were not taken once the infusion was stopped, when distribution processes between compartments would likely be most apparent. Thus, the limited sample size and lack of sampling following withdrawal of midazolam likely reduced the ability to detect multiple compartments. Moreover, a 1-compartment model is inconsistent with the observation that midazolam is generally described as declining in an at least biexponential fashion (e.g. (Thummel and Wilkinson 1998).

For 1'-OH midazolam, the best structural model found in the current evaluation was a 3-compartment model, although a 2-compartment model may also have been acceptable. This is in contrast to other models, where 1'-OH midazolam was found to be best described using a 1-compartment model (Brussee et al. 2018; Nguyen et al. 2016; Seng et al. 2014; Tomalik-Scharte et al. 2014; van Rongen et al. 2015). Of note, two of the models also included 1 or 2 compartments for 1'-OH midazolam glucuronide (Seng et al. 2014; van Rongen et al. 2015), and the clearance into and between these compartments may have been partly captured by the 1'-OH midazolam structure in the present model. In addition, the small sample sizes noted earlier would have provided additional limitations in the structural assessments for the models. Another difference for at least the model by Brussee et al. is the fact that it was developed on a paediatric population, where CYP3A activity would not be as mature (children were between the ages of 1 and 18 years) and where sampling is generally less extensive (at least in the younger populations), limiting one's capacity to identify multiple compartments.

Thus, while some discrepancies existed for the 1'-OH midazolam model structure, which has not been examined in many of the existing models, the composite model structure was still largely concordant with the structures of midazolam models developed to date.

4.2.2 Statistical and covariate models

The statistical model providing the best results for midazolam models has been relatively consistent. Specifically, in the majority of literature, as well as in the current work, a proportional error model was found to best describe the residual unexplained variance. Consistent with Yang et al. (Yang et al. 2018) a two-step error approach was applied to the residual error, given the observation that there was greater error for the earlier time points than for the later time points. In contrast to the error model used here, Brussee et al. (Brussee et al. 2018) and van Groen et al. (van Groen et al. 2019) found that a combined proportional and additive error model was best-suited for describing residual variability. However, both groups examined paediatric populations where physiological processes would be at various levels of maturation, possibly accounting for the need to include the extra additive error term.

Examination of covariates affecting CYP3A activity has generally resulted in mixed conclusions. Although some studies have found an effect of sex, weight, and/or age (Brill et al. 2014; Brussee et al. 2018; Chen et al. 2006; Dresser et al. 2000; van Rongen et al. 2015), others have found no effect of these covariates (Kashuba et al. 1998; Thummel et al. 1996; Tomalik-Scharte et al. 2014). In the current model, the population consisted of a good proportion of males to females (59:40), which should allow reliable conclusions to be drawn regarding the covariate of sex. The ages included were within a restricted range (19 to 52 years) and all weights were within a healthy range for adults, so extrapolation to paediatric or elderly populations or to obese populations would require additional investigation. Despite these limitations, a relationship between weight and metabolite inter-compartmental clearance were observed and included in the composite model. Although age was found to be correlated with k_{met} , the addition of age to the model did not improve the model fit or decrease variability, suggesting it may have been a spurious finding. Thus, it was not included in the final composite model. Sex was not found to be a significant covariate of any of the model parameters and in the midazolam only model, no covariate relationships were found to be present.

Although other groups have found weight to be related to midazolam parameters, these models have generally examined special populations. Specifically, weight was found to be a significant covariate of midazolam parameters in models examining paediatric populations and obese populations (Brill et al. 2014; Brussee et al. 2018; van Rongen et al. 2015), although the relationship with weight found by van Rongen et al. was more related to excess body weight. Visual examination of the plots provided by Brill et al. also suggested that their correlation with weight was more related to excess body weight, as it was not apparent in the healthy volunteers. Other models examining midazolam pharmacokinetics in healthy adults did not find weight to be a covariate of midazolam parameters (Tomalik-Scharte et al. 2014; Yang et al. 2018), which is in-line with the examination performed for the midazolam only model. Consistent with the finding that weight was related to 1'-OH midazolam parameters, in one of the few models which also examined metabolite concentrations, weight was found to be a covariate of 1'-OH midazolam clearance and volume of distribution (Seng et al. 2014). Given the limited number of models including 1'-OH midazolam, the correlation with weight and metabolite exposure should be further assessed in future models to confirm the relationship found here and by Seng et al.

In contrast to the results of the presented model, Yang et al. found both age and sex to be significant covariates of midazolam clearance and central compartment volume, although only the effect on volume was retained in the final model (Yang et al. 2018). 1'-OH midazolam was not included in the model, thus, potential relationships with the metabolite concentrations are unknown. As ages included in the model development by Yang et al. were also relatively restricted (similar age range to the current analyses), further modelling activities including an expanded age range would be needed to determine if relationships are true or spurious.

4.2.3 Final models with constitutive CYP3A activity

Midazolam model estimates for CL, F, V_c , Q_{p1} , and Q_{p2} were in-line with those found by others (Brill et al. 2014; Yang et al. 2018), although k_a was estimated to be lower than in other models. Proportional error estimates were found to be comparable with the estimates from the model by Yang et al. (Yang et al. 2018), whose residual error approach was similar to that in the present model. As further support for the appropriateness of the final models, estimates for CL and F were in-line with the pharmacokinetics of midazolam found in clinical studies

(Heizmann et al. 1983), showing physiological plausibility. Model estimates of CL_{met} for 1'-OH midazolam were also in general accordance with previous models (Brussee et al. 2018; Seng et al. 2014; Tomalik-Scharte et al. 2014; van Rongen et al. 2015), and with the values found in the microdosing study described in Section 3.1.3. As other models generally described 1'-OH midazolam using a 1-compartment model, comparisons between other metabolite parameters cannot be made.

The final models displayed both good internal and external validity, as evidenced by visual predictive checks conducted on both the data used to develop the model, as well as on the data from the prospective studies. Median values and the 97.5th percentile values were almost always within the confidence intervals provided by the VPC simulations, although the 2.5th percentile was sometimes under-predicted by the model. As the models covered various situations, including different dosing regimens (oral, iv, or semi-simultaneous oral + iv administration), different conditions (fasted vs fed), and different sites of data collection, this suggests that the model should be fairly robust and applicable for numerous settings. Thus, the model was found to perform well under constitutive CYP3A activity levels and was subsequently examined for CYP3A inhibition and induction.

4.2.4 Drug-drug interaction assessment

Treatment effects for inhibition and induction were added to the final composite and midazolam only models. Applying treatment effects to midazolam clearance, bioavailability, and central volume of distribution for the midazolam only model, with the addition of treatment effects on pre-systemic rate of metabolism, and metabolic clearance for the composite model generally resulted in a good description of the midazolam data following CYP3A inhibition and induction with potent perpetrators. 1'-OH midazolam concentrations were less well-described, although model fit was still adequate. The reason for the less well-described metabolite concentrations may be due to a number of factors. First, inhibition via both reversible and irreversible inhibitors were included in the dataset; as these have different mechanisms of action, they would not necessarily be expected to impact exposure in the same way. Including an additional term for irreversible inhibition on metabolic clearance and on midazolam's central volume of distribution provided a better fit for the data, but still resulted in a less ideal overall fit of 1'-OH midazolam concentrations compared to the other CYP3A

conditions. More data using each of the different inhibitor types would help to further tease out the impact of the different inhibitors on metabolite concentrations.

Another potential reason for the less well-described 1'-OH midazolam concentrations is likely related to the differing levels of CYP3A activity at the intestinal and hepatic levels, as well as to the fact that 1'-OH midazolam goes on to be further metabolised. The further glucuronidation of 1'-OH midazolam would increase variability of the model, both for constitutive and modulated CYP3A activity, resulting in additional variability that can be hard to account for. Moreover, 1'-OH midazolam is not the only metabolite produced via CYP3A metabolism and while midazolam clearance would look the same, regardless, differing amounts of each of the produced metabolites may contribute to increased variability in the 1'-OH midazolam portion of the model that cannot be accounted for without additional information pertaining to the minor metabolites. The increased variability for 1'-OH midazolam is consistent with the findings of Study 3 of the midazolam microdosing studies, whereby the gMean concentration-time profiles also indicated a greater variability in 1'-OH midazolam exposure. This suggests the increased variability, whether due to differences in metabolite formation, further metabolism or for other reasons, provides a reasonable explanation for a decreased ability to describe these data well in the model. All-in-all, however, the model described the data relatively well for all conditions and, thus, was considered to be a good model for assessment of CYP3A DDIs.

The utility of the model was further assessed through the determination of model predicted cut-points that may help in identifying if a midazolam profile is based on constitutive levels of CYP3A activity, inhibited levels of activity, or induced levels of activity. The parameter with cut-points that were most accurate in categorising the individual cases was midazolam clearance via metabolism. Given that metabolism is the process affected by CYP3A modulation, this outcome is not surprising. Less than 2% of cases were incorrectly identified using the cut-points from the composite model. Those cases that were falsely categorised tended to be constitutive activity cases that were classified as inhibition cases, meaning that the presence of interactions would generally not be missed. As such, the model predictions can be useful not just during drug development, but also in clinics when baseline conditions are not necessarily available for classification of a DDI.

4.2.5 Limited sampling assessment

As a final assessment of the model utility, simulations were conducted using limited sampling schemes from the model development dataset, as well as from the prospective studies and an external validation set. Simulations were mostly in-line with the observed data, although the 90% prediction interval for induction with the external dataset showed an under-prediction for concentrations, suggesting that a larger effect of induction would be predicted by the model than what is actually seen. As such, the model would likely benefit from additional induction datasets, in order to improve the estimation of this effect. In general, however, the model shows good predictive ability, even when only limited sampling is provided. Thus, the model may be combined with limited sampling for facilitating assessment of the presence of CYP3A DDIs.

4.2.6 Limitations

A number of limitations were present in the current model. Specifically, the 1'-OH midazolam concentrations could not be as well described as those of midazolam itself, likely due to varying levels of CYP3A activity, both at the intestinal and hepatic levels, as described in the sections above. Furthermore, in the composite model, the 1 µg and lower doses were particularly hard to model for 1'-OH midazolam and, thus, were removed from the dataset (note that for midazolam, only the nanomolar doses caused the model to become unstable). This limitation with the lower doses mostly stems from the fact that the lower limit of quantification for the 1'-OH metabolite resulted in a large number of measurements below the limit of quantification. Given that the model adequately described the data between 3 µg and 4 mg and that most studies would likely be using doses within this range, this limitation is not considered particularly problematic.

Another limitation of the presented model was that the amount of data for induction was relatively limited (only 1 study with full profiles, consisting of only 12 subjects). As such, although the individual predictions were generally well described, the fit for the overall population would likely have been better with the inclusion of more data.

Finally, with regards to covariate analyses, as mentioned previously, the age and weight ranges included were still relatively limited (19-52 years and 47-111 kg), so results from the

model presented here do not necessarily extend to paediatric or elderly populations, or to obese individuals.

4.2.7 Model development conclusion

Both the developed composite parent-to-metabolite PopPK model and the midazolam only PopPK model were able to describe CYP3A activity in healthy adults during constitutive CYP3A activity, inhibited CYP3A activity, and induced CYP3A activity. Furthermore, the model was able to describe such activity over a broad range of doses, allowing it to be combined with microdosing approaches for reduced subject or patient burden. Simulations using limited sampling time points resulted in adequate predictions, suggesting the combination of a population pharmacokinetic model with limited sampling offers a good ability to detect clinically relevant pharmacokinetic DDIs. The obtained cut-points for clearance were able to categorise the vast majority of interactions correctly and, thus, may be useful indicators of interaction presence when only a single profile is available, making it particularly convenient for clinical practice. Examination with moderate or weak moderators would give additional benefit for the usefulness of these cut-points. Further research examining the applicability of the model to paediatric and elderly populations is warranted.

4.3 Overall Conclusions

Midazolam microdosing was successfully implemented in early clinical development studies. The results indicated that liability of the test compounds as being CYP3A perpetrators, despite all compounds exceeding the *in vitro* determined concentration thresholds for CYP3A DDI liability, was minimal at most. Partial AUC ratios showed good agreement with $AUC_{0-\infty}$ ratios, suggesting a limited sampling approach may be appropriate to assess the presence of DDIs. Furthermore, the developed PopPK models were able to adequately describe CYP3A activity interactions and, thus, would provide a useful tool for combining with limited sampling in the assessment of CYP3A DDIs. As such, the current dissertation has shown the feasibility of using midazolam microdosing and limited sampling in clinical studies, as well as providing three separate, complementary tools for the assessment of CYP3A DDIs.

5. SUMMARY

5.1 English

Due to its abundance in the human liver and gut, as well as the important role it plays in drug metabolism, CYP3A is a significant liability for drug-drug interactions. As such, efficient and accurate methods for detecting CYP3A drug-drug interactions are needed to facilitate assessment both in drug development and in the clinic. Several methods are considered in this work, including midazolam microdosing, a limited sampling approach, and population pharmacokinetic modelling. Microdosing consists of administration of a pharmacologically inactive dose that is no more than 1/100th of the therapeutic dose, which allows such doses to be administered with other substances without worry that they may influence the pharmacokinetics or pharmacodynamics of the co-administered substance. Limited sampling approaches use 1 to 4 samples to determine exposure of a drug, rather than obtaining a full pharmacokinetic profile. These approaches are ideal candidates for combining with population pharmacokinetic modelling, which can estimate full profiles from sparse sampling. Thus, the current dissertation had the following aims: 1) establish a method of incorporating midazolam microdosing in multiple rising dose studies for early detection of CYP3A drug-drug interactions; 2) develop a population pharmacokinetic model to describe midazolam exposure during constitutive, inhibited, and induced CYP3A activity; and 3) assess the capability of limited sampling to complement the two preceding aims. As an exploratory objective, model estimated parameters were assessed for potential cut-points that may allow for determination of drug-drug interactions when a baseline profile is not available.

For the establishment of midazolam microdosing in early clinical development, three early clinical studies were conducted with substances (Compounds A, B, and C) which gave positive CYP3A perpetrator signals *in vitro*. A 75 µg dose of midazolam was administered alone (baseline CYP3A activity) followed by administration with the highest dose groups tested for each compound on Day 1/3 and Day 14 or Day 17. Midazolam exposure ($AUC_{0-\infty}$, C_{max}) during administration with the test substances was compared to baseline data via an analysis of variance on log-transformed data. Partial AUC_{2-4} ratios were also compared to $AUC_{0-\infty}$ ratios using linear regression on log-transformed data. The data obtained from these studies were further used for external validation, following development of a composite midazolam-1'-OH midazolam population pharmacokinetic model for CYP3A drug-drug

interactions. The composite model was also evaluated using limited sampling profiles, both from the model development set, as well as from an external validation set.

The implementation of midazolam microdosing in early clinical studies proved to be feasible: Midazolam concentrations were quantifiable over the full profiles for all subjects in all studies and AUC and C_{max} values could, thus, be accurately determined. Results from the test compounds indicated that, based on the C_{max} values exceeding relevant thresholds, drug-drug interactions were expected. Point estimates of the midazolam $AUC_{0-\infty}$ gMean ratios ranged from 108.3 to 127.1% for Compound A, from 93.3 to 114.5% for Compound B, and from 92.0 to 96.7% for the two highest dose groups of Compound C. C_{max} gMean ratios were in the same range. Thus, despite the expectation of drug-drug interactions from *in vitro* results, midazolam microdosing results indicated no relevant interactions were present. AUC_{2-4} ratios, based on the limited sampling scheme suggested for subsequent studies (2, 2.5, 3, and 4 h), were comparable to the $AUC_{0-\infty}$ ratios in the conducted studies.

A composite model was developed, which adequately described midazolam and 1'-OH midazolam concentrations for constitutive, inhibited, and induced CYP3A activity. The model showed good internal and external validity, both with full profiles and limited sampling (2, 2.5, 3, and 4 h), and the model estimated parameters were congruent with values found in clinical studies. Assessment of potential cut-points for model estimated parameters to identify drug-drug interaction liability with a single profile suggested that midazolam clearance may reasonably be used to detect inhibition (6.81-16.8 L/h), induction (43.3-86.6 L/h), and no modulation (16.8-43.3 L/h). Sensitivities for potent inhibition and induction were 98.7% and 100%, respectively, and specificity was 99.2% for no modulation.

Thus, the current dissertation indicated that 1) midazolam microdosing incorporated into early clinical studies is a feasible tool for reducing dedicated drug-drug interaction studies; 2) a population pharmacokinetic approach can provide efficient and accurate CYP3A drug-drug liability detection; and 3) limited sampling can be a useful complementary tool for both midazolam microdosing and population pharmacokinetic modelling. Therefore, the current dissertation provides three separate, complementary tools for the assessment of CYP3A drug-drug interactions, either in drug development or in clinical practice.

5.2 Deutsch

Aufgrund seiner Menge in der Leber und im Darm sowie der wichtigen Rolle, die es im Arzneistoffmetabolismus spielt, ist CYP3A eine bedeutende Ursache für Arzneimittelinteraktionen. Daher sind effiziente und verlässliche Methoden zum Nachweis von CYP3A-Interaktionen erforderlich, um die Beurteilung sowohl in der Entwicklung als auch in der Klinik zu erleichtern. In dieser Arbeit werden Midazolam-Mikrodosierung, ein limitierter Probenentnahmeansatz und die Populations-Pharmakokinetik als Optionen berücksichtigt. Die Mikrodosierung besteht aus der Verabreichung einer pharmakologisch inaktiven Dosis, die nicht mehr als 1/100 der therapeutischen Dosis beträgt, wodurch solche Dosen mit anderen Substanzen verabreicht werden können, ohne befürchten zu müssen, dass sie die Pharmakokinetik/Pharmakodynamik der gleichzeitig verabreichten Substanz beeinflussen. Bei Ansätzen mit limitierter Probenentnahme werden 1 bis 4 Proben verwendet, um die Exposition eines Arzneimittels zu bestimmen. Diese Ansätze sind ideale Kandidaten für die Kombination mit der Populationsanalyse mit den vollständigen Profilen aus spärliche Messwerte geschätzt werden können. Daher hatte die aktuelle Dissertation folgende Ziele: 1) Etablierung einer Methode zur Einbeziehung der Midazolam-Mikrodosierung in frühen Studien mit steigender Dosis zur Früherkennung von CYP3A-Interaktionen; 2) Entwicklung eines populationspharmakokinetischen Modells zur Beschreibung der Midazolam-Exposition während der konstitutiven, inhibierten und induzierten CYP3A-Aktivität; und 3) Bewertung einer limitierten Probenentnahme zur Ergänzung der vorhergehenden Ziele. Als exploratives Ziel wurden vom Modell geschätzte Parameter potenzielle Grenzwerte bewertet, die die Bestimmung von Interaktionen ermöglichen können, wenn kein Basisprofil verfügbar ist.

Zur Etablierung einer Midazolam-Mikrodosierung in der frühen klinischen Entwicklung wurden drei frühe klinische Studien mit Substanzen (Substanzen A, B und C) durchgeführt, die *in vitro* positive CYP3A-Modulatorsignale ergaben. Eine 75 µg Dosis von Midazolam wurde allein verabreicht (Basis-CYP3A-Aktivität), gefolgt von der Verabreichung mit den höchsten Dosisgruppen, die für jede Substanz am Tag 1/3 und am Tag 14 oder Tag 17 getestet wurden. Midazolam-Exposition ($AUC_{0-\infty}$, C_{max}) während der Verabreichung mit den Testsubstanzen wurden über eine Varianzanalyse der logarithmisch transformierten Daten mit den Basisdaten verglichen. Partielle AUC_{2-4} Verhältnisse wurden auch mit $AUC_{0-\infty}$ Verhältnissen verglichen. Die aus diesen Studien erhaltenen Daten wurden nach der Entwicklung eines

pharmakokinetischen Populationsmodells für CYP3A-Interaktionen weiter als externe Validierung verwendet. Das finale Modell wurde auch unter Verwendung limitierter Stichprobenprofile bewertet.

Die Implementierung einer Midazolam-Mikrodosierung erwies sich als machbar: die Midazolam-Konzentrationen waren über die vollständigen Profile quantifizierbar, und die AUC- und C_{max} -Werte konnten somit genau bestimmt werden. Die Ergebnisse der Testsubstanzen zeigten, dass basierend auf den C_{max} -Werten, die die relevanten Grenzen überschreiten, Arzneimittelinteraktionen erwartet wurden. Die Punktschätzungen der Midazolam $AUC_{0-\infty}$ gMean-Verhältnisse lagen zwischen 108,3 und 127,1% für Substanz A, zwischen 93,3 und 114,5% für Substanz B und zwischen 92,0 und 96,7% für die beiden höchsten Dosisgruppen von Substanz C. C_{max} gMean-Verhältnisse lagen im gleichen Bereich. Trotz der Erwartung von Interaktionen, zeigten die Ergebnisse der Midazolam-Mikrodosierung, dass keine relevanten Interaktionen vorhanden waren. Die AUC_{2-4} -Verhältnisse waren mit den $AUC_{0-\infty}$ Verhältnissen in den durchgeführten Studien vergleichbar.

Es wurde ein Midazolam-1'-OH-Midazolam-Modell für konstitutive, inhibierte und induzierte CYP3A-Aktivität entwickelt. Das Modell zeigte eine gute interne und externe Validität, sowohl mit vollständigen Profilen als auch mit limitierter Stichprobe (2, 2,5, 3 und 4 Stunden); die geschätzte Parameter des Modells stimmten mit den in klinischen Studien gefundenen Werten überein. Die Bewertung möglicher Grenzwerte für vom Modell geschätzte Parameter zur Bewertung der Interaktionen mit einem einzigen Profil zeigte, dass die Clearance von Midazolam vernünftigerweise zum Nachweis von Hemmung (6,81-16,8 L/h), Induktion (43,3-86,6 L/h) und keine Modulation (16,8-43,3 L/h) verwendet werden kann. Die Empfindlichkeit für eine starke Hemmung war 98,7% und für die Induktion war 100%. Die Spezifität für keine Modulation war 99,2%.

Daher zeigte diese Dissertation, dass 1) Midazolam-Mikrodosierung ein praktikables Instrument zur Reduzierung dedizierter Interaktionsstudien darstellt wenn es in frühen Studien enthalten ist; 2) eine populationspharmakokinetische Analyse kann einen effizienten und genauen Nachweis der CYP3A-Interaktion liefern; und 3) eine limitierter Probenentnahme kann ein nützliches ergänzendes Instrument sowohl für die Midazolam-Mikrodosierung als auch für die populationspharmakokinetische Modellierung sein.

6. REFERENCES

- Ahsman, M. J., Hanekamp, M., Wildschut, E. D., Tibboel, D. and Mathot, R. A. (2010). **Population pharmacokinetics of midazolam and its metabolites during venoarterial extracorporeal membrane oxygenation in neonates.** *Clinical pharmacokinetics* 49, 407-419.
- Anzenbacher, P. and Anzenbacherova, E. (2001). **Cytochromes P450 and metabolism of xenobiotics.** *Cellular and Molecular Life Sciences CMLS* 58, 737-747.
- Atkins, W. M. (2005). **Non-Michaelis-Menten kinetics in cytochrome P450-catalyzed reactions.** *Annu. Rev. Pharmacol. Toxicol.* 45, 291-310.
- Atkinson Jr, A. and Lalonde, R. (2007). **Introduction of quantitative methods in pharmacology and clinical pharmacology: a historical overview.** *Clinical Pharmacology & Therapeutics* 82, 3-6.
- Baron, K. T., Gastonguay, M. R., Bioavailability, A., SS, I. and ADDL, M. (2015). **Simulation from ODE-based population PK/PD and systems pharmacology models in R with mrgsolve.** *Omega* 2, 1x1.
- Bauer, R. J. (2019). **NONMEM Tutorial Part II: Estimation Methods and Advanced Examples.** *CPT: pharmacometrics & systems pharmacology* 8, 538-556.
- Bayer, J., Heinrich, T., Burhenne, J., Haefeli, W. and Mikus, G. (2009). **Potential Induction of CYP3A4 after a Single-Dose of Efavirenz Using Midazolam Pharmacokinetics as a Marker: Abstract: 59.** *Basic & Clinical Pharmacology & Toxicology* 104.
- Benet, L. Z. (2009). **The drug transporter– metabolism alliance: uncovering and defining the interplay.** *Molecular pharmaceutics* 6, 1631-1643.
- Bergstrand, M., Hooker, A. C., Wallin, J. E. and Karlsson, M. O. (2011). **Prediction-corrected visual predictive checks for diagnosing nonlinear mixed-effects models.** *The AAPS journal* 13, 143-151.
- Bornemann, L., Min, B., Crews, T., Rees, M., Blumenthal, H., Colburn, W. and Patel, I. (1985). **Dose dependent pharmacokinetics of midazolam.** *European journal of clinical pharmacology* 29, 91-95.
- Bosgra, S., Vlaming, M. L. and Vaes, W. H. (2016). **To apply microdosing or not? Recommendations to single out compounds with non-linear pharmacokinetics.** *Clinical pharmacokinetics* 55, 1-15.
- Brendel, K., Comets, E., Laffont, C., Laveille, C. and Mentré, F. (2006). **Metrics for external model evaluation with an application to the population pharmacokinetics of gliclazide.** *Pharmaceutical research* 23, 2036-2049.

REFERENCES

- Brill, M. J., Väitalo, P. A., Darwich, A. S., van Ramshorst, B., Van Dongen, H., Rostami–Hodjegan, A., Danhof, M. and Knibbe, C. A. (2016). **Semiphysiologically based pharmacokinetic model for midazolam and CYP3A mediated metabolite 1-OH-midazolam in morbidly obese and weight loss surgery patients**. *CPT: pharmacometrics & systems pharmacology* 5, 20-30.
- Brill, M. J., van Rongen, A., Houwink, A. P., Burggraaf, J., van Ramshorst, B., Wiezer, R. J., van Dongen, E. P. and Knibbe, C. A. (2014). **Midazolam pharmacokinetics in morbidly obese patients following semi-simultaneous oral and intravenous administration: a comparison with healthy volunteers**. *Clinical pharmacokinetics* 53, 931-941.
- Brussee, J. M., Yu, H., Krekels, E. H., Palić, S., Brill, M. J., Barrett, J. S., Rostami-Hodjegan, A., de Wildt, S. N. and Knibbe, C. A. (2018). **Characterization of Intestinal and Hepatic CYP3A-Mediated Metabolism of Midazolam in Children Using a Physiological Population Pharmacokinetic Modelling Approach**. *Pharmaceutical research* 35, 182.
- Buckeridge, C., Duvvuri, S. and Denney, W. S. (2015). **Simple, automatic noncompartmental analysis: the PKNCA R package**. *J Pharmacokinet Pharmacodyn* 42, S65.
- Burhenne, J., Halama, B., Maurer, M., Riedel, K.-D., Hohmann, N., Mikus, G. and Haefeli, W. E. (2012). **Quantification of femtomolar concentrations of the CYP3A substrate midazolam and its main metabolite 1'-hydroxymidazolam in human plasma using ultra performance liquid chromatography coupled to tandem mass spectrometry**. *Analytical and bioanalytical chemistry* 402, 2439-2450.
- Burk, O. and Wojnowski, L. (2004). **Cytochrome P450 3A and their regulation**. *Naunyn-Schmiedeberg's archives of pharmacology* 369, 105-124.
- Burt, T., Yoshida, K., Lappin, G., Vuong, L., John, C., de Wildt, S., Sugiyama, Y. and Rowland, M. (2016). **Microdosing and other phase 0 clinical trials: facilitating translation in drug development**. *Clinical and translational science* 9, 74.
- CDC/National Center for Health Statistics (2010). **Reliability of Estimates**. . URL: https://www.cdc.gov/nchs/ahcd/ahcd_estimation_reliability.htm [as of February 25, 2020].
- Chaobal, H. N. and Kharasch, E. D. (2005). **Single-point sampling for assessment of constitutive, induced, and inhibited cytochrome P450 3A activity with alfentanil or midazolam**. *Clinical Pharmacology & Therapeutics* 78, 529-539.
- Chen, M., Ma, L., Drusano, G. L., Bertino Jr, J. S. and Nafziger, A. N. (2006). **Sex differences in CYP3A activity using intravenous and oral midazolam**. *Clinical Pharmacology & Therapeutics* 80, 531-538.
- CHMP, C. f. M. P. f. H. U. (2004). **Position Paper on non-clinical safety studies to support clinical trials with a single microdose**. Position paper CPMP/SWP/2599. European Medicines Agency, London.

REFERENCES

- Croft, M., Keely, B., Morris, I., Tann, L. and Lappin, G. (2012). **Predicting drug candidate victims of drug-drug interactions, using microdosing.** *Clinical pharmacokinetics* 51, 237-246.
- Cummins, C. L., Jacobsen, W., Christians, U. and Benet, L. Z. (2004). **CYP3A4-transfected Caco-2 cells as a tool for understanding biochemical absorption barriers: studies with sirolimus and midazolam.** *Journal of Pharmacology and Experimental Therapeutics* 308, 143-155.
- De Wildt, S., De Hoog, M., Vinks, A., Van Der Giesen, E. and Van Den Anker, J. (2003). **Population pharmacokinetics and metabolism of midazolam in pediatric intensive care patients.** *Critical care medicine* 31, 1952-1958.
- Dresser, G. K., Spence, J. D. and Bailey, D. G. (2000). **Pharmacokinetic-pharmacodynamic consequences and clinical relevance of cytochrome P450 3A4 inhibition.** *Clinical pharmacokinetics* 38, 41-57.
- Eap, C. B., Buclin, T., Cucchia, G., Zullino, D., Hustert, E., Bleiber, G., Golay, K. P., Aubert, A.-C., Baumann, P. and Telenti, A. (2004). **Oral administration of a low dose of midazolam (75 µg) as an in vivo probe for CYP3A activity.** *European journal of clinical pharmacology* 60, 237-246.
- Egorin, M. J., Forrest, A., Belani, C. P., Ratain, M. J., Abrams, J. S. and Van Echo, D. A. (1989). **A limited sampling strategy for cyclophosphamide pharmacokinetics.** *Cancer research* 49, 3129-3133.
- Eichbaum, C., Cortese, M., Blank, A., Burhenne, J. and Mikus, G. (2013). **Concentration effect relationship of CYP3A inhibition by ritonavir in humans.** *European journal of clinical pharmacology* 69, 1795-1800.
- Einolf, H., Chen, L., Fahmi, O., Gibson, C., Obach, R., Shebley, M., Silva, J., Sinz, M., Unadkat, J. and Zhang, L. (2014). **Evaluation of various static and dynamic modeling methods to predict clinical CYP3A induction using in vitro CYP3A4 mRNA induction data.** *Clinical Pharmacology & Therapeutics* 95, 179-188.
- EMA-CHMP (2012 Jun). **Guideline on the investigation of drug interactions: final (CPMP/EWP/560/95/Rev. 1 corr. 2).** URL: http://www.ema.europa.eu/docs/en_GB/document_library/Scientific_guideline/2012/07/WC500129606.pdf [as of 14. Jun 2019].
- Ette, E. I., Williams, P. J., Kim, Y. H., Lane, J. R., Liu, M. J. and Capparelli, E. V. (2003). **Model appropriateness and population pharmacokinetic modeling.** *The Journal of Clinical Pharmacology* 43, 610-623.
- EUMAPP, E. M. A. P. P. (2012). **Outcomes from EUMAPP—a study comparing in vitro, in silico, microdose and pharmacological dose pharmacokinetics.**

REFERENCES

- Evans, W. E. and Relling, M. V. (1999). **Pharmacogenomics: translating functional genomics into rational therapeutics**. *science* 286, 487-491.
- FDA, U. (2006). **guidance for industry, investigators and reviewers: exploratory IND studies**. US Department of Health and Human Services www.fda.gov/downloads/Drugs/GuidanceComplianceRegulatoryInformation/Guidances/UCM078933.pdf (Accessed March 2010).
- Fetzner, L., Burhenne, J., Weiss, J., Völker, M., Unger, M., Mikus, G. and Haefeli, W. E. (2011). **Daily honey consumption does not change CYP3A activity in humans**. *The Journal of Clinical Pharmacology* 51, 1223-1232.
- Fisher, D. and Shafer, S. (2007). **Pharmacokinetic and pharmacodynamic analysis with NONMEM. Basic concepts**. Paper presented at: NONMEM Workshop: Introduction to NONMEM: 2007; Ghent.
- Fuchs, I., Hafner-Blumenstiel, V., Markert, C., Burhenne, J., Weiss, J., Haefeli, W. E. and Mikus, G. (2013). **Effect of the CYP3A inhibitor ketoconazole on the PXR-mediated induction of CYP3A activity**. *European journal of clinical pharmacology* 69, 507-513.
- Guthrie, B., Makubate, B., Hernandez-Santiago, V. and Dreischulte, T. (2015). **The rising tide of polypharmacy and drug-drug interactions: population database analysis 1995–2010**. *BMC medicine* 13, 74.
- Hafner, V., Jäger, M., Matthée, A. K., Ding, R., Burhenne, J., Haefeli, W. and Mikus, G. (2010). **Effect of simultaneous induction and inhibition of CYP3A by St John's Wort and ritonavir on CYP3A activity**. *Clinical Pharmacology & Therapeutics* 87, 191-196.
- Halama, B., Hohmann, N., Burhenne, J., Weiss, J., Mikus, G. and Haefeli, W. E. (2013). **A nanogram dose of the CYP3A probe substrate midazolam to evaluate drug interactions**. *Clin Pharmacol Ther* 93, 564-571, doi: 10.1038/clpt.2013.27.
- He, P., Court, M. H., Greenblatt, D. J. and von Moltke, L. L. (2005). **Genotype-phenotype associations of cytochrome P450 3A4 and 3A5 polymorphism with midazolam clearance in vivo**. *Clinical Pharmacology & Therapeutics* 77, 373-387.
- Heizmann, P., Eckert, M. and Ziegler, W. (1983). **Pharmacokinetics and bioavailability of midazolam in man**. *British journal of clinical pharmacology* 16, 43S-49S.
- Heizmann, P. and Ziegler, W. (1981). **Excretion and metabolism of 14C-midazolam in humans following oral dosing**. *Arzneimittel-forschung* 31, 2220-2223.
- Hohmann, N., Kocheise, F., Carls, A., Burhenne, J., Haefeli, W. E. and Mikus, G. (2015). **Midazolam microdose to determine systemic and pre-systemic metabolic CYP3A activity in humans**. *British journal of clinical pharmacology* 79, 278-285.

REFERENCES

- Hohmann, N., Kocheise, F., Carls, A., Burhenne, J., Weiss, J., Haefeli, W. E. and Mikus, G. (2016). **Dose-dependent bioavailability and CYP3A inhibition contribute to non-linear pharmacokinetics of voriconazole.** *Clinical pharmacokinetics* 55, 1535-1545.
- Holte, R. C. (1993). **Very simple classification rules perform well on most commonly used datasets.** *Machine learning* 11, 63-90.
- Hostler, D., Zhou, J., Tortorici, M. A., Bies, R. R., Rittenberger, J. C., Empey, P. E., Kochanek, P. M., Callaway, C. W. and Poloyac, S. M. (2010). **Mild hypothermia alters midazolam pharmacokinetics in normal healthy volunteers.** *Drug metabolism and disposition* 38, 781-788.
- Kanto, J. H. (1985). **Midazolam: The first water-soluble benzodiazepine; Pharmacology, pharmacokinetics and efficacy in insomnia and anesthesia.** *Pharmacotherapy: The Journal of Human Pharmacology and Drug Therapy* 5, 138-155.
- Karlsson, M. and Savic, R. (2007). **Diagnosing model diagnostics.** *Clinical Pharmacology & Therapeutics* 82, 17-20.
- Karlsson, M. and Sheiner, L. (1993). **The importance of modeling interoccasion variability in population pharmacokinetic analyses.** *Journal of pharmacokinetics and biopharmaceutics* 21, 735-750.
- Karlsson, M. O., Beal, S. L. and Sheiner, L. B. (1995). **Three new residual error models for population PK/PD analyses.** *Journal of pharmacokinetics and biopharmaceutics* 23, 651-672.
- Kashuba, A. D., Bertino, J. S., Rocci, M. L., Kulawy, R. W., Beck, D. J. and Nafziger, A. N. (1998). **Quantification of 3-month intraindividual variability and the influence of sex and menstrual cycle phase on CYP3A activity as measured by phenotyping with intravenous midazolam.** *Clinical Pharmacology & Therapeutics* 64, 269-277.
- Katzenmaier, S., Markert, C. and Mikus, G. (2010). **Proposal of a new limited sampling strategy to predict CYP3A activity using a partial AUC of midazolam.** *European journal of clinical pharmacology* 66, 1137-1141.
- Katzenmaier, S., Markert, C., Riedel, K., Burhenne, J., Haefeli, W. and Mikus, G. (2011). **Determining the time course of CYP3A inhibition by potent reversible and irreversible CYP3A inhibitors using a limited sampling strategy.** *Clinical Pharmacology & Therapeutics* 90, 666-673.
- Keubler, A., Weiss, J., Haefeli, W. E., Mikus, G. and Burhenne, J. (2012). **Drug interaction of efavirenz and midazolam: efavirenz activates the CYP3A-mediated midazolam 1'-hydroxylation in vitro.** *Drug Metabolism and Disposition* 40, 1178-1182.
- Kiene, K., Hayasi, N., Burhenne, J., Uchitomi, R., Sünderhauf, C., Schmid, Y., Haschke, M., Haefeli, W. E., Krähenbühl, S. and Mikus, G. (2019). **Microdosed midazolam for the determination of**

REFERENCES

- cytochrome P450 3A activity: Development and clinical evaluation of a buccal film.** European Journal of Pharmaceutical Sciences *135*, 77-82.
- Kim, J. S., Nafziger, A. N., Tsunoda, S. M., Choo, E. F., Streetman, D. S., Kashuba, A. D., Kulawy, R. W., Beck, D. J., Rocci Jr, M. L. and Wilkinson, G. R. (2002). **Limited sampling strategy to predict AUC of the CYP3A phenotyping probe midazolam in adults: application to various assay techniques.** The Journal of Clinical Pharmacology *42*, 376-382.
- Kirby, B., Kharasch, E. D., Thummel, K. T., Narang, V. S., Hoffer, C. J. and Unadkat, J. D. (2006). **Simultaneous measurement of in vivo P-glycoprotein and cytochrome P450 3A activities.** The Journal of Clinical Pharmacology *46*, 1313-1319.
- Kliwer, S. A., Goodwin, B. and Willson, T. M. (2002). **The nuclear pregnane X receptor: a key regulator of xenobiotic metabolism.** Endocrine reviews *23*, 687-702.
- Koch, I., Weil, R., Wolbold, R., Brockmüller, J., Hustert, E., Burk, O., Nuessler, A., Neuhaus, P., Eichelbaum, M. and Zanger, U. (2002). **Interindividual variability and tissue-specificity in the expression of cytochrome P450 3A mRNA.** Drug Metabolism and Disposition *30*, 1108-1114.
- Krecic-Shepard, M. E., Barnas, C. R., Slimko, J. and Schwartz, J. B. (2000). **Faster clearance of sustained release verapamil in men versus women: Continuing observations on sex-specific differences after oral administration of verapamil.** Clinical Pharmacology & Therapeutics *68*, 286-292.
- Kronbach, T., Mathys, D., Umeno, M., Gonzalez, F. J. and Meyer, U. A. (1989). **Oxidation of midazolam and triazolam by human liver cytochrome P450III A4.** Molecular pharmacology *36*, 89-96.
- Krupka, E., Venisse, N., Lafay, C., Gendre, D., Diquet, B., Bouquet, S. and Perault, M.-C. (2006). **Probe of CYP3A by a single-point blood measurement after oral administration of midazolam in healthy elderly volunteers.** European journal of clinical pharmacology *62*, 653-659.
- Lalonde, R., Kowalski, K., Hutmacher, M., Ewy, W., Nichols, D., Milligan, P., Corrigan, B., Lockwood, P., Marshall, S. and Benincosa, L. (2007). **Model-based drug development.** Clinical Pharmacology & Therapeutics *82*, 21-32.
- Lappin, G., Kuhn, W., Jochemsen, R., Kneer, J., Chaudhary, A., Oosterhuis, B., Drijfhout, W. J., Rowland, M. and Garner, R. C. (2006). **Use of microdosing to predict pharmacokinetics at the therapeutic dose: experience with 5 drugs.** Clinical Pharmacology & Therapeutics *80*, 203-215.
- Lappin, G., Noveck, R. and Burt, T. (2013). **Microdosing and drug development: past, present and future.** Expert opinion on drug metabolism & toxicology *9*, 817-834.
- Lee, L. S., Bertino Jr, J. S. and Nafziger, A. N. (2006). **Limited sampling models for oral midazolam: midazolam plasma concentrations, not the ratio of 1-hydroxymidazolam to midazolam**

REFERENCES

- plasma concentrations, accurately predicts AUC as a biomarker of CYP3A activity.** *The Journal of Clinical Pharmacology* 46, 229-234.
- Lin, J. H. and Lu, A. Y. (1998). **Inhibition and induction of cytochrome P450 and the clinical implications.** *Clinical pharmacokinetics* 35, 361-390.
- Liu, Y.-T., Hao, H.-P., Liu, C.-X., Wang, G.-J. and Xie, H.-G. (2007). **Drugs as CYP3A probes, inducers, and inhibitors.** *Drug metabolism reviews* 39, 699-721.
- Ma, J., Nguyen, E., Tsunoda, S., Greenberg, H., Gorski, J., Penzak, S. and Lee, L. (2010). **Assessment of oral midazolam limited sampling strategies to predict area under the concentration time curve (AUC) during cytochrome P450 (CYP) 3A baseline, inhibition and induction or activation.** *International journal of clinical pharmacology and therapeutics* 48, 847-853.
- Masters, J. C., Harano, D. M., Greenberg, H. E., Tsunoda, S. M., Jang, I.-J. and Ma, J. D. (2015). **Limited sampling strategy of partial area-under-the-concentration-time-curves to estimate midazolam systemic clearance for cytochrome P450 3A phenotyping.** *Therapeutic drug monitoring* 37, 84.
- Menten, L. and Michaelis, M. (1913). **Die kinetik der invertinwirkung.** *Biochem Z* 49, 5.
- Mikus, G. (2019). **Probes and cocktails for drug-drug interaction evaluation: The future is microdosing?** *Clin Pharmacol Ther* 105, 1335-1337, doi: 10.1002/cpt.1350.
- Mikus, G., Heinrich, T., Bödigeimer, J., Röder, C., Matthee, A. K., Weiss, J., Burhenne, J. and Haefeli, W. E. (2017). **Semisimultaneous midazolam administration to evaluate the time course of CYP3A activation by a single oral dose of efavirenz.** *The Journal of Clinical Pharmacology* 57, 899-905.
- Miyazaki, M., Fujiwara, Y., Takahashi, T., Isobe, T., Ohune, T., Tsuya, T. and Yamakido, M. (1997). **Limited-sampling models for estimation of the carboplatin area under the curve.** *Anticancer research* 17, 4571-4575.
- Mould, D. and Upton, R. (2012). **Basic concepts in population modeling, simulation, and model-based drug development.** *CPT: pharmacometrics & systems pharmacology* 1, 1-14.
- Mould, D. and Upton, R. N. (2013). **Basic concepts in population modeling, simulation, and model-based drug development—part 2: introduction to pharmacokinetic modeling methods.** *CPT: pharmacometrics & systems pharmacology* 2, 1-14.
- Mueller, S. C. and Drewelow, B. (2013). **Evaluation of limited sampling models for prediction of oral midazolam AUC for CYP3A phenotyping and drug interaction studies.** *European journal of clinical pharmacology* 69, 1127-1134.

REFERENCES

- Murphy, C. C., Fullington, H. M., Alvarez, C. A., Betts, A. C., Lee, S. J. C., Haggstrom, D. A. and Halm, E. A. (2018). **Polypharmacy and patterns of prescription medication use among cancer survivors**. *Cancer* 124, 2850-2857.
- Nebert, D. W. and Russell, D. W. (2002). **Clinical importance of the cytochromes P450**. *The Lancet* 360, 1155-1162.
- Nguyen, T., Mouksassi, M. S., Holford, N., Al-Huniti, N., Freedman, I., Hooker, A. C., John, J., Karlsson, M. O., Mould, D. and Ruixo, J. P. (2017). **Model evaluation of continuous data pharmacometric models: metrics and graphics**. *CPT: pharmacometrics & systems pharmacology* 6, 87-109.
- Nguyen, T. T., Bénech, H., Pruvost, A. and Lenuzza, N. (2016). **A limited sampling strategy based on maximum a posteriori Bayesian estimation for a five-probe phenotyping cocktail**. *European journal of clinical pharmacology* 72, 39-51.
- Paine, M. F., Hart, H. L., Ludington, S. S., Haining, R. L., Rettie, A. E. and Zeldin, D. C. (2006). **The human intestinal cytochrome P450 "pie"**. *Drug Metabolism and Disposition* 34, 880-886.
- Penzak, S. R., Busse, K. H., Robertson, S. M., Formentini, E., Alfaro, R. M. and Davey Jr, R. T. (2008). **Limitations of using a single postdose midazolam concentration to predict CYP3A-mediated drug interactions**. *The Journal of Clinical Pharmacology* 48, 671-680.
- PMDA (2014). **Pharmaceuticals & Medical Device Agency-Japan. Drug interaction guideline for drug development and labeling recommendations (draft for public comment)** URL: [http://www.solvobiotech.com/documents/Japanese_DDI_guideline_\(draft\)_2014Jan.pdf](http://www.solvobiotech.com/documents/Japanese_DDI_guideline_(draft)_2014Jan.pdf) [as of 13.Mar.2017].
- Prueksaritanont, T., Tatosian, D. A., Chu, X., Railkar, R., Evers, R., Chavez-Eng, C., Lutz, R., Zeng, W., Yabut, J., Chan, G. H., Cai, X., Latham, A. H., Hehman, J., Stypinski, D., Brejda, J., Zhou, C., Thornton, B., Bateman, K. P., Fraser, I. and Stoch, S. A. (2016). **Validation of a microdose probe drug cocktail for clinical drug interaction assessments for drug transporters and CYP3A**. *Clin Pharmacol Ther*, doi: 10.1002/cpt.525.
- Qato, D. M., Alexander, G. C., Conti, R. M., Johnson, M., Schumm, P. and Lindau, S. T. (2008). **Use of prescription and over-the-counter medications and dietary supplements among older adults in the United States**. *Jama* 300, 2867-2878.
- Quintela, O., Cruz, A., Concheiro, M., Castro, A. d. and López-Rivadulla, M. (2004). **A sensitive, rapid and specific determination of midazolam in human plasma and saliva by liquid chromatography/electrospray mass spectrometry**. *Rapid communications in mass spectrometry* 18, 2976-2982.
- R Core Team (2018). **R: A language and environment for statistical computing**. (R Foundation for Statistical Computing, Vienna, Austria).

REFERENCES

- Ratain, M. J. and Vogelzang, N. J. (1987). **Limited sampling model for vinblastine pharmacokinetics.** *Cancer treatment reports* 71, 935-939.
- Reitman, M. L., Chu, X., Cai, X., Yabut, J., Venkatasubramanian, R., Zajic, S., Stone, J. A., Ding, Y., Witter, R., Gibson, C., Roupe, K., Evers, R., Wagner, J. A. and Stoch, A. (2011). **Rifampin's acute inhibitory and chronic inductive drug interactions: experimental and model-based approaches to drug-drug interaction trial design.** *Clin Pharmacol Ther* 89, 234-242, doi: 10.1038/clpt.2010.271.
- Rendic, S. (2002). **Summary of information on human CYP enzymes: human P450 metabolism data.** *Drug metabolism reviews* 34, 83-448.
- Riley, R. J. and Wilson, C. E. (2015). **Cytochrome P450 time-dependent inhibition and induction: advances in assays, risk analysis and modelling.** *Expert opinion on drug metabolism & toxicology* 11, 557-572.
- Rogers, J. F., Nafziger, A. N., Kashuba, A. D., Streetman, D. S., Rocci Jr, M. L., Choo, E. F., Wilkinson, G. R. and Bertino Jr, J. S. (2002). **Single plasma concentrations of 1'-hydroxymidazolam or the ratio of 1'-hydroxymidazolam: midazolam do not predict midazolam clearance in healthy subjects.** *The Journal of Clinical Pharmacology* 42, 1079-1082.
- Savic, R. M., Jonker, D. M., Kerbusch, T. and Karlsson, M. O. (2007). **Implementation of a transit compartment model for describing drug absorption in pharmacokinetic studies.** *Journal of pharmacokinetics and pharmacodynamics* 34, 711-726.
- Seng, K. Y., Hee, K. H., Soon, G. H., Sapari, N. S., Soong, R., Goh, B. C. and Lee, L. S. U. (2014). **CYP3A5*3 and bilirubin predict midazolam population pharmacokinetics in Asian cancer patients.** *The Journal of Clinical Pharmacology* 54, 215-224.
- Sevrioukova, I. F. and Poulos, T. L. (2013). **Understanding the mechanism of cytochrome P450 3A4: recent advances and remaining problems.** *Dalton transactions* 42, 3116-3126.
- Sheiner, L. B. (1997). **Learning versus confirming in clinical drug development.** *Clinical Pharmacology & Therapeutics* 61, 275-291.
- Sheiner, L. B., Rosenberg, B. and Melmon, K. L. (1972). **Modelling of individual pharmacokinetics for computer-aided drug dosage.** *Computers and Biomedical Research* 5, 441-459.
- Sherwin, C. M., Kiang, T. K., Spigarelli, M. G. and Ensom, M. H. (2012). **Fundamentals of population pharmacokinetic modelling.** *Clinical pharmacokinetics* 51, 573-590.
- Smith, M., Eadie, M. and Brophy, T. R. (1981). **The pharmacokinetics of midazolam in man.** *European journal of clinical pharmacology* 19, 271-278.

REFERENCES

- Steyerberg, E. W. and Harrell, F. E. (2016). **Prediction models need appropriate internal, internal-external, and external validation.** *Journal of clinical epidemiology* 69, 245-247.
- Stoll, F., Burhenne, J., Lausecker, B., Weiss, J., Thomsen, T., Haefeli, W. E. and Mikus, G. (2013). **Reduced exposure variability of the CYP3A substrate simvastatin by dose individualization to CYP3A activity.** *The Journal of Clinical Pharmacology* 53, 1199-1204.
- Sugiyama, Y. and Yamashita, S. (2011). **Impact of microdosing clinical study—why necessary and how useful?** *Advanced drug delivery reviews* 63, 494-502.
- Sun, H., Fadiran, E. O., Jones, C. D., Lesko, L., Huang, S.-M., Higgins, K., Hu, C., Machado, S., Maldonado, S. and Williams, R. (1999). **Population pharmacokinetics.** *Clinical pharmacokinetics* 37, 41-58.
- Svendsen, P., El-Galaly, T. C., Dybkær, K., Bøgsted, M., Laursen, M. B., Schmitz, A., Jensen, P. and Johnsen, H. E. (2016). **The application of human phase 0 microdosing trials: a systematic review and perspectives.** *Leukemia & lymphoma* 57, 1281-1290.
- Swart, E. L., Zuideveld, K. P., De Jongh, J., Danhof, M., Thijs, L. G. and Strack van Schijndel, R. M. (2004). **Comparative population pharmacokinetics of lorazepam and midazolam during long-term continuous infusion in critically ill patients.** *British journal of clinical pharmacology* 57, 135-145.
- Thelen, K. and Dressman, J. B. (2009). **Cytochrome P450-mediated metabolism in the human gut wall.** *Journal of pharmacy and pharmacology* 61, 541-558.
- Thummel, K. and Wilkinson, G. (1998). **In vitro and in vivo drug interactions involving human CYP3A.** *Annual review of pharmacology and toxicology* 38, 389-430.
- Thummel, K. E., O'Shea, D., Paine, M. F., Shen, D. D., Kunze, K. L., Perkins, J. D. and Wilkinson, G. R. (1996). **Oral first-pass elimination of midazolam involves both gastrointestinal and hepatic CYP3A-mediated metabolism.** *Clinical Pharmacology & Therapeutics* 59, 491-502.
- Tomalik-Scharte, D., Suleiman, A. A., Frechen, S., Kraus, D., Kerkweg, U., Rokitta, D., Di Gion, P., Queckenberg, C. and Fuhr, U. (2014). **Population pharmacokinetic analysis of circadian rhythms in hepatic CYP3A activity using midazolam.** *The Journal of Clinical Pharmacology* 54, 1162-1169.
- US-FDA (2012 Feb). **Guidance for industry: Drug interaction studies - study design, data analysis, implications for dosing, and labeling recommendations (draft guidance).** URL: <https://www.fda.gov/media/108130/download> [as of 14 Jun. 2019].
- US-FDA (2020a). **Guidance for industry: clinical drug interaction studies - cytochrome P450 enzyme- and transporter-mediated drug interactions,** Services, U. S. D. o. H. a. H., ed. (

REFERENCES

- US-FDA (2020b). **Guidance for industry: in vitro drug interaction studies - cytochrome P450 enzyme- and transporter-mediated drug interactions**, Services, U. S. D. o. H. a. H., ed. (
- van Groen, B. D., Vaes, W. H., Park, B. K., Krekels, E. H., van Duijn, E., K rgvee, L. T., Maruszak, W., Grynkiewicz, G., Garner, R. C. and Knibbe, C. A. (2019). **Dose-linearity of the pharmacokinetics of an intravenous [14C] midazolam microdose in children**. *British journal of clinical pharmacology* *85*, 2332-2340.
- van Rongen, A., Vaughns, J. D., Moorthy, G. S., Barrett, J. S., Knibbe, C. A. and van den Anker, J. N. (2015). **Population pharmacokinetics of midazolam and its metabolites in overweight and obese adolescents**. *British journal of clinical pharmacology* *80*, 1185-1196.
- Vieira, M. L., Kirby, B., Ragueneau-Majlessi, I., Galetin, A., Chien, J., Einolf, H., Fahmi, O., Fischer, V., Fretland, A. and Grime, K. (2014). **Evaluation of various static in vitro–in vivo extrapolation models for risk assessment of the CYP3A inhibition potential of an investigational drug**. *Clinical Pharmacology & Therapeutics* *95*, 189-198.
- Wade, J. R., Beal, S. L. and Sambol, N. C. (1994). **Interaction between structural, statistical, and covariate models in population pharmacokinetic analysis**. *Journal of pharmacokinetics and biopharmaceutics* *22*, 165-177.
- Whiting, B., Kelman, A. W. and Grevel, J. (1986). **Population pharmacokinetics theory and clinical application**. *Clinical pharmacokinetics* *11*, 387-401.
- Wilkinson, G. R. (2005). **Drug metabolism and variability among patients in drug response**. *New England Journal of Medicine* *352*, 2211-2221.
- Yang, J., Patel, M., Nikanjam, M., Capparelli, E. V., Tsunoda, S. M., Greenberg, H. E., Penzak, S. R., Aubrey Stoch, S., Bertino Jr, J. S. and Nafziger, A. N. (2018). **Midazolam single time point concentrations to estimate exposure and cytochrome P450 (CYP) 3A constitutive activity utilizing limited sampling strategy with a population pharmacokinetic approach**. *The Journal of Clinical Pharmacology* *58*, 1205-1213.
- Zadoyan, G., Rokitta, D., Klement, S., Diemel, A., Hoerr, R., Gramatt , T. and Fuhr, U. (2012). **Effect of Ginkgo biloba special extract EGb 761® on human cytochrome P450 activity: a cocktail interaction study in healthy volunteers**. *European journal of clinical pharmacology* *68*, 553-560.
- Zhou, S.-F. (2008). **Drugs behave as substrates, inhibitors and inducers of human cytochrome P450 3A4**. *Current drug metabolism* *9*, 310-322.
- Ziesenitz, V. C., Burhenne, J., Koenig, S. K. and Haefeli, W. E. (2012). **Midazolam pharmacokinetics are not influenced by polymorphisms of hepatic OATP 1B1 in healthy volunteers**. Paper presented at: *Clinical Pharmacology & Therapeutics* (NATURE PUBLISHING GROUP 75 VARICK ST, 9TH FLR, NEW YORK, NY 10013-1917 USA).

REFERENCES

- Ziesenitz, V. C., König, S. K., Mahlke, N. S., Skopp, G., Haefeli, W. E. and Mikus, G. (2015).
Pharmacokinetic interaction of intravenous fentanyl with ketoconazole. *The Journal of Clinical Pharmacology* 55, 708-717.
- Zomorodi, K., Donner, A., Somma, J., Barr, J., Sladen, R., Ramsay, J., Geller, E. and Shafer, S. L. (1998).
Population pharmacokinetics of midazolam administered by target controlled infusion for sedation following coronary artery bypass grafting. *Anesthesiology: The Journal of the American Society of Anesthesiologists* 89, 1418-1429.

7. PUBLICATIONS

Wiebe, S. T., Meid, A. D. and Mikus, G. (2020). **Composite midazolam and 1'-OH midazolam population pharmacokinetic model for constitutive, inhibited and induced CYP3A activity.** *Journal of Pharmacokinetics and Pharmacodynamics (Submitted).*

Wiebe, S. T., Huennemeyer, A., Kadus, W., Goettel, M., Jambrecina, A., Schultz, A., Vinisko, R., Schlieker, L., Herich, L. and Mikus, G. (2020). **Midazolam microdosing applied in early clinical development for drug-drug interaction assessment.** *British Journal of Clinical Pharmacology (Submitted).*

APPENDICES

PK Parameter Tables for Midazolam Microdosing Implementation

Tab. A1: Non-compartmental PK parameters of midazolam administered alone and after multiple oral administration of Compound A or placebo to healthy male participants – Study 1

| PK Parameter | Midazolam + Compound A | | Midazolam + Placebo | |
|-----------------------------------|------------------------|----------------------|---------------------|-----------------------|
| | N | gMean (gCV [%]) | N | gMean (gCV [%]) |
| Baseline (Midazolam only) | | | | |
| AUC _{0-tz} [pM·h] | 18 | 3310 (36.9) | 6 | 4220 (37.6) |
| AUC _{0-∞} [pM·h] | 18 | 3650 (39.6) | 6 | 4550 (39.0) |
| AUC ₂₋₄ [pM·h] | 18 | 970 (45.3) | 6 | 1360 (38.0) |
| CL/F [L·h ⁻¹] | 18 | 63.8 (39.0) | 6 | 51.0 (38.1) |
| C _{max} [pM] | 18 | 1090 (36.1) | 6 | 1230 (39.0) |
| t _{max} ¹ [h] | 18 | 1.00 (0.250 to 2.00) | 6 | 1.00 (0.500 to 2.00) |
| Day 3 of Compound A | | | | |
| AUC _{0-tz} [pM·h] | 18 | 3680 (32.5) | 6 | 4210 (30.8) |
| AUC _{0-∞} [pM·h] | 18 | 4100 (36.3) | 6 | 4610 (30.8) |
| AUC ₂₋₄ [pM·h] | 18 | 1060 (35.2) | 6 | 1280 (39.9) |
| CL/F [L·h ⁻¹] | 18 | 56.9 (36.0) | 6 | 50.4 (30.8) |
| C _{max} [pM] | 18 | 1270 (33.3) | 6 | 1310 (29.3) |
| t _{max} ¹ [h] | 18 | 1.00 (0.250 to 1.02) | 6 | 0.750 (0.500 to 2.00) |
| Day 14 of Compound A | | | | |
| AUC _{0-tz} [pM·h] | 18 | 4070 (29.2) | 6 | 4230 (25.2) |
| AUC _{0-∞} [pM·h] | 18 | 4490 (30.1) | 6 | 4600 (25.6) |
| AUC ₂₋₄ [pM·h] | 18 | 1240 (33.3) | 6 | 1310 (28.7) |
| CL/F [L·h ⁻¹] | 18 | 52.2 (29.7) | 6 | 50.9 (25.4) |
| C _{max} [pM] | 18 | 1320 (34.0) | 6 | 1390 (31.9) |
| t _{max} ¹ [h] | 18 | 1.00 (0.500 to 2.00) | 6 | 0.759 (0.450 to 2.00) |

¹ For t_{max}, the median and range (minimum-maximum) are given.

APPENDICES – PK PARAMETER TABLES

Tab. A2: Non-compartmental PK parameters of midazolam in plasma after oral administration alone and following multiple oral administration of Compound B or placebo – Study 2

| PK Parameter | Midazolam + Compound B | | Midazolam + Placebo | |
|-----------------------------------|------------------------|----------------------|---------------------|----------------------|
| | N | gMean (gCV [%]) | N | gMean (gCV [%]) |
| Baseline (Midazolam alone) | | | | |
| AUC _{0-tz} [pM·h] | 32 | 3660 (42.8) | 8 | 4360 (36.4) |
| AUC _{0-∞} [pM·h] | 32 | 4130 (44.9) | 8 | 5140 (42.4) |
| AUC ₂₋₄ [pM·h] | 32 | 1110 (50.9) | 8 | 1410 (35.1) |
| CL/F [L·h ⁻¹] | 32 | 56.6 (44.9) | 8 | 45.7 (41.3) |
| C _{max} [pM] | 32 | 1140 (40.5) | 8 | 1200 (33.6) |
| t _{max} ¹ [h] | 32 | 1.00 (0.250 to 2.50) | 8 | 1.00 (0.500 to 2.00) |
| Day 17 of Compound B | | | | |
| AUC _{0-tz} [pM·h] | 30 | 3850 (47.1) | 8 | 4480 (15.3) |
| AUC _{0-∞} [pM·h] | 30 | 4420 (49.7) | 8 | 5170 (17.7) |
| AUC ₂₋₄ [pM·h] | 30 | 1230 (52.8) | 8 | 1500 (18.3) |
| CL/F [L·h ⁻¹] | 30 | 52.9 (49.2) | 8 | 45.1 (16.9) |
| C _{max} [pM] | 30 | 1080 (42.0) | 8 | 1200 (16.5) |
| t _{max} ¹ [h] | 30 | 1.00 (0.250 to 2.00) | 8 | 1.50 (0.300 to 2.50) |

¹ For t_{max}, the median and range (minimum-maximum) are given.

APPENDICES – PK PARAMETER TABLES

Tab. A3: Non-compartmental PK parameters of midazolam and 1'-OH midazolam in plasma after oral administration alone and following single and multiple oral administration of Compound C or placebo – Study 3

| PK Parameter | Midazolam + Compound C | | | Midazolam + Placebo | | |
|-----------------------------------|------------------------|-------------------|-------------------|---------------------|-------------------|-------------------|
| | | MDZ | 1'-OH MDZ | | MDZ | 1'-OH MDZ |
| | N | gMean (gCV [%]) | gMean (gCV [%]) | N | gMean (gCV [%]) | gMean (gCV [%]) |
| Baseline (Midazolam alone) | | | | | | |
| AUC _{0-tz} [pM·h] | 40 | 3220 (34.5) | 852 (28.9) | 10 | 3030 (28.6) | 907 (20.7) |
| AUC _{0-∞} [pM·h] | 40 | 3630 (37.5) | 920 (29.0) | 10 | 3370 (32.3) | 998 (22.2) |
| AUC ₂₋₄ [pM·h] | 40 | 987 (37.6) | 283 (34.9) | 10 | 933 (33.4) | 306 (25.2) |
| CL/F [L·h ⁻¹] | 40 | 64.0 (37.2) | 252 (28.9) | 10 | 68.5 (32.7) | 231 (22.9) |
| C _{max} [pM] | 40 | 1000 (32.9) | 268 (30.5) | 10 | 929 (25.6) | 255 (18.3) |
| t _{max} ¹ [h] | 40 | 1.00 (0.500-2.00) | 1.00 (0.500-2.50) | 10 | 1.00 (0.500-2.00) | 1.00 (0.500-2.50) |
| Day 1 of Compound C | | | | | | |
| AUC _{0-tz} [pM·h] | 40 | 3050 (35.0) | 862 (28.3) | 10 | 2960 (31.8) | 998 (26.7) |
| AUC _{0-∞} [pM·h] | 40 | 3410 (37.4) | 937 (28.8) | 10 | 3280 (35.1) | 1110 (28.0) |
| AUC ₂₋₄ [pM·h] | 40 | 912 (40.6) | 279 (33.3) | 10 | 943 (37.3) | 356 (27.8) |
| CL/F [L·h ⁻¹] | 40 | 68.5 (36.5) | 247 (28.9) | 10 | 71.2 (35.2) | 210 (28.4) |
| C _{max} [pM] | 40 | 1010 (29.6) | 283 (30.6) | 10 | 913 (26.2) | 274 (26.1) |
| t _{max} ¹ [h] | 40 | 1.00 (0.500-2.00) | 1.00 (0.500-2.50) | 10 | 1.00 (0.500-2.50) | 1.50 (0.500-2.00) |
| Day 14 of Compound C | | | | | | |
| AUC _{0-tz} [pM·h] | 38 | 3380 (33.6) | 752 (24.4) | 10 | 3200 (28.9) | 800 (23.3) |
| AUC _{0-∞} [pM·h] | 38 | 3870 (38.5) | 830 (24.9) | 10 | 3690 (33.9) | 893 (24.5) |
| AUC ₂₋₄ [pM·h] | 38 | 1070 (36.2) | 252 (32.0) | 10 | 1050 (24.5) | 285 (22.1) |
| CL/F [L·h ⁻¹] | 38 | 60.5 (38.3) | 280 (24.9) | 10 | 63.5 (33.4) | 259 (24.8) |
| C _{max} [pM] | 38 | 991 (31.4) | 224 (28.7) | 10 | 887 (27.1) | 230 (23.8) |
| t _{max} ¹ [h] | 38 | 1.00 (0.500-2.50) | 1.00 (0.500-2.50) | 10 | 1.00 (0.500-2.00) | 2.00 (0.500-2.00) |

¹ For t_{max}, the median and range (minimum-maximum) are given.

Figure A1: Composite Model Diagnostic Plots

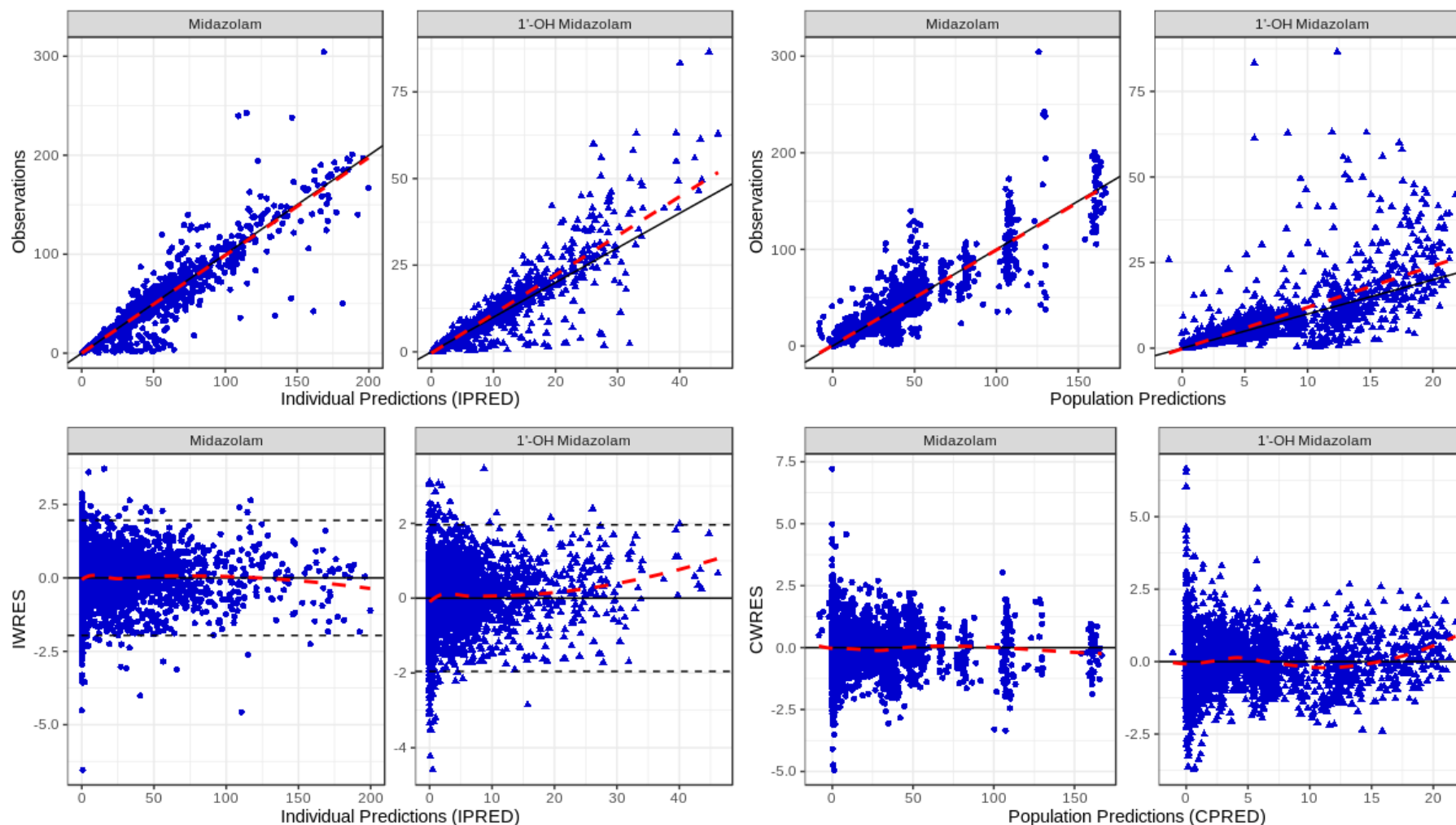
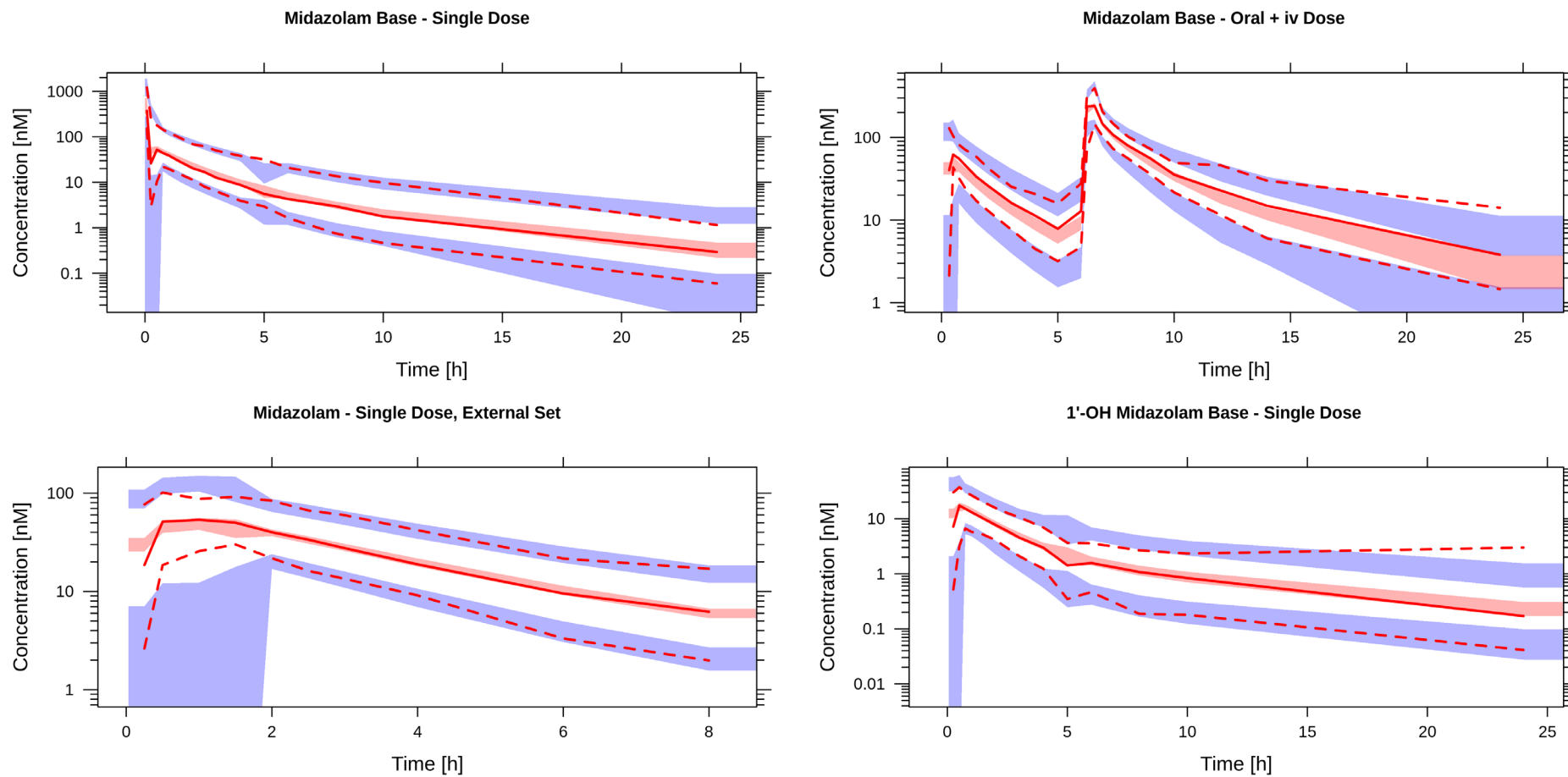


Fig. A1: Goodness-of-fit plots for the final composite model. Blue points denote individual values; black solid lines represent unity (top panels); red-dashed line is a linear smoothing function (top panels) or a loess smoothing function (bottom panels); black dashed lines represent ± 1.96 standard deviations (bottom left panels). CWRES = conditional weighted residual error; IWRES = individual weighted residual error.

Figure A2: Composite Model VPC



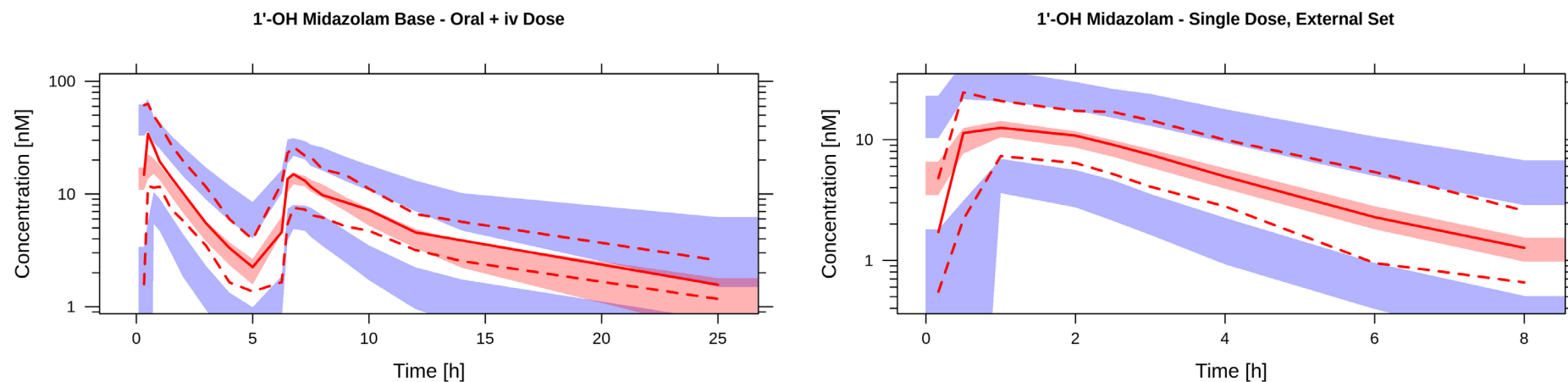
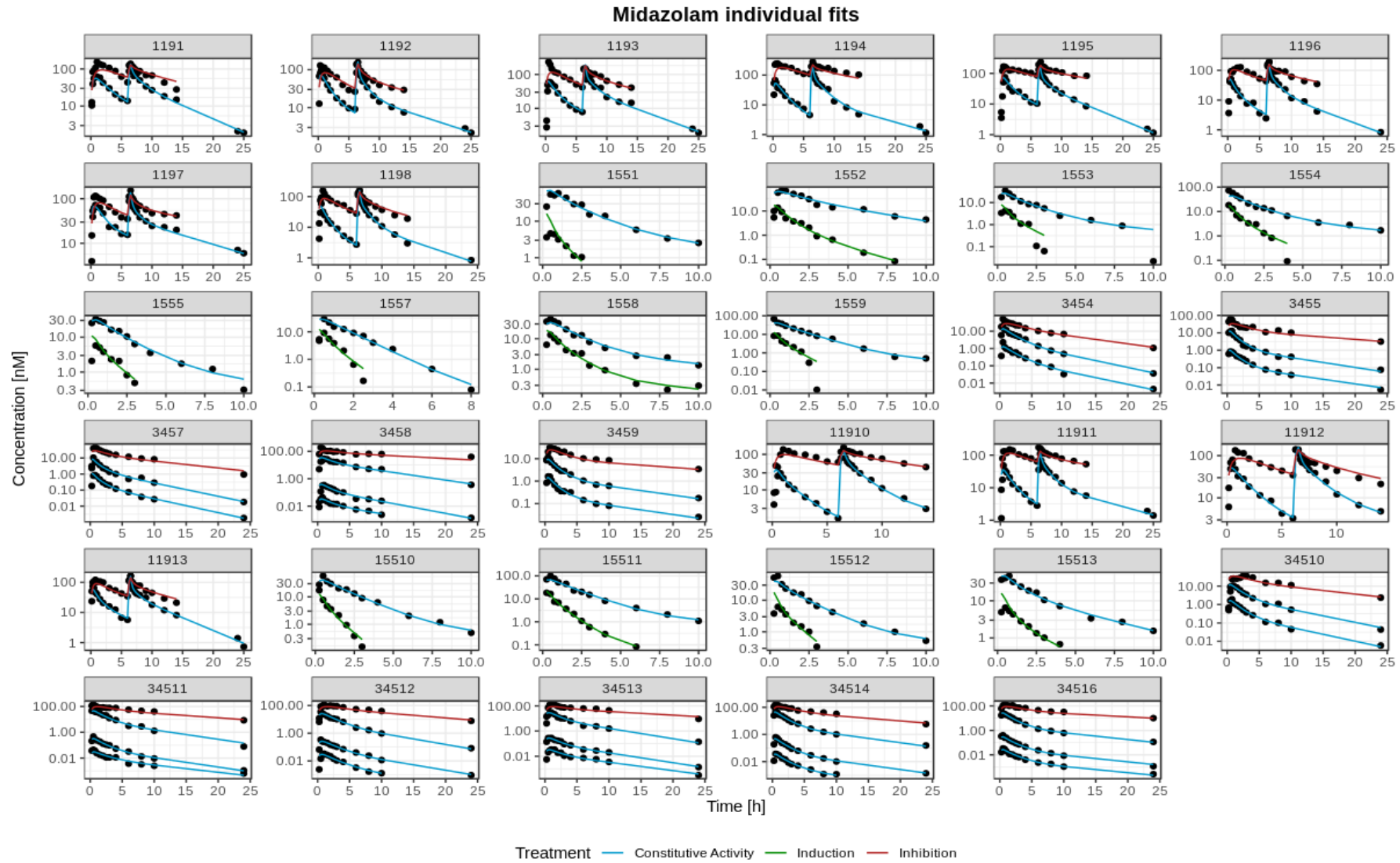
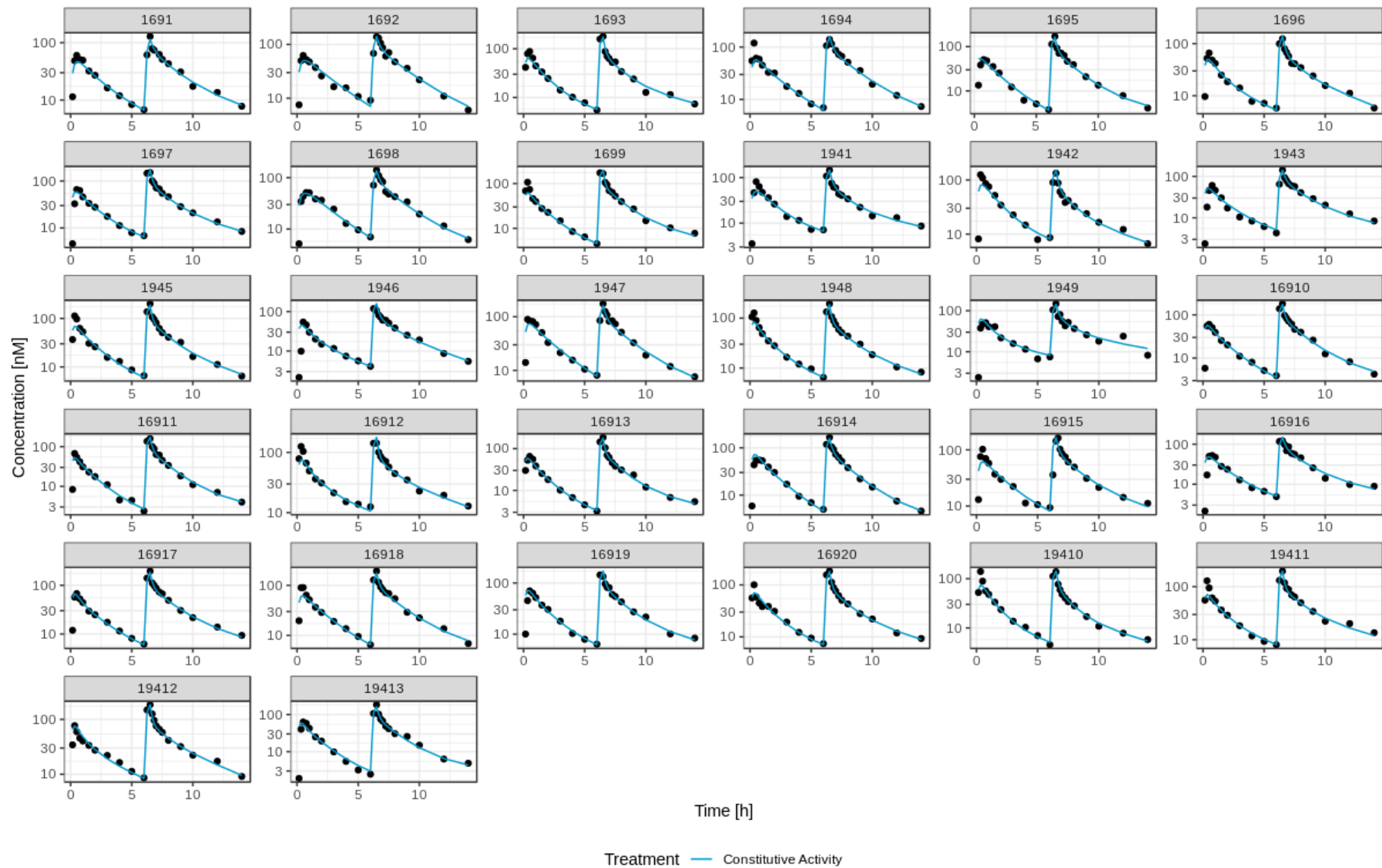


Fig. A2: Visual predictive check of the final composite model. 1000 simulations were used and data are displayed on a semi-log scale. The first two panels for each analyte are run on the dataset used to build the model, while the third panel includes only data from the prospective studies ('External Set'). The solid red line depicts the observed median concentrations, while the dotted lines depict the observed 97.5th and 2.5th percentiles. The shaded red area pertains to the 90% confidence interval for the predicted medians, while the shaded blue areas pertain to the 90% confidence interval for the 97.5th and 2.5th percentile predictions. Data are normalised to a midazolam dose of 4 mg. Single doses refer to a single oral or iv dose during the dosing interval. nM = nanomolar; h = hours.

Figure A3: Midazolam Individual Fits for Interaction Model



APPENDICES – COMPOSITE MODEL INDIVIDUAL FITS FOR INTERACTION



APPENDICES – COMPOSITE MODEL INDIVIDUAL FITS FOR INTERACTION

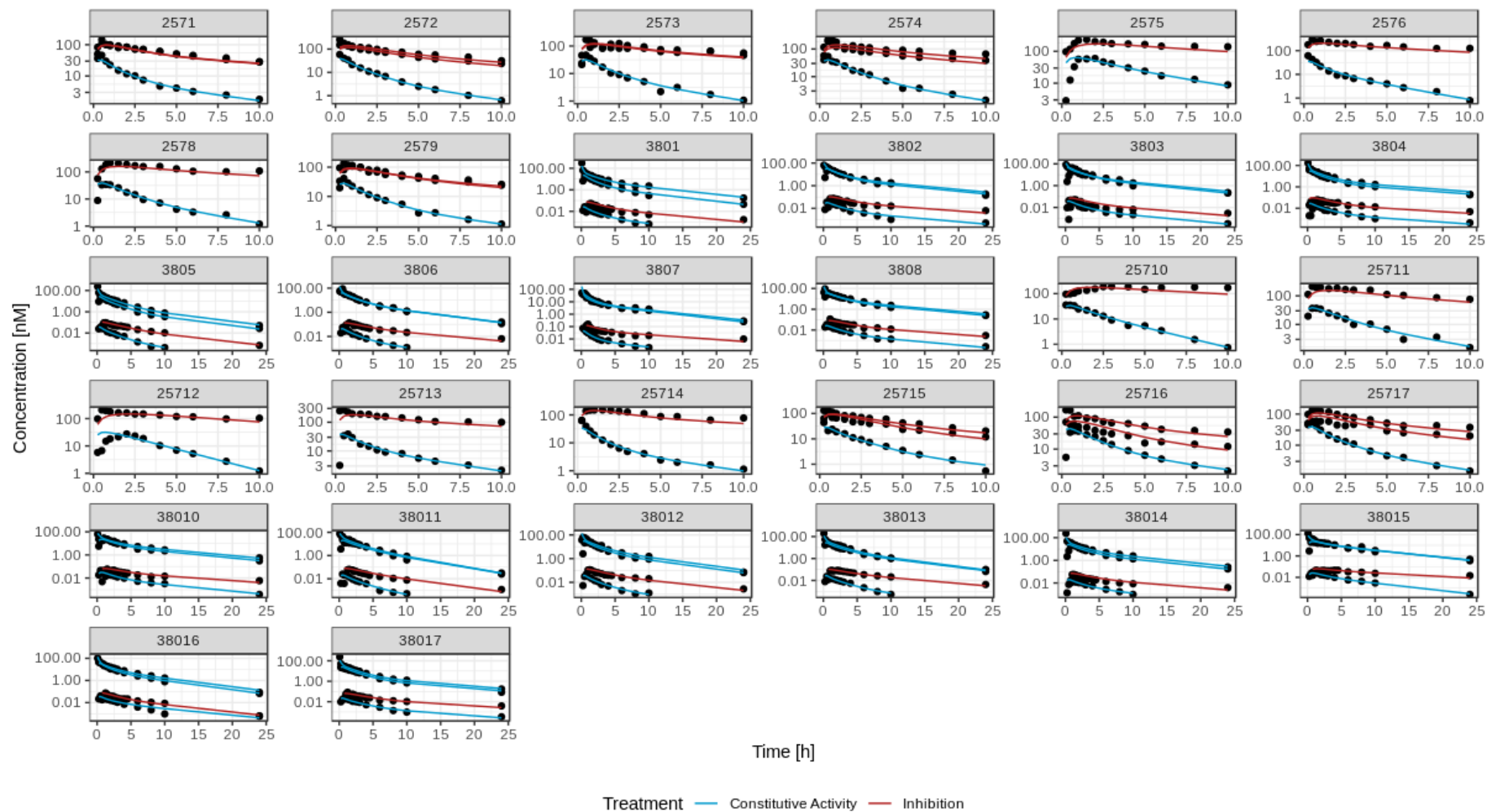
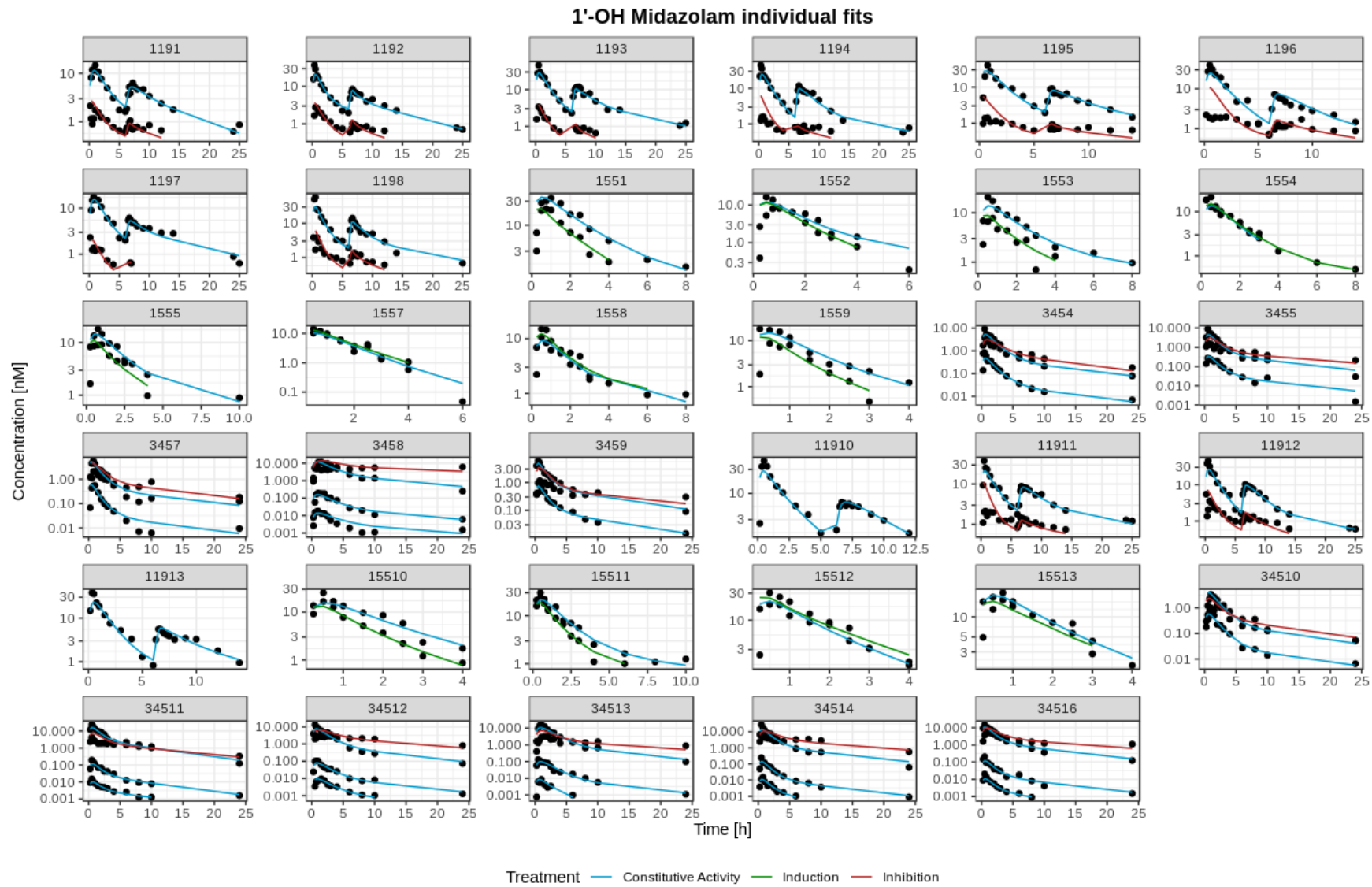
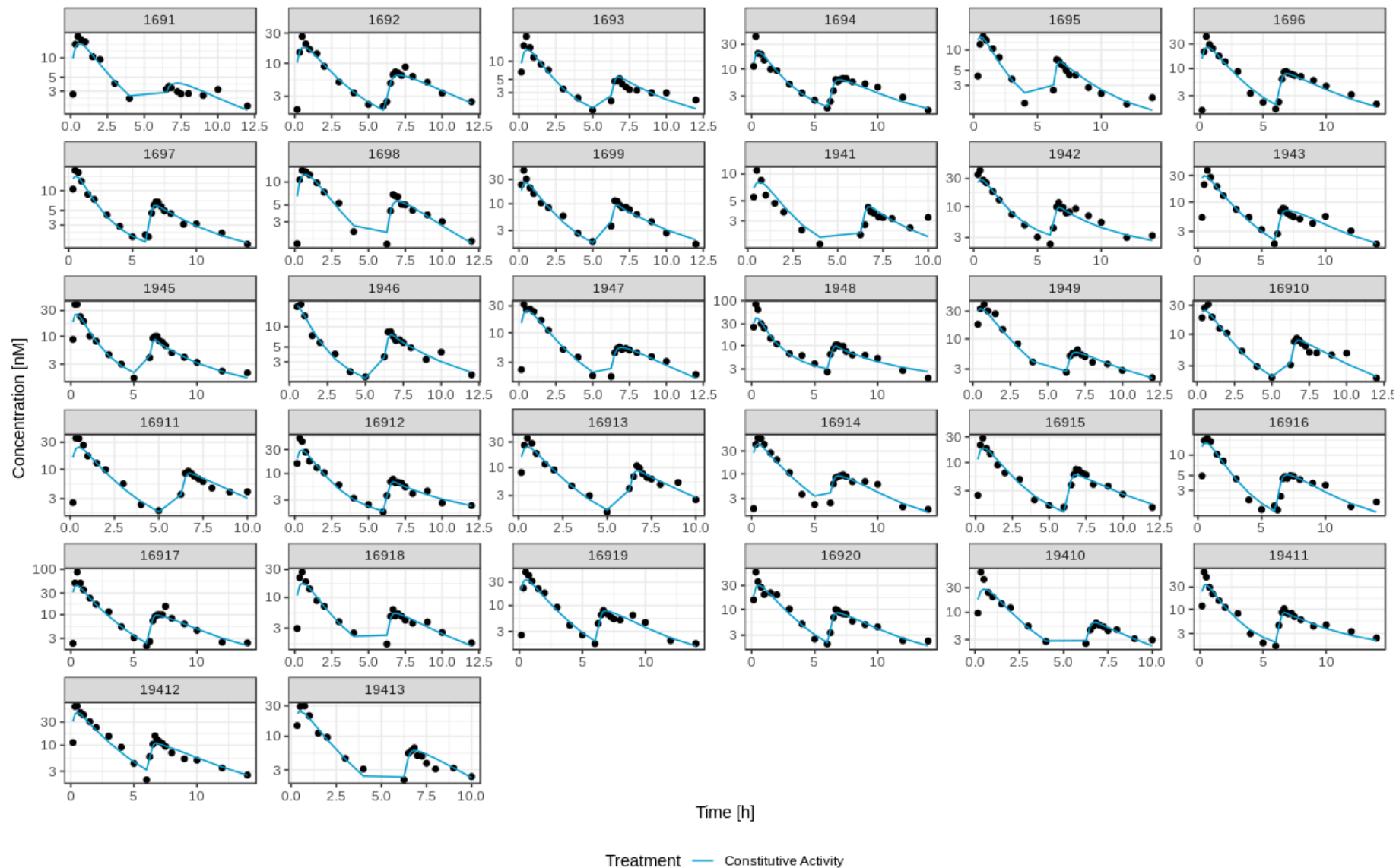


Fig. A3: Individual fits for all CYP3A conditions based on the composite model predictions. Profiles are for midazolam concentrations and are plotted on a semi-log scale; lines represent predicted profiles, while black circles represent actual observations.

Figure A4: 1'-OH Midazolam Individual Fits for Interaction Model



APPENDICES – COMPOSITE MODEL INDIVIDUAL FITS FOR INTERACTION



APPENDICES – COMPOSITE MODEL INDIVIDUAL FITS FOR INTERACTION

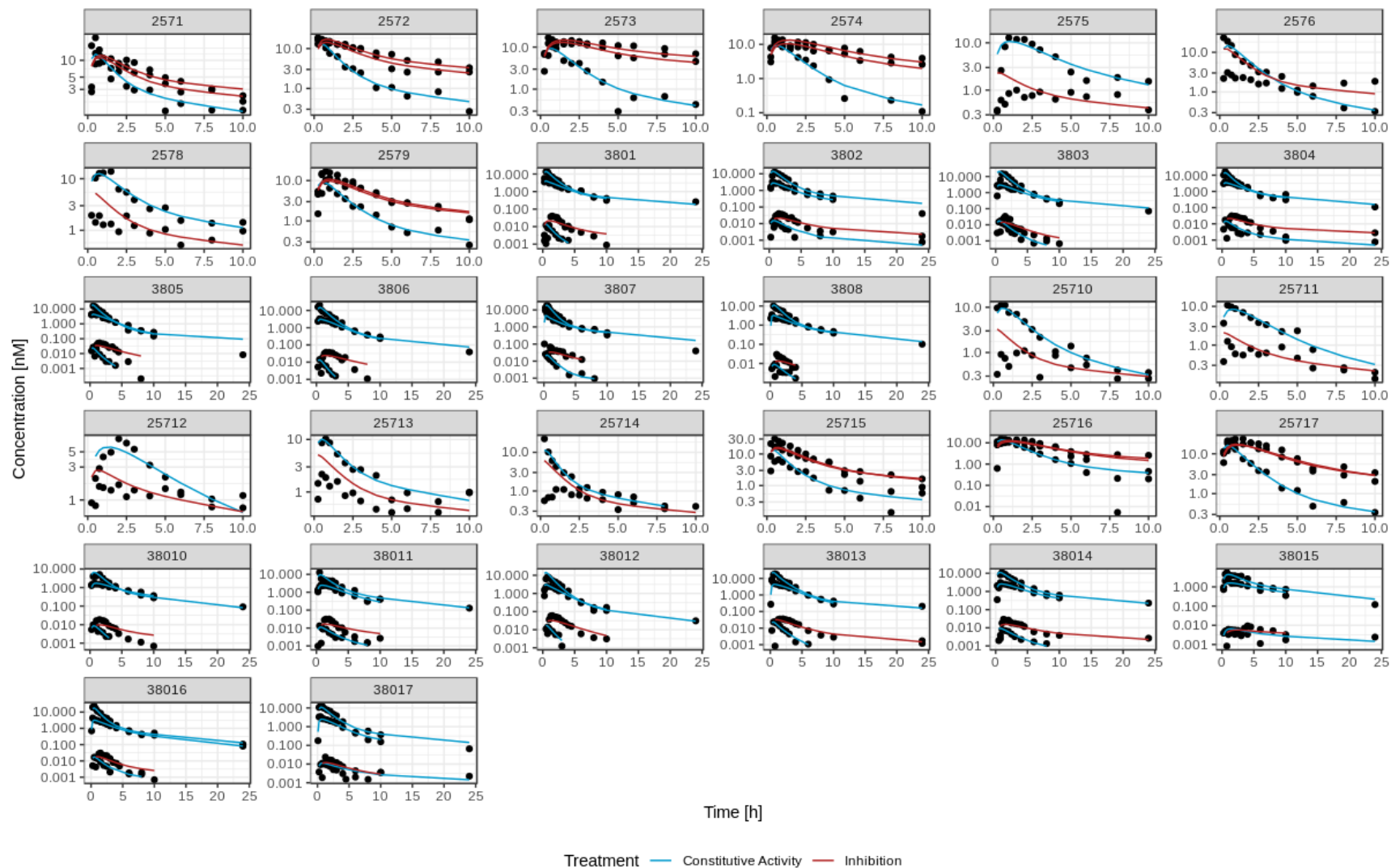
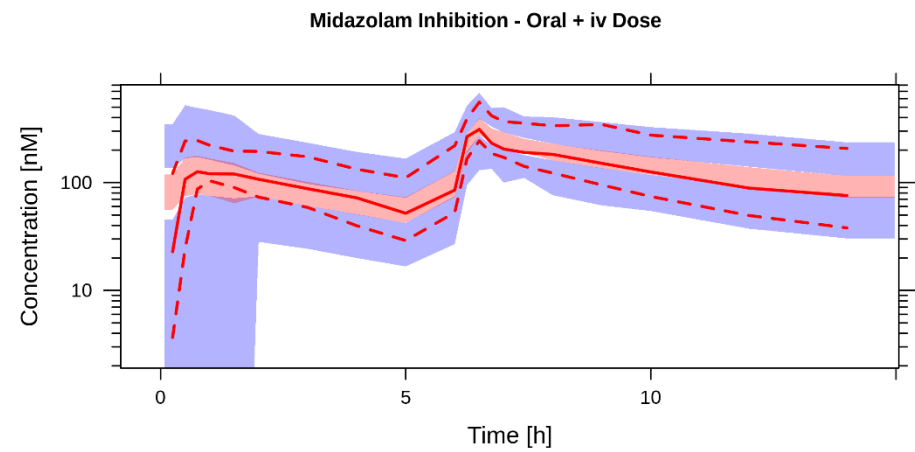
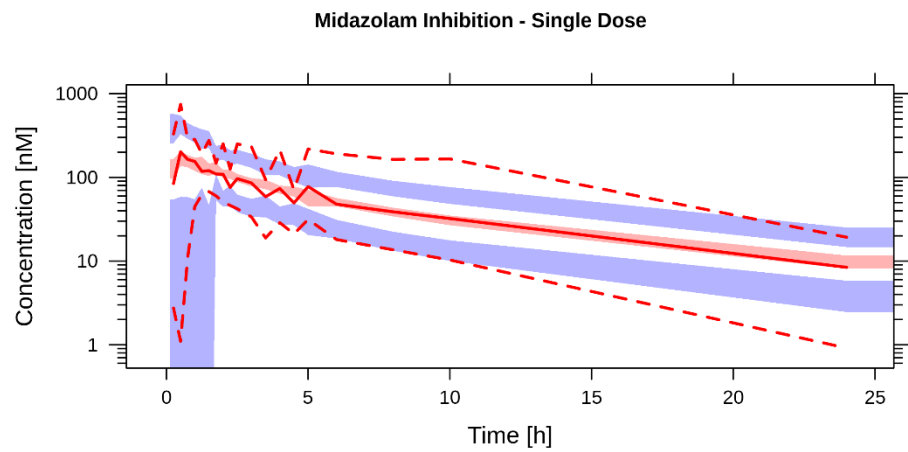
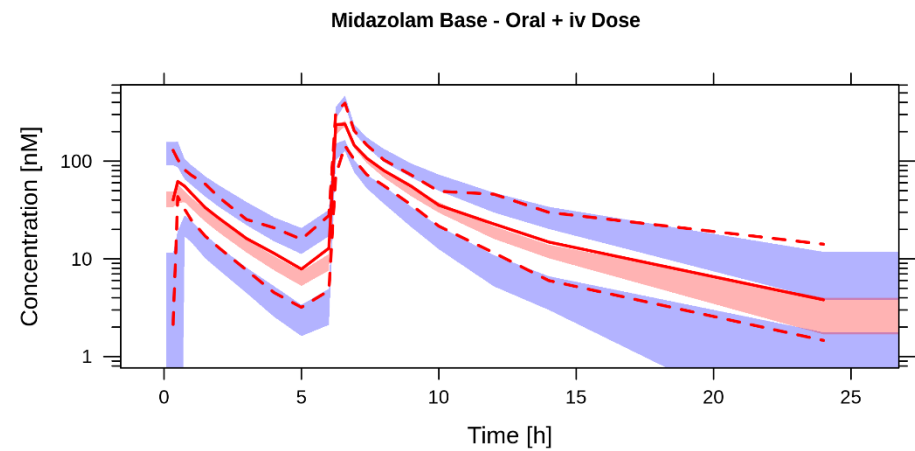
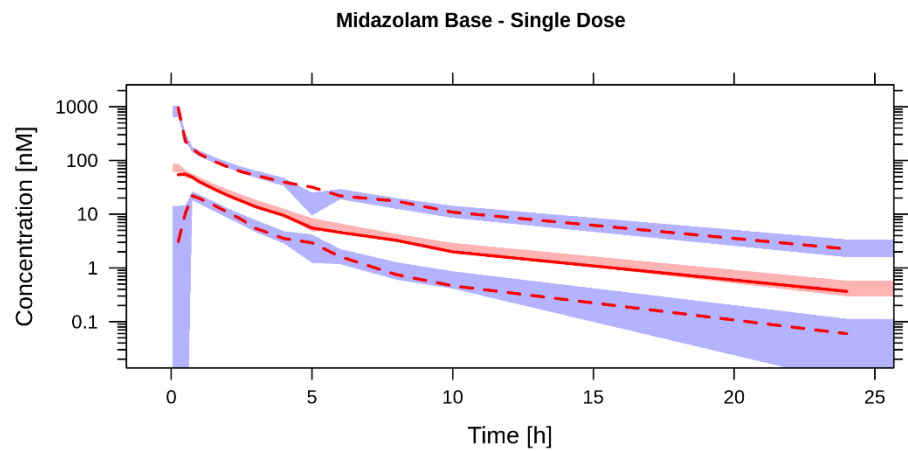


Fig. A4: Individual fits for all CYP3A conditions based on the composite model predictions. Profiles are for 1'-OH midazolam concentrations and are plotted on a semi-log scale; lines represent predicted profiles, while black circles represent actual observations.

Figure A5: Midazolam Interaction Model VPC



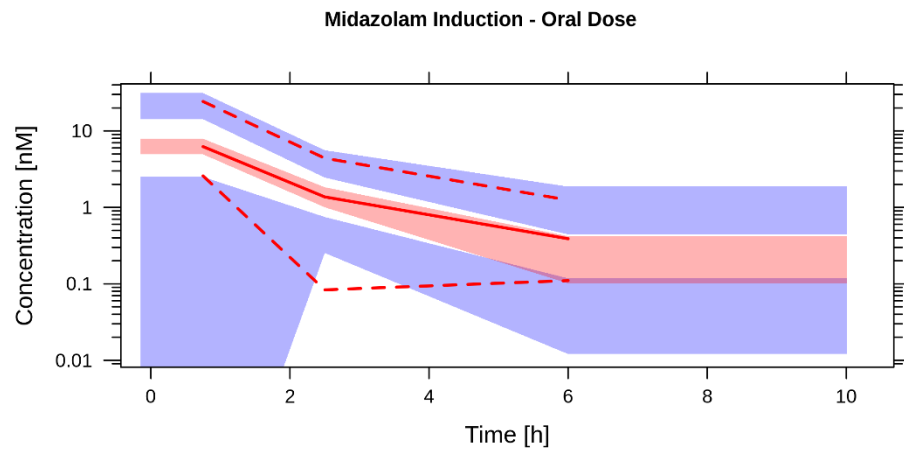


Fig. A5: Visual predictive check of the interaction effect on midazolam using the final midazolam model with interaction. 1000 simulations were used and data are displayed on a semi-log scale. The solid red line depicts the observed median concentrations, while the dotted lines depict the observed 97.5th and 2.5th percentiles. The shaded red area pertains to the 90% confidence interval for the predicted medians, while the shaded blue areas pertain to the 90% confidence interval for the 97.5th and 2.5th percentile predictions. Data are normalised to a midazolam dose of 4 mg. Single doses refer to a single oral or iv dose during the dosing interval. nM = nanomolar; h = hours.

Figure A6: Simulations Based on Limited Sampling – Internal Set

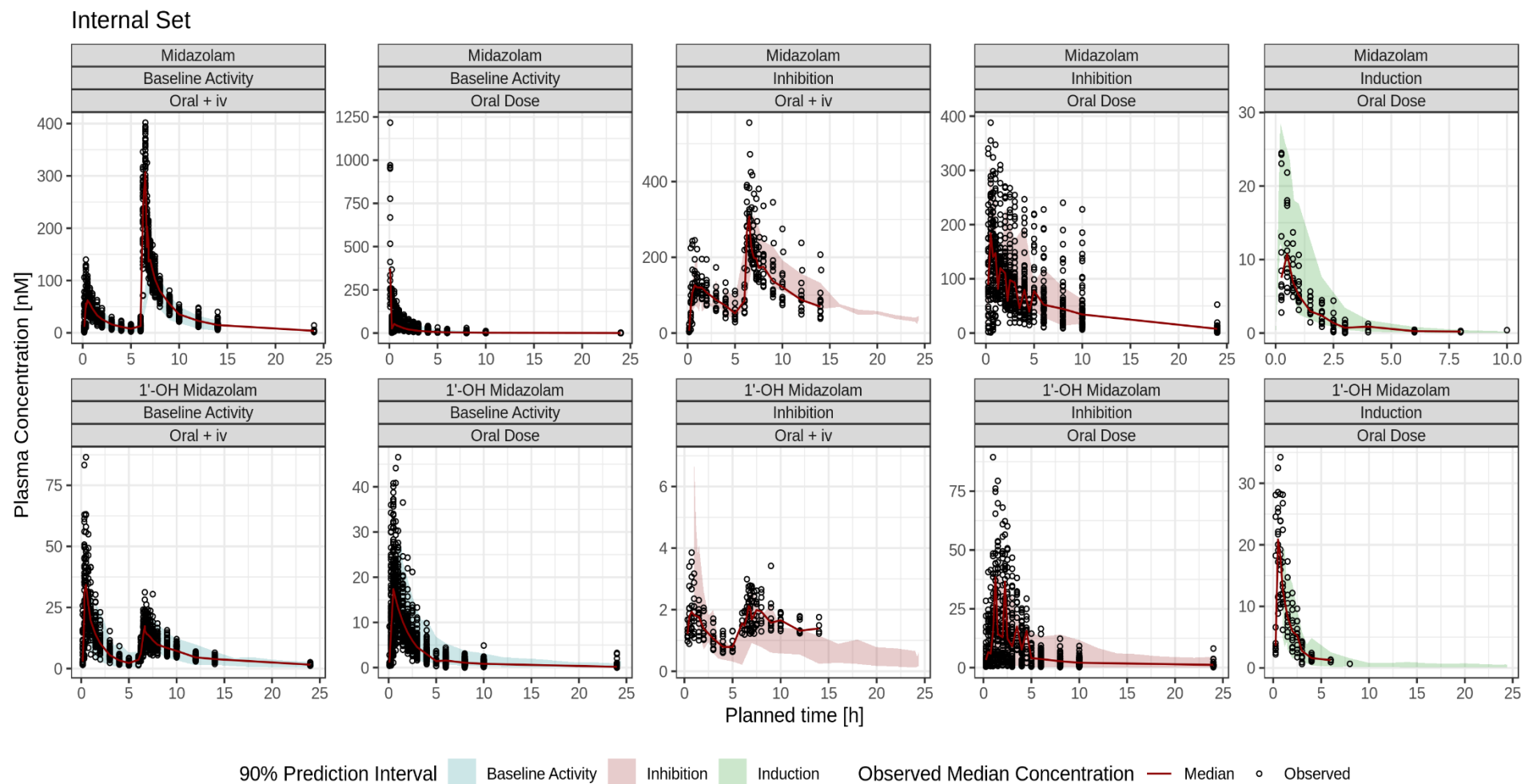


Fig. A6: Observed versus predicted midazolam and 1'-OH midazolam concentrations, based on limiting sampling and the final interaction model. Prediction intervals are simulated based on times 2, 2.5, 3, and 4 h from the original dataset. Black dots show all the actual observations, not just those used for simulations.

Figure A7: Simulations Based on Limited Sampling – External Set

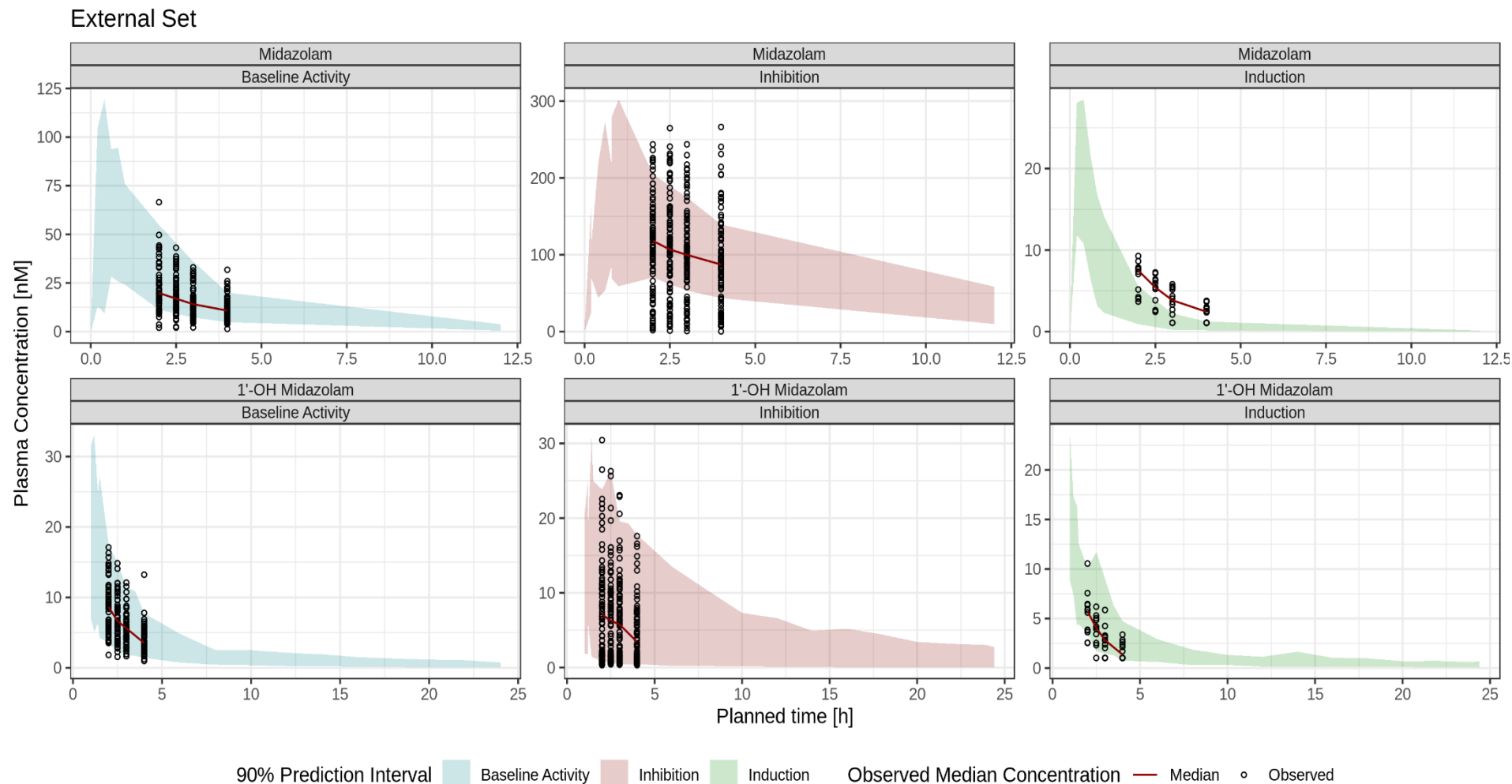


Fig. A7: Observed versus predicted midazolam and 1'-OH midazolam concentrations, based on limiting sampling and the final interaction model. Prediction intervals are simulated based on times 2, 2.5, 3, and 4 h from the external validation dataset.

Adopted Midazolam Model Control Stream with Interaction and Food Effect

```

$PROB      MDZ PopPK Model with Interaction and Food Effect
$INPUT     C ID XTIME=TIME TAFD AMT AMT2 DOSE CMT ANA XDV LDV=DROP DV
           MDV SEX AGE WT EVID RATE TRT TRT2 VIS STDY OCC BIS LLOQ
           LLOQ_Unit=DROP TRT3 STYP$DATA
$DATA     Combined_Set_w_TRT.csv
           IGNORE=C IGNORE=(ANA.EQ.1)
$SUBROUTINE ADVAN6 TOL=4
$MODEL     COMP(ABSORB)
           COMP(CENTRAL,DEFOBS)
           COMP(PERIPH)
           COMP(PERIPH2)
;===== PARAMETER DEFINITIONS =====
$PK
;----- FED STATUS -----
FED = 0

IF(FOOD.EQ.1) FED = 1
;----- TREATMENT -----
INH1 = 0 ; for reversible inhibition
INH2 = 0 ; for irreversible inhibition
IND = 0

IF(TRT3.EQ.2) INH1 = 1
IF(TRT3.EQ.5) INH2 =1
IF(TRT3.EQ.3) IND = 1
;----- INTEROCCASION VARIABILITY -----
OCC1=0
OCC2=0
OCC3=0
OCC4=0

IF(OCC.EQ.1) OCC1=1
IF(OCC.EQ.2) OCC2=1
IF(OCC.EQ.3) OCC3=1
IF(OCC.EQ.4) OCC4=1

IOF1 = OCC1*ETA(8)+OCC2*ETA(9)+OCC3*ETA(10)+OCC4*ETA(11)
IOCL = OCC1*ETA(12)+OCC2*ETA(13)+OCC3*ETA(14)+OCC4*ETA(15)
;----- PK MODEL -----
TVVC      = THETA(1)+INH2*THETA(17)+FED*THETA(20)
VC        = TVVC*EXP(ETA(1))      ; central compartment volume with food effect

TVVP1     = THETA(2)
VP1       = TVVP1*EXP(ETA(2))    ; peripheral compartment1 volume

TVVP2     = THETA(3)
VP2       = TVVP2*EXP(ETA(6))    ; peripheral compartment2 volume

TVQP1     = THETA(4)
QP1       = TVQP1*EXP(ETA(3))    ; inter-compartmental clearance (PER1)

```

APPENDICES – CONTROL STREAMS

TVQP2 = THETA(5)
 QP2 = TVQP2 ; inter-compartmental clearance (PER2)

TVCL = THETA(6)+ INH1*THETA(15)+INH2*THETA(15)+IND*THETA(16)
 CL = TVCL*EXP(ETA(4)+IOCL) ; elimination of parent with treatment effect

TVKA = THETA(7)+FED*THETA(21)
 KA = TVKA*EXP(ETA(7)) ; absorption rate constant with food effect

TVF1 = THETA(8)+INH1*THETA(13)+INH2*THETA(13)+IND*THETA(14)+FED*THETA(22)
 F1 = TVF1*EXP(ETA(5)+IOF1) ; bioavailability with treatment and food effects

K20 = CL/VC
 K23 = QP1/VC
 K32 = QP1/VP1
 K24 = QP2/VC
 K42 = QP2/VP2

S2=VC

;;===== DIFFERENTIAL EQUATIONS =====

\$DES

DADT (1) = - KA*A(1)
 DADT (2) = KA*A(1) - K23*A(2) + K32*A(3) - K24*A(2) + K42*A(4) - K20*A(2)
 DADT (3) = K23*A(2) - K32*A(3)
 DADT (4) = K24*A(2) - K42*A(4)

;;===== MODEL FIT =====

\$ERROR

FPROP = THETA(9) ; proportional RUV (early)
 FADD = THETA(10) ; additive RUV (early - fixed to 0)
 FPROP2 = THETA(11) ; proportional RUV (late)
 FADD2 = THETA(12) ; additive RUV (late - fixed to 0)
 FPROP3 = THETA(18) ; proportional RUV (late)
 FADD3 = THETA(19) ; additive RUV (late - fixed to 0)

;;Uppsala method for expressing error and weighted residuals:

IPRED = A(2)/S2

AUC = F1*DOSE/CL

W = SQRT((FPROP**2)*(IPRED**2)+(FADD**2))

IF(TRT.NE.2.AND.TIME.GT.0.5) W = SQRT((FPROP2**2)*(IPRED**2)+(FADD2**2)) ; to account for
 ; additional noise at early time points

IF(FED.EQ.1.OR.TR.TEQ.2.AND.TIME.GT.1.5) W = SQRT((FPROP3**2)*(IPRED**2)+(FADD3**2))
 ; to account for later tmax

IRES = DV - IPRED

IWRES = IRES/W

APPENDICES – CONTROL STREAMS

Y = IPRED+W*EPS(1) ; MDZ early prediction
IF(TRT.NE.2.AND.TIME.GT.0.5) Y = IPRED+W*EPS(2) ; MDZ late prediction
IF(FED.EQ.1.OR.TRT.EQ.2.AND.TIME.GT.1.5) Y = IPRED+W*EPS(3) ; MDZ late – inhibition/fed

IF(ICALL.EQ.4.AND.Y.LE.0) Y = 0.00001 ; to allow for log-transformed VPCs
;===== INITIAL ESTIMATES =====
\$THETA
20.6932 FIX ; 1 VC L
44.0251 FIX ; 2 VP1 L
23.6997 FIX ; 3 VP2 L
8.02466 FIX ; 4 QP1 L/h
45.7333 FIX ; 5 QP2 L/h
24.088 FIX ; 6 CL L/h
2.32486 FIX ; 7 KA /h
0.277613 FIX ; 8 F1
0.473118 FIX ; 9 FPROP
0 FIX ; 10 FADD
-0.155528 FIX ; 11 FPROP2
0 FIX ; 12 FADD2
0.529075 FIX ; 13 F1~INH
-0.199376 FIX ; 14 F1~IND
-15.1216 FIX ; 15 CL~INH
39.7503 FIX ; 16 CL~IND
16.6395 FIX ; 17 V2~INH2
-0.195234 ; 18 FPROP3 ; allowed to vary, as both fed and inhibition conditions have later tmax
0 FIX ; 19 FADD3
11.34 FIX ; 20 VC~FED
-1.076 FIX ; 21 KA~FED
0.1775 FIX ; 22 F1~FED

\$OMEGA
0.103977 FIX ; IIV_VC
0.184672 FIX ; IIV_VP1
0.220718 FIX ; IIV_QP1

\$OMEGA BLOCK(2) FIX
0.00724547 ; IIV_CL
-0.0127034 0.057301 ; IIV_F1

\$OMEGA
0.0339725 FIX ; IIV_VP2
0.0907368 FIX ; IIV_KA

\$OMEGA BLOCK(1) FIX
0.0204782 ; IOV FOR F1
\$OMEGA BLOCK(1) SAME
\$OMEGA BLOCK(1) SAME
\$OMEGA BLOCK(1) SAME

\$OMEGA BLOCK(1) FIX
0.0191667 ; IOV FOR CL
\$OMEGA BLOCK(1) SAME

APPENDICES – CONTROL STREAMS

\$OMEGA BLOCK(1) SAME
\$OMEGA BLOCK(1) SAME

\$SIGMA

1 FIX
1 FIX
1 FIX

;;===== ESTIMATION METHOD =====

\$ESTIMATION METHOD=1 INTERACTION MAXEVAL=9999 NOABORT PRINT=5 NSIG=3
SIGL=9 ; FOCE-I

\$COVARIANCE PRINT=E

;;===== TABLES =====

\$TABLE ID STDY TIME DOSE AMT CMT MDV EVID RATE VIS OCC BIS TRT
ETAS(1:LAST) STYP; Standard parameters
IPRED IWRES CIPRED CPRED CRES CWRES CIWRES NOPRINT
ONEHEADER FILE=sdtab11.7446

\$TABLE ID AUC CL VC VP1 VP2 QP1 QP2 KA F1 AGE WT SEX TRT TRT3; Model params
FPROP FADD FPROP2 FADD2 ETAS(1:LAST) NOPRINT NOAPPEND
ONEHEADER FILE=patab11.7446

\$TABLE ID SEX ; categorical covariate parameters
IPRED IWRES CIPRED CPRED CRES CWRES CIWRES NOPRINT
NOAPPEND ONEHEADER FILE=catab11.7446

\$TABLE ID AGE WT ; continuous covariate parameters
IPRED IWRES CIPRED CPRED CRES CWRES CIWRES NOPRINT
NOAPPEND ONEHEADER FILE=cotab11.7446

Adopted 1'-OH Midazolam Control Stream with Food Effect

```

$PROB      1'-OH MDZ PopPK Base Model
$INPUT     C ID TIME TAFD AMT CMT CMT2=DROP ANA DV LDV=DROP MDV SEX
           AGE WT EVID RATE TRT=DROP VIS=DROP STDY OCC BIS
$DATA      Combined_Set_1OH_MDZ.csv
           IGNORE=C IGNORE=(OCC.GT.1)
$SUBROUTINE ADVAN6 TOL=3
$MODEL     COMP(ABSORB)
           COMP(CENTRAL,DEFOBS)
           COMP(PERIPH)
           COMP(PERIPH2)
           COMP(PARENT)

;===== PARAMETER DEFINITIONS =====
$PK
;----- FED STATUS -----
FED = 0

IF(STDY.EQ.3) FED = 1 ; Study 3 gave midazolam following continental breakfast
;----- PK MODEL -----

TVVMET     = THETA(1)+FED*THETA(15) ; central compartment volume with food effect
VMET       = TVVMET*EXP(ETA(1))

TVVMP      = THETA(2) ; peripheral compartment volume
VMP        = TVVMP*EXP(ETA(3))

TVVMP2     = THETA(3) ; peripheral2 compartment volume
VMP2       = TVVMP2*EXP(ETA(8))

TVQMP      = THETA(4)+FED*THETA(17) ; intercompartmental clearance with food effect
QMP        = TVQMP*EXP(ETA(2))

TVQMP2     = THETA(5) ; intercompartmental clearance2
QMP2       = TVQMP2

TVCLM      = THETA(6) ; elimination of metabolite
CLM        = TVCLM*EXP(ETA(4))

TVKMET     = THETA(7)+FED*THETA(16) ; oral dose metabolic rate constant with food effect
KMET       = TVKMET*EXP(ETA(7))

TVF1       = THETA(8)
F1         = TVF1*EXP(ETA(5)) ; fraction metabolised/available following oral administration

TVF5       = THETA(9)
F5         = TVF5*EXP(ETA(6)) ; fraction metabolised/available following iv administration

KA         = THETA(10) ; rate of metabolism/"absorption" (following iv administration)
IF(CMT.EQ.1) KA = KMET

```

APPENDICES – CONTROL STREAMS

K20 = CLM/VMET
 K23 = QMP/VMET
 K32 = QMP/VMP
 K24 = QMP2/VMET
 K42 = QMP2/VMP2

S2=VMET

\$DES

DADT (1) = - KMET*A(1)
 DADT (2) = KMET*A(1) - K23*A(2) + K32*A(3) - K24*A(2) + K42*A(4) + F5*KA*A(5) - K20*A(2)
 DADT (3) = K23*A(2) - K32*A(3)
 DADT (4) = K24*A(2) - K42*A(4)
 DADT (5) = - F5*KA*A(5)

;;===== MODEL FIT =====
 \$ERROR

FPROP = THETA(11)
 FADD = THETA(12)
 FPROP2 = THETA(13)
 FADD2 = THETA(14)

;;Uppsala method for expressing error and weighted residuals:

IPRED = A(2)/S2
 W = SQRT((FPROP**2)*(IPRED**2)+(FADD**2))
 IF(TIME.GT.0.75) W = SQRT((FPROP2**2)*(IPRED**2)+(FADD2**2)) ; late cut-point for 1'-OH MDZ

IRES = DV - IPRED
 IWRES = IRES/W
 Y = IPRED+W*EPS(1) ; 1'-OH MDZ early prediction
 IF(TIME.GT.0.75) Y = IPRED+W*EPS(2) ; 1'-OH MDZ late prediction

IF(ICALL.EQ.4.AND.Y.LE.0) Y=0.0001 ; to be able to produce log-transformed VPCs

;;===== INITIAL ESTIMATES =====
 \$THETA

59.2791 FIX ; 1 VMET L
 2488.52 FIX ; 2 VMP L
 56.8482 FIX ; 3 VMP2 L
 114.423 FIX ; 4 QMP L/h
 24.7025 FIX ; 5 QMP L/h
 129.467 FIX ; 6 CLM L/h
 0.802675 FIX ; 7 KMET /h
 0.811246 FIX ; 8 F1
 0.796446 FIX ; 9 F5
 0.426855 FIX ; 10 KA
 -0.487011 FIX ; 11 FPROP
 0.00001 FIX ; 12 FADD
 0.181784 FIX ; 13 FPROP2
 0.00001 FIX ; 14 FADD2

APPENDICES – CONTROL STREAMS

120 ; 15 VMET~FED
-0.2279 ; 16 KMET~FED
-42 ; 17 QMP~FED

\$OMEGA

0.435663 FIX ; IIV_VMET
0.413409 FIX ; IIV_QMP
0.373184 FIX ; IIV_VMP

\$OMEGA BLOCK(2) FIX

0.0990933 ; IIV_CLM
-0.0354774 0.0127039 ; IIV_F1

\$OMEGA

0.0126279 FIX ; IIV_F5
0.00863727 FIX; IIV_KMET
0.83752 FIX ; IIV_VMP2

\$SIGMA

1 FIX
1 FIX

;;===== ESTIMATION METHOD =====

\$ESTIMATION METHOD=1 INTERACTION MAXEVAL=9999 NOABORT PRINT=5 NSIG=3
SIGL=9 ; FOCE-I

\$COVARIANCE PRINT=E

;;===== TABLES =====

\$TABLE ID TIME AMT CMT MDV EVID RATE STDY BIS STYP ETAS(1:LAST) ; Standard parameters
IPRED IWRES CIPRED CPRED CRES CWRES CIWRES NOPRINT
ONEHEADER FILE=sdtab42.345

\$TABLE ID CLM VMET VMP VMP2 Q1 Q2 F1 F5 KMET AGE WT SEX ; Model parameters
FPROP FADD ETAS(1:LAST) IPRED IWRES CIPRED CPRED CRES
CWRES CIWRES NOPRINT NOAPPEND ONEHEADER FILE=patab42.345

\$TABLE ID SEX ; categorical covariate parameters
IPRED IWRES CIPRED CPRED CRES CWRES CIWRES NOPRINT
NOAPPEND ONEHEADER FILE=catab42.345

\$TABLE ID AGE WT ; continuous covariate parameters
IPRED IWRES CIPRED CPRED CRES CWRES CIWRES NOPRINT
NOAPPEND ONEHEADER FILE=cotab42.345

Adopted Composite Model Control Stream with Interaction

```

$SIZES          LVR=50 ; increase number of allowed etas+epsilons to 50
$PROBLEM        Combined MDZ+1-OH MDZ PopPK Model
$INPUT          C ID XTIME=TIME TAFD=DROP AMT DOSE CMT ANA DV LDV=DROP NDV
                MDV SEX AGE WT EVID RATE TRT TRT2 VIS STDY OCC BIS BIS2
                LLOQ LLOQ_Unit=DROP TRT3 STYP
$DATA          Combined_Set_w_TRT_no1ug.csv IGNORE=C
                IGNORE=(BIS.EQ.1)
$SUBROUTINE    ADVAN6 TOL=4
$MODEL          COMP(ABSORB)
                COMP(CENTRAL)
                COMP(PERIPH1)
                COMP(PERIPH2)
                COMP(METABOL)
                COMP(MET_PER)
                COMP(MET_PER2)
;===== PARAMETER DEFINITIONS =====
$PK
;----- INTERACTION -----
INH1 = 0 ; reversible inhibition
INH2 = 0 ; irreversible inhibition
IND = 0 ; induction

IF(TRT3.EQ.2) INH1 = 1
IF(TRT3.EQ.5) INH2 = 1
IF(TRT3.EQ.3) IND = 1
;----- INTEROCCASION VARIABILITY -----
OCC1=0
OCC2=0
OCC3=0
OCC4=0
OCC5=0

IF(OCC.EQ.1) OCC1=1
IF(OCC.EQ.2) OCC2=1
IF(OCC.EQ.3) OCC3=1
IF(OCC.EQ.4) OCC4=1
IF(OCC.EQ.5) OCC5=1

IOQMET = OCC1*ETA(10)+OCC2*ETA(11)+OCC3*ETA(12)+OCC4*ETA(13)+OCC5*ETA(14)
IOCLM  = OCC1*ETA(15)+OCC2*ETA(16)+OCC3*ETA(17)+OCC4*ETA(18)+OCC5*ETA(19)
IOF1   = OCC1*ETA(20)+OCC2*ETA(21)+OCC3*ETA(22)+OCC4*ETA(23)+OCC5*ETA(24)
;----- PK MODEL -----
; - MDZ -
TVVC      = THETA(1)+INH2*THETA(25)
VC        = TVVC*EXP(ETA(2)) ; central compartment volume

TVVP1     = THETA(2)
VP1       = TVVP1*EXP(ETA(5)) ; peripheral compartment1 volume

TVVP2     = THETA(3)
VP2       = TVVP2 ; peripheral compartment2 volume

```

APPENDICES – CONTROL STREAMS

TVQP1 = THETA(4)
QP1 = TVQP1*EXP(ETA(6)) ; intercompartmental clearance (PER1)

TVQP2 = THETA(5)
QP2 = TVQP2 ; intercompartmental clearance (PER2)

TVQMET = THETA(10)+INH1*THETA(26)+INH2*THETA(26)+IND*THETA(27)
QMET = TVQMET*EXP(ETA(3)+IOQMET) ; 1-OH MDZ systemic formation rate

TVF1 = THETA(7)+INH1*THETA(28)+INH2*THETA(28)+IND*THETA(29)
F1 = TVF1*EXP(ETA(7)+IOF1) ; availability of parent+metabolite

FM = 1 ; fraction metabolised, fixed to 1

; - 1-OH MDZ -

TVKMET = THETA(8)+INH1*THETA(30)+INH2*THETA(30)+IND*THETA(31)
KMET = TVKMET*EXP(ETA(8)) ; pre-systemic metabolism rate

TVVMET = THETA(9)
VMET = TVVMET*EXP(ETA(1)) ; metabolic central compartment volume

TVCLM = THETA(11)+INH1*THETA(32)+INH2*THETA(33)+IND*THETA(34)
CLM = TVCLM*EXP(ETA(4)+IOCLM) ; metabolic clearance

TVVMP = THETA(12)
VMP = TVVMP ; volume of metabolic peripheral compartment 1

TVQMP = THETA(13)*(WT/70)**THETA(24)
QMP = TVQMP*EXP(ETA(9)) ; metabolic inter-compartmental clearance 1

TVVMP2 = THETA(14)
VMP2 = TVVMP2 ; volume of metabolic peripheral compartment 2

TVQMP2 = THETA(15)
QMP2 = TVQMP2 ; metabolic inter-compartmental clearance 2

IF(ANA.EQ.0) KA = THETA(6) ; absorption rate constant
IF(ANA.EQ.1) KA = KMET ; first-pass/pre-systemic metabolism rate

K23 = QP1/V2
K32 = QP1/VP1
K24 = QP2/V2
K42 = QP2/VP2
K56 = QMP/VMET
K65 = QMP/VMP
K57 = QMP2/VMET
K75 = QMP2/VMP2
K2M = FM*QMET/V2
KM0 = CLM/VMET

APPENDICES – CONTROL STREAMS

S2=V2

S5=VMET

;;===== DIFFERENTIAL EQUATIONS =====

\$DES

DADT (1) = - KA*A(1) - KMET*A(1)

DADT (2) = KA*A(1) - K23*A(2) + K32*A(3) - K24*A(2) + K42*A(4) - K2M*A(2)

DADT (3) = K23*A(2) - K32*A(3)

DADT (4) = K24*A(2) - K42*A(4)

DADT (5) = KMET*A(1) - K57*A(5) + K75*A(7) - K56*A(5) + K65*A(6) + K2M*A(2) - KM0*A(5)

DADT (6) = K56*A(5) - K65*A(6)

DADT (7) = K57*A(5) - K75*A(7)

;;===== MODEL FIT =====

\$ERROR

IPRED = F

IPRED = A(2)/S2

IF(ANA.EQ.1) IPRED = A(5)/S5

FPROP1 = THETA(16) ; proportional residual error

FADD1 = THETA(17) ; additive residual error

FPROP2 = THETA(18)

FADD2 = THETA(19)

FPROP3 = THETA(20)

FADD3 = THETA(21)

FPROP4 = THETA(22)

FADD4 = THETA(23)

FPROP5 = THETA(35)

FADD5 = THETA(36)

FPROP6 = THETA(37)

FADD6 = THETA(38)

IF(TRT.NE.2.AND.ANA.EQ.0.AND.TIME.LE.0.5) W = SQRT((FPROP1**2)*(IPRED**2)+(FADD1**2))

IF(TRT.NE.2.AND.ANA.EQ.0.AND.TIME.GT.0.5) W = SQRT((FPROP3**2)*(IPRED**2)+(FADD3**2))

IF(TRT.NE.2.AND.ANA.EQ.1.AND.TIME.LE.0.5) W = SQRT((FPROP2**2)*(IPRED**2)+(FADD2**2))

IF(TRT.NE.2.AND.ANA.EQ.1.AND.TIME.GT.0.5) W = SQRT((FPROP4**2)*(IPRED**2)+(FADD4**2))

IF(TRT.EQ.2.AND.TIME.LE.1.5) W = SQRT((FPROP5**2)*(IPRED**2)+(FADD5**2))

IF(TRT.EQ.2.AND.TIME.GT.1.5) W = SQRT((FPROP6**2)*(IPRED**2)+(FADD6**2))

Y1 = IPRED+W*EPS(1) ; MDZ prediction [P]

Y2 = IPRED+W*EPS(2) ; 1'-OH MDZ prediction [P]

IRES= DV - IPRED

IWRES = IRES/W

Y = ANA*Y2+(1-ANA)*Y1 ; Combine both analytes for predictions

IF(ICALL.EQ.4.AND.Y.LE.0) Y=0.0001

APPENDICES – CONTROL STREAMS

;;===== INITIAL ESTIMATES =====

\$THETA

19.4929 FIX ; 1 VC L
41.28 FIX ; 2 VP1 L
23.679 FIX ; 3 VP2 L
8.1232 FIX ; 4 QP1 L/h
45.4305 FIX ; 5 QP2 L/h
0.68347 FIX ; 6 KA parent /h
0.931754 FIX ; 7 F1
1.59436 FIX ; 8 KMET /h
178.663 FIX ; 9 VMET L
24.2406 FIX ; 10 QMET L/h
199.081 FIX ; 11 CLM L/h
695.65 FIX ; 12 VMP L
60.2326 FIX ; 13 QMP /h
64.9128 FIX ; 14 VMP2 L
128.035 FIX ; 15 QMP2 /h
0.500352 FIX ; 16 FPROP1
0 FIX ; 17 FADD1
0.542515 FIX ; 18 FPROP2
0.00001 FIX ; 19 FADD2
0.147547 FIX ; 20 FPROP3
0 FIX ; 21 FADD3
-0.215408 FIX ; 22 FPROP4
0.00001 FIX ; 23 FADD4
1.177 FIX ; 24 QMP~WT
23.1644 ; VC~INH2
-14.0604 ; QMET~INH
38.6969 ; QMET~IND
0.777008 ; F1~INH
-0.391097 ; F1~IND
-1.03554 ; KMET~INH
1.56394 ; KMET~IND
-78.6676 ; CLM~INH1
1159.2 ; CLM~INH2
-47.3111 ; CLM~IND
0.531725 ; FPROP5
0 FIX ; FADD5
-0.309011 ; FPROP6
0 FIX ; FADD6

\$OMEGA BLOCK(2) FIX

0.119028 ; IIV_VMET
0.0811696 0.135856 ; IIV_VC

\$OMEGA

0.00678604 FIX ; IIV_QMET
0.0221803 FIX ; IIV_CLM
0.173052 FIX ; IIV_VP1
0.249102 FIX ; IIV_QP1
0.0468617 FIX ; IIV_F1
0.0848403 FIX ; IIV_KMET

APPENDICES – CONTROL STREAMS

0.303653 FIX ; IIV_QMP

\$OMEGA BLOCK(1) FIX
0.0230267 ; IOV FOR QMET
\$OMEGA BLOCK(1) SAME
\$OMEGA BLOCK(1) SAME
\$OMEGA BLOCK(1) SAME
\$OMEGA BLOCK(1) SAME

\$OMEGA BLOCK(1) FIX
0.0904157 ; IOV FOR CLM
\$OMEGA BLOCK(1) SAME
\$OMEGA BLOCK(1) SAME
\$OMEGA BLOCK(1) SAME
\$OMEGA BLOCK(1) SAME

\$OMEGA BLOCK(1) FIX
0.0261093 ; IOV FOR F1
\$OMEGA BLOCK(1) SAME
\$OMEGA BLOCK(1) SAME
\$OMEGA BLOCK(1) SAME
\$OMEGA BLOCK(1) SAME

\$SIGMA

1 FIX ; MDZ proportional
1 FIX ; 1'-OH MDZ proportional

;;===== ESTIMATION METHOD =====
\$ESTIMATION METHOD=1 INTERACTION MAXEVAL=9999 NOABORT PRINT=5 NSIG=3 ; FOCE-I
\$COVARIANCE PRINT=E

;;===== TABLES =====

\$TABLE ANA ID TIME AMT DOSE CMT MDV EVID RATE SEX AGE WT STDY VIS
TRT TRT3 TRT2 STYP ETAS(1:LAST) IPRED IWRES CIPRED CPRED
CRES CWRES CIWRES NOPRINT ONEHEADER FILE=sdtab247.69

\$TABLE ANA ID CLM V2 VP1 VP2 VMET VMP VMP2 QP1 QP2 QMET QMP QMP2 KA
F1 KMET TRT TRT2 SEX AGE WT FPROP1 FADD1 FPROP2 FADD2
FPROP3 FADD3 ETAS(1:LAST) IPRED IWRES CIPRED CPRED CRES
CWRES CIWRES NOPRINT ONEHEADER FILE=patab247.69

CURRICULUM VITAE

Sabrina Wiebe
Am Bächle 6
88437 Lauperthausen
Birth date: May 9, 1982
Nationality: Canadian

HIGHER EDUCATION

Doctoral Candidate, sc. hum. (Clinical Pharmacology), Heidelberg University, Germany,
Finish foreseen: 2020

M.Sc. (Experimental Psychology), McGill University, Canada, 2007

B.Sc. (Honours Psychology), University of Ottawa, Canada, 2005 (Summa Cum Laude)

CAREER

2019-present: Pharmacometrician, Boehringer-Ingelheim, Biberach an der Riss, Germany

2017-present: Scientific Aid, Universitätsklinikum Heidelberg, Heidelberg, Germany

2013-2019: Trial Clinical Pharmacokineticist, Boehringer-Ingelheim, Biberach an der Riss,
Germany

2012-2013: Research Assistant in Neuroscience, Animal Research Lab, McGill University,
Canada

2009-2012: Laboratory/Research Coordinator, Attention, Behaviour and Sleep Laboratory,
Douglas Mental Health Institution, McGill University, Canada

2006-2009: Statistical Consultant in Health and Social Sciences, employed by multiple
Canadian Universities

Ort und Datum

Unterschrift

ACKNOWLEDGMENTS

First and foremost, I would like to thank my supervisors and mentors, Prof. Dr. med. Gerd Mikus and Dr. Andreas Meid for giving me the opportunity to learn about and work on the topic of midazolam microdosing and population pharmacokinetic modelling applied to CYP3A drug-drug interactions. Furthermore, I would like to thank them for their support in achieving the results of the work herein.

Additionally, I would like to thank Dr. Peter Stopfer, Dr. Ashish Sharma, Dr. Thomas Giessman and Dr. Fabian Mueller for their encouragement and support in pursuing this work. I would also like to thank Boehringer-Ingelheim for funding of the early clinical studies where midazolam microdosing was integrated.

A very big thank you to Dr. Ben Weber, Dr. Valerie Nock, Dr. Alexander Staab, Dr. Oskar Clewe, and other fellow pharmacometricians for sharing their insight and providing me much needed support, despite their already heavy workloads and limited time schedules.

Lastly, and perhaps most importantly, I would like to thank my husband, Mathieu Parisien, and my children, Kaya and Lea, who have had to sacrifice many “mummy-time hours” so that I would be able to accomplish this undertaking. Their encouragement, love, and patience during the process have been integral to being able to move forward and achieve such a big endeavour.

EIDESSTATTLICHE VERSICHERUNG

1. Bei der eingereichten Dissertation zu dem Thema
Midazolam Microdosing and Population Pharmacokinetic Modelling to Assess CYP3A Drug-Drug Interactions in Early Clinical Development
handelt es sich um meine eigenständig erbrachte Leistung.
2. Ich habe nur die angegebenen Quellen und Hilfsmittel benutzt und mich keiner unzulässigen Hilfe Dritter bedient. Insbesondere habe ich wörtlich oder sinngemäß aus anderen Werken übernommene Inhalte als solche kenntlich gemacht.
3. Die Arbeit oder Teile davon habe ich bislang nicht an einer Hochschule des In- oder Auslands als Bestandteil einer Prüfungs- oder Qualifikationsleistung vorgelegt.
4. Die Richtigkeit der vorstehenden Erklärungen bestätige ich.
5. Die Bedeutung der eidesstattlichen Versicherung und die strafrechtlichen Folgen einer unrichtigen oder unvollständigen eidesstattlichen Versicherung sind mir bekannt. Ich versichere an Eides statt, dass ich nach bestem Wissen die reine Wahrheit erkläre und nichts verschwiegen habe.

Ort und Datum

Unterschrift